GRADUATE AERONAUTICAL LABORATORIES
CALIFORNIA INSTITUTE OF TECHNOLOGY

THEORETICAL AND EXPERIMENTAL STUDY ON THE EJECTOR AUGMENTED JET FLAP

NASA Grant NGR 05-002-239

Firestone Flight Sciences Laboratory

Guggenheim Aeronautical Laboratory

Karman Laboratory of Fluid Mechanics and Jet Propulsion

Pasadena

FINAL REPORT

Grant NGR 05-002-239
NASA Ames Research Center

THEORETICAL AND EXPERIMENTAL STUDY ON THE EJECTOR AUGMENTED JET FLAP

August 1, 1974

Submitted by:

for H. J. Stewart BS

H. J. Stewart
Professor of Aeronautics

B. Sturtevant

B. Sturtevant
Executive Officer for Aeronautics

Graduate Aeronautical Laboratories
California Institute of Technology
Pasadena, California

TABLE OF CONTENTS

PART I

INTRODUCTION AND SUMMARY

I. INTRODUCTION AND SUMMARY

Introduction

A general limitation in the system analysis of jet flap or related propulsive systems suitable for VTOL or STOL applications arises from the paucity of analytical models which can rationally represent the complex flow problems observed in real machines. The jet flap theory developed by Spence* has been generally useful in these considerations even though it represents a limiting idealization of the flow phenomena. The work of Shollenburger** on a propulsive biplane brought forth the possibility of relaxing one of the idealizations of Spence's theory by incorporating a finite fluid flow into the propulsive system.

It was felt to be desirable to extend the concept of Shollenburger's work to a configuration more nearly resembling actual propulsive-lifting wings in order to investigate more realistically the usefulness of the analytical concept. Accordingly, the present work, supported by a grant from the NASA Ames Laboratory, was undertaken.

The configuration chosen was a two dimensional wing with a biplane flap, having a jet injected on the upper surface of the wing at the flap hinge axis and discharging into the channel between the two elements of the flap. The work was carried out in two parts, the first analytical and the second experimental.

The analytical work, carried out by Laurent Sidor as a thesis project, is a potential flow solution in which the wing geometry (with thickness effects neglected) is represented by bound vortex sheets. The

---

* See Ref. 6 of Part II

** See Ref. 8 of Part II

propulsive effects are, in effect, represented by an actuator disc spanning the gap between the trailing edges and introducing a uniform total head jump into all the fluid flowing through this region. The total head jump then requires that, in the wake, the propulsive fluid be separated from the outer fluid by free vortex sheets. The solutions obtained, with one minor and unimportant exception (see Appendix B), represent the full nonlinear solution of the potential flow boundary value problem. This work is presented in the next section of this report.

The experimental work was carried out in a special two-dimensional test installation in the GALCIT 10-foot subsonic wind tunnel. The model description, the test conditions and the summary of the experimental results are presented in the third part of this report.

Summary

The analytical work, Part II of this report, is self-contained and requires no further comment at this point except to note (see Fig. 11) the excellent correlation between the computed lift due to propulsion at zero angle of attack and the lift variation predicted by the "equivalent sink" concept. In noting this correlation it must be remembered that the actuator disc formally corresponds to a singularity system having zero mass injection but a finite momentum injection as measured by the jump in total head.

The report of the experimental tests (Part III) is also complete in itself. There remains, then, the analysis of the experimental data in the light of the theoretical analysis to illustrate the usefulness of the theoretical concepts. For this purpose it is convenient to restate the analysis in a form more directly related to the experimentally obtained

data.

For any two-dimensional wing in the presence of a sink of strength Q, the lift increment at any given angle of attack (for example, $\alpha = 0°$) is proportional to Q and is given by (see Eq. 55, Part II)

$$\Delta C_L = 2\left(\frac{Q}{c U_\infty}\right)\bar{k}$$

where $\bar{k}$ is a geometrically determined constant. In the analysis the "equivalent sink" strength due to the jet was taken to be

$$\frac{Q}{c U_\infty} = \frac{h}{c}\left[(1+C_H)^{1/2}-1\right]$$

This formula assumes the jet width to be essentially the same far from the wing and at the trailing edge. The Kutta condition makes this formula asymptotically correct for large values of C_H and the computed variation (with finite values of C_H) was at most only a few percent. The theoretical calculation for this configuration shows best correlation for $k = \frac{h}{c}\bar{k} = 0.1625$.

The experimental measurements of total head at the trailing edge station show that relatively poor mixing was achieved by the simple slot injection and C_H varies strongly across the channel, however a proper measure of the "equivalent sink" can be obtained by integration across the wake. In addition, it is necessary to make a correction for the volume of fluid injected (a negative sink) through the slot. For the test series this volume flux was held constant at 21.45 cu. ft./sec. A rake survey over the 3 ft span of the slot shows reasonably uniform conditions except that a 30% deficit in flux occurred for a distance of 2.5 in. at each end of the model. The effective span is thus 2 7/8 ft. for determining the two-dimensional source (negative sink) strength. The magnitude of this

correction at the various test dynamic pressures is as follows:

q (lbs/ft^2)	2.25	3	5	10
Q'/cU_∞	-0.083	-0.0072	-0.056	-0.040

The theoretical analysis was carried out for $\frac{h}{c} = 0.15$; thus the procedure for calculating an equivalent uniform total head increment C_H^* for relating the experimental results with the analytical theory is

$$0.15\left\{\sqrt{1 + C_H^*} - 1\right\} = \int_{\text{wake}} \left\{\sqrt{1 + C_H} - 1\right\} d\left(\frac{z}{c}\right) + \left(Q'/cU_\infty\right)$$

where z is the distance along the total head rake survey station.

The test data shows, in addition to the low level of mixing, indications of flow separation and a standing, trapped, vortex below the main wing at the hinge station. Accordingly the data analysis was limited to consideration of the lift increments produced by blowing. Table I shows the observed results. Because the effective total head increment obtained (C_H^*) was fairly low, it can be expected (see Fig. 16 of Part II) that the lift increment will be proportional to C_H^*; the ratio $\Delta C_L/C_H^*$ is computed for comparison with the analytical result from Fig. 16, $\Delta C_L/C_H = 0.4$.

The experimentally obtained values of $\Delta C_L/C_H^*$ show a wide variation; however the average value $\Delta C_L/C_H^* = 0.41$ is essentially identical to the analytical result. It is also apparent from this analysis that, for a given momentum input to the propulsive duct, the resulting magnitude of C_H^*, and thus the lift due to blowing, is strongly and adversely affected by non-uniformities in the mixing.

4

TABLE I

LIFT INCREMENT DUE TO BLOWING

	Runs		q	C_L		ΔC_L	C_H^*	$\Delta C_L / C_H^*$
$h_s = 1.80''$	$C_j \neq 0$	$C_j = 0$		$C_j \neq 0$	$C_j = 0$			
$\alpha = 0°$	45	40	2.25	1.530	1.078	0.452	2.240	0.20
	46	41	3	1.513	1.040	.473	1.434	0.33
	47	42	5	1.458	1.009	.449	0.940	0.48
	48	43	10	1.393	0.997	.396	0.585	0.68
$\alpha = 6°$	45	40	2.25	1.918	1.328	0.590	1.732	0.34
	46	41	3	1.874	1.311	.563	1.560	0.36
	47	42	5	1.845	1.307	.538	1.053	0.51
	48	43	10	1.783	1.259	.524	0.598	0.88
$h_s = 2.25''$								
$\alpha = 0°$	2	9	2.25	1.650	1.163	0.487	1.890	0.26
	3	10	3	1.610	1.185	.425	1.690	0.25
	4	11	5	1.541	1.082	.459	1.250	0.37
	5	12	10	1.462	1.048	.414	0.790	0.52
$\alpha = 6°$	2	9	2.25	1.998	1.406	0.592	1.890	0.31
	3	10	3	1.957	1.434	.523	1.538	0.34
	4	11	5	1.885	1.331	.554	1.152	0.48
	5	12	10	1.811	1.297	.514	0.737	0.70

TABLE I (con't)

LIFT INCREMENT DUE TO BLOWING

	Runs		q	C_L		ΔC_L	C_H^*	$\Delta C_L / C_H^*$
	$C_j \neq 0$	$C_j = 0$		$C_j \neq 0$	$C_j = 0$			
$\alpha = 6^\circ$	32	36	2.25	2.035	1.491	0.544	2.686	0.20
	33	37	3	1.980	1.412	.568	1.179	0.48
	34	38	5	1.925	1.348	.577	1.412	0.41
	35	39	10	1.850	1.297	.553	0.869	0.64
$h_s = 2.70''$								
$\alpha = 0^\circ$	32	36	2.25	1.671	1.232	0.439	2.637	0.17
	33	37	3	1.660	1.155	.505	2.240	0.23
	34	38	5	1.582	1.101	.481	1.332	0.36
	35	39	10	1.505	1.053	.452	0.924	0.49

PART II

THEORETICAL

AN INVESTIGATION OF THE EJECTOR-POWERED JET-FLAP

Thesis by

Laurent B. Sidor

In Partial Fulfillment of the Requirements

For the Degree of

Aeronautical Engineer

California Institute of Technology

Pasadena, California

1974

(Submitted September 10, 1973)

8

ACKNOWLEDGEMENTS

The author expresses his gratitude to Dr. Gordon L. Harris for suggesting the topic and providing guidance in the early part of the work. Also, he is grateful to Dr. Homer J. Stewart for his interest and his guidance in the completion of this work. In addition, the financial support of the National Aeronautics and Space Administration, Ames Research Center is deeply appreciated. And finally, he thanks Mrs. Elizabeth Fox for the typing of the thesis.

ABSTRACT

The inviscid and incompressible potential flow aspects associated with a two-dimensional ejector-powered jet-flap configuration are investigated. The energy addition due to the mixing process in the ejector results in a non-homogeneous flow and is represented by an actuator disk located between the lifting surfaces and a powered wake. A set of singularities is developed to represent the lifting surfaces, to include camber and flap deflection, and the powered wake. A numerical procedure is used to compute the total system vorticity needed to satisfy exactly all the prescribed boundary conditions. The lift and moment coefficients are evaluated as a function of the head change prescribed across the actuator disk. A simple interpretation of the resulting lift curves is proposed in terms of analytical results obtained for single-airfoil configurations - a flat-plate airfoil and sink system, and a conventional single element jet flap. The sink effect of the actuator accounts for a finite lift at zero angle of attack, and the lift increment due to angle of attack only can be predicted by using Spence's theory of the jet flap.

TABLE OF CONTENTS

TABLE OF CONTENTS (Cont'd)

TABLE OF CONTENTS (Cont'd)

I. INTRODUCTION

1. General Background

The past few years have seen a widened interest in the area of V/STOL flight, spurred by potentially attractive civilian and military applications. These applications establish as a foremost requirement for the lifting system a high wing loading, necessary for range and good ride quality.

Toward the satisfaction of this requirement, new aerodynamic configurations have been developed to exploit directly the power available from the propulsion system for the generation of lift by blowing on the lifting surfaces. Various schemes have been investigated, and are shown in Fig. 1. They are:

The externally blown flap (a good review of configurations of this type is in Ref. 29) and over the wing blowing (Ref. 28) configurations use the jet engine exhaust directly over the upper side of the flap or wing surface. These configurations are characterized by the simplicity of the mechanical devices used to direct the exhaust airflow.

Other configurations use an extensive internal ducting system, driven by the high pressure stage of the engine compressor, to distribute the blowing over a major spanwise portion of the wing. The conventional jet-flap (Refs. 30-31) and augmentor-type wings operate on this principle.

In a conventional jet-flap, the jet sheet created by the blowing action mixes with the surrounding air producing a secondary effect on the lift by fact rather than design; it will be discussed later in this

section. On the other hand, the name "augmentor wings" is reserved for configurations intended to exploit this mixing effect to "augment" the primary airstream with the entrained secondary in installations known as "ejectors." The specific purpose for which the ejector is designed separates augmentor wings into two categories.

(a) The ejector can develop extra thrust on its inlet lip and sidewalls, thus supplementing the direct thrust generated by the primary for a vertical lift system.

A family of ejectors designed toward this end has been under development at the Aerospace Research Laboratories, Wright Patterson AFB (Refs. 19, 20). It is specifically tailored for the needs of vertical take-off and landing operations.

(b) The other type of augmentor wing is the ejector-powered jet-flap, which is the subject of the present investigation. The purpose of the ejector in this case is to augment the primary jet momentum with the entrained secondary, the intent being to produce an increase in circulation around the wing as compared to a conventional jet-flap design, other things being equal. In addition, the design is purported to offer a potential remedy to the noise problem associated with conventional jet-flaps. The ejector-powered jet-flap is aimed at producing the high lift coefficients needed for sustaining flight at low forward speeds: this is the domain of STOL. The Large-Scale Aerodynamics facility at NASA/Ames has tested several full-scale versions of this scheme (Refs. 26, 27).

The present work is concerned with the analysis of some aspects of the flow field around a two-dimensional section of this

type. Let us describe now in more specific terms the flow field and how the conventional modelling techniques can be extended to the present problem.

2. Representation of the Effects of the Mixing Zone on the Lifting Surfaces

The effects of the mixing zone are represented by the inflow velocity associated with the jet entrainment, and a net momentum flow downstream resulting in a powered wake. The inflow velocity can in turn be represented as an equivalent distribution of sinks located on the jet centerline (Ref. 33), the strength of these sinks being equal to the rate of entrainment. The net momentum flux in the powered wake is representative of the mixing efficiency of the ejector. The specific parameters used depend on the wake model used and are discussed in the next section.

3. Solutions to the Lifting Problem for Multi-energy Flows

A wide variety of multi-energy potential flows have been investigated over the past fifteen years or so, and are quite intimately associated to new developments in lifting systems. The flow models can be classified into two families: thin wake models and thick wake models. The independent parameter used to describe the energy addition will depend on which wake model is used.

Spence, in his analysis of jet-flap configurations (Refs. 5, 6, 13), used a thin wake model, in which the real powered wake is replaced by a single vortex sheet. In addition the boundary conditions are linearized. This model is valid in the limit of a jet of negligibly small mass flux but finite momentum flux (it is the independent

parameter energy addition due to the jet).

His analysis was extended by Wygnanski and Newman (Ref. 7) to include the effects of entrainment by adding sinks on the airfoil chordline. The strength of the sinks, for a given jet momentum, is related to the entrainment as mentioned previously. It is found that although significant, the contribution of the sinks to the over-all lift increment is quite small, and possibly dependent on the particular mixing model used.

Thick wake work has been largely associated with the prediction of propeller configurations, with the exception of C. A. Shollenberger's investigation of the two-dimensional propulsive biplane (Ref. 8). The independent parameter, in this case, is the head change ΔH normalized in the form $C_H = \frac{\Delta H}{\frac{1}{2}\rho U_\infty^2}$; it results from the action of an actuator disk which raises the head of entrained fluid from H_o to $H_o + \Delta H$.

Efforts have been directed toward the solution of the flow field generated by a heavily loaded actuator disk at zero angle of attack and to include the effects of non-uniform loading (Ref. 3), and at a finite angle of attack (Ref. 12). More directly relevant to our problem, Chaplin (Ref. 2) has investigated the performance of shrouded propellers at zero angle of attack and no forward speed. His treatment of the wake is quite similar to the one of the present work, described in Section II. A review of shrouded propeller work can be found in Weissinger and Maas' article (Ref. 9). The emphasis of this work being toward propellers, the configurations investigated are always two-dimensional axisymmetric, making the results of

use for our particular configuration as general reference only.

The potential flow model proposed in Section II is an extension of C. A. Shollenberger's analysis of the two-dimensional propulsive wing with rectilinear lifting surfaces. It accounts for camber, and in particular for flap deflection. This will be described in the next section.

II. POTENTIAL FLOW PROBLEM

1. Formulation of the Problem

This section provides the theoretical background for a numerical calculation of the potential flow around the lifting section represented in Fig. 2. It was found that the singularity system proposed in Ref. 8 for rectilinear chordlines can be extended to this more general geometry.

(a) Field Equation and Elementary Solutions

In this section, we will formulate the problem of the incompressible, inviscid homogeneous and irrotational flow about a system of lifting surfaces of specified shape in which the amount of energy addition is specified through the head change ΔH.

The lifting surfaces will be represented by cambered thin lines, in the usual thin airfoil theory formalism.

We will assume that the powered wake fluid does not substantially mix with the surrounding fluid, so that it can be assumed to be bounded by two infinitely thin vortex sheets. This assumption will model the jump in velocity between inside and outside of the wake.

In the conditions stated above, the stream function ψ of the system, and its derivatives, the velocity components u_x and u_y, satisfy the Laplace equation throughout the field (including the wake) except on the boundaries where a jump in tangential velocity occurs.

$$\nabla^2 \psi = 0$$

$$\nabla^2 u_x = \nabla^2 u_y = 0$$

19

We will work with the velocity components u_x and u_y because the boundary conditions are more readily expressed in terms of u_x and u_y rather than ψ.

Using the jump condition across the vortex sheet, we may decompose the tangential velocity field into a regular part, $u_{other}(x)$, due to all the other singularities in the field, and a single-valued part, representing the self-induced velocity field due to the local vorticity:

$$\lim_{y \to \pm 0} u(x, y) = u_{other} \pm u_{s \cdot i} \tag{1}$$

where $u_{si} = \frac{1}{2}\gamma(x)$ for two-dimensional vortex sheets.

Let $\vec{s} = \vec{s}(\sigma)$ specify the position of a vortex sheet (Fig. 3) of intensity $|\vec{\gamma}(\sigma)|$. Then the velocity field $\Delta\vec{u}(\vec{r})$ due to the vortex elements between σ_1 and σ_2 at any point away from the discontinuity is given by:

$$\Delta\vec{u}(\vec{r}) = \frac{1}{2\pi} \int_{\sigma_1}^{\sigma_2} \frac{\vec{\gamma}(\sigma) d\sigma \times (\vec{r} - \vec{s})}{|\vec{r} - \vec{s}|^2} \tag{2}$$

The total velocity field at that point, $\vec{u}(\vec{r})$, is found by superposing the contribution from all the vortex elements in the field. The choice of specific vortex elements is dictated by the particular problem treated. Each is referred to as an "elementary vortex" and, within this context, (2) is an elementary solution to the field equation (Poisson solution to the Laplace equation).

We have found a general expression for the solution to the field equation, expressed in terms of the singularities in that field. The next step is to find a suitable set of singularities. These are imposed by the boundary conditions.

(b) Boundary Conditions

The boundary conditions are imposed both by the airfoil surfaces and the powered wake. These can be separated into two distinct classes: those that are linear in the velocity field and those that are not.

(i) The Kinematic or Streamline Condition: Let α be the local slope of the streamline, referred to the freestream direction (local angle of attack). Then we must have the following relationship between the velocity components:

$$\frac{v_y}{U_\infty + u_x} = \tan\alpha \qquad (3)$$

Since there is no flow through the surfaces representing the airfoils, this relates the geometry of the system to the velocity field, the standard problem of thin airfoil theory.

In addition, the relation must be true in particular at the vortex sheets bounding the wake from the outside fluid. However, in this case, both α and the velocity components are a priori unknown.

Also, the presence of the powered wake imposes finite velocity perturbations at downstream infinity. We will show how this boundary condition is satisfied by the wake model we will choose.

(ii) The Pressure or Dynamic Boundary Condition in the Wake: The mixing process occurring in the ejector raises the total pressure of the entrained fluid from atmospheric head H_o to $H_o + \Delta H$. Applying the Bernoulli equation on the upper and lower side of the wake vortex sheets (Fig. 2), we get

$H_o = p_o + \frac{1}{2}\rho u_o^2$ outside wake

$H_o + \Delta H = p_1 + \frac{1}{2}\rho u_1^2$ inside wake

Continuity of static pressure across the vortex sheet requires $p_o = p_1$

$$\Delta H = \tfrac{1}{2}\rho(u_1 + u_o)(u_1 - u_o) \tag{4}$$

where ΔH is specified for this problem. Using (1), we can directly translate this into a condition for the vorticity:

$$\rho\, u_{other} \cdot \gamma(x) = \Delta H \tag{5}$$

The difficulty of satisfying this boundary condition is two-fold--it is non-linear in the velocity field, and the location at which it should be applied is a priori unknown.

The solution to the problem is completely determined, in principle, given the representation (2) of the velocity field and the set of boundary conditions (3) and (5). We must now find suitable elementary solutions and a practical scheme to actually solve the problem.

2. Vortex Distributions to Represent the Airfoil System

The chordwise distribution of vorticity in the presence of discontinuities in the shape of the boundary has been discussed extensively in Refs. 5, 6 and 16. These discontinuities occur at the leading edge, at the sharp corner representing the deflection of a flap, and possibly at the trailing edge. A singularity in the vorticity distribution at the trailing edge means flow around the trailing

edge due to jet discharge angle. This is known as "singular blowing" (Ref. 30). In our problem, the jet discharges parallel to the flap line, thus removing this condition ("regular blowing").

In the final analysis, these singularities are of two types: square root at the leading edge and logarithmic for the other two. The different nature of these singularities shows in the integrated effect: the square root singularity produces a net thrust in addition to the normal force, while the logarithmic singularity is too "weak" to produce a thrust term. It is these criteria that dictate the choice of a particular type of vortex distribution.

(a) The Leading Edge Singularity

A well-known result of thin airfoil theory is the square-root leading edge singularity of the vorticity distribution of a flat plate airfoil at an angle of attack:

$$\gamma_f(x) \sim \frac{\Gamma_f}{\sqrt{x}} \quad \text{as } x \to 0 \tag{6}$$

The flow around the leading edge of the thin section is interpreted as the limit of the flow about the round nose section of finite thickness. In both cases, this singularity produces a finite suction force $S = 2\pi\Gamma_f^2$, directed along the slope of the camberline at the leading edge.

The Kutta-Joukowsky flow about a lifting flat plate has the required behavior at the leading edge. It is described by the following analytic function:

$$w(z) = u - iv$$

$$= i\Gamma_f \left[1 - \sqrt{\frac{z-1}{z}}\right] \tag{7}$$

In particular, it gives a constant downwash $v = \Gamma_f$ on the chordline.

Further properties of this flow are listed in Appendix 1.

The chordwise distribution of vorticity for a flat plate due to the nose singularity becomes:

$$\gamma_f(x) = \Gamma_f \sqrt{\frac{1-x}{x}} \tag{8}$$

where $\tilde{\Gamma}_f = \sin\alpha$ for an isolated flat plate and is otherwise unknown for an arbitrary system (see Appendix B, page 38).

(b) The Trapezoidal Distribution of Vorticity

The logarithmic singularity occurring at flap deflection can also be handled in a similar fashion by finding the flow function due to a sharp break in the airfoil chordline. Ref. 17 has taken advantage of this approach.

In the present investigation, we found that the singularity could be adequately handled by assuming a trapezoidal distribution of vorticity between neighboring points:

$$\gamma(x) = \Gamma_i + (\Gamma_{i+1} - \Gamma_i) \cdot \frac{x}{\sigma_i} \tag{9}$$

Provided the step size σ_i is chosen small enough, the agreement in overall lift with thin airfoil theory has been found to be excellent. The pressure distribution is of course quite different in the neighborhood of the flap hinge, but then the sharp break in

camberline is not a realistic representation of the flap deflection anyway.

The field due to (9) can be calculated at any point using (2). The details of the calculation and properties of the field are listed in Appendix 1.

(c) Total Chordwise Distribution of Vorticity and Downwash

We may now superpose the contributions (8) and (9) to the vortex distribution which becomes:

$$\gamma(x_i \leq x \leq (x_i+\sigma_i)) = 2\Gamma_f \sqrt{\frac{1-x}{x}} + \Gamma_i + (\Gamma_{i+1}-\Gamma_i)\frac{x}{\sigma_i} \qquad (10)$$

where x is referred to the mean chordline of each airfoil. The resulting downwash distribution on the camberline is

$$v(x_i \leq x \leq (x_i+\sigma_i)) = \Gamma_f + \frac{1}{2\pi}\left[\Gamma_i \text{ Log } \left|\frac{x}{\sigma_i - x}\right| + (\Gamma_{i+1}-\Gamma_i)\left(-1 + \frac{x}{\sigma_i}\cdot \text{ Log } \left|\frac{x}{\sigma_i - x}\right|\right)\right] + v_{other} \qquad (11)$$

The Γ_f and [ ] terms represent the downwash induced by the ith element on itself, while v_{other} represents the field generated by all the other vortex elements in the lifting system (including those on its own airfoil).

The constant term Γ_f in the downwash corresponds to a thin airfoil approximation, but it should be emphasized that the downwash component is computed at the actual location of the boundary condition on the camberline, and in the local coordinate system defined by the slope of the element at that point. In contrast, thin airfoil theories handling the downwash distribution in terms of integrals

of the vortex distribution are of necessity limited to computing the downwash as if the boundary condition were imposed at the mean-chord. Regardless of whether the approximation is justified or not, the present numerical scheme obviates the need for making it in the first place.

Having the expression of the downwash as a function of the unknown vortex distributions, we may use boundary condition (3) and solve for the distributions. This is the subject of the next section.

(d) Endpoints and Control Points on the Airfoil System

Let n be the number of segments chosen to represent the camberline for the lower airfoil, and m for the upper one.

The set of unknowns representing the vorticity of the airfoil system is:

$$\vec{G} = [\Gamma_{fl}, \Gamma_2, \ldots, \Gamma_n, \Gamma_{fu}, \ldots, \Gamma_{n+m+1}] \qquad (12)$$

It contains the two leading edge singularity terms, Γ_{fl} and Γ_{fu}, and the trapezoidal terms.

We have omitted the trapezoidal terms at the leading edge of each airfoil. They may as well be taken to be zero, because the square root singularity dominates anyway. At the trailing edge, the vorticity is specified by the Kutta condition, so that $\Gamma_{n+1} = \Gamma_{n+m+2} = 0$, of course, in the unpowered case. In the powered case, the vorticity is specified otherwise; we will return to this point later.

Thus, the total number of unknown vortex intensities is the same as the total number of segments representing the system. We may select in particular the midpoints of these segments to compute the downwash, whence it takes the particularly simple form

$$v(x = \frac{\sigma}{2}) = \Gamma_f + \frac{\Gamma_i - \Gamma_{i+1}}{2\pi} + v_{other} \qquad (13)$$

We call these midpoints "control points".

We may now solve for the vortex distribution as a function of the slope of the camberline. Boundary condition (3) involves velocity components parallel and perpendicular to free-stream. Writing (13) for all (n+m) control points, and rotating to the proper coordinate system, we can write symbolically

$$u_x = U_{11}\Gamma_{f\ell} + U_{12}\Gamma_2 + \ldots + U_{1n}\Gamma_n + U_{1n+1}\Gamma_{fu} +$$

$$\ldots\ldots + U_{1n+m+1}\Gamma_{n+m+1} \equiv \underline{\underline{U}} \cdot \underline{G} \text{ for control point \#1,}$$

and similarly $u_y = \underline{\underline{V}} \cdot \underline{G}$ for all control points (14)

$\underline{\underline{U}}$ and $\underline{\underline{V}}$ are the induction functions by which given a vorticity distribution $\underline{G}$ the velocity can be calculated at any point. Conversely, given boundary condition (3) the vorticity distribution may be computed as follows:

Define $\underline{\underline{H}} = \underline{\underline{V}} - \underline{\underline{U}} \tan\alpha$

Then (3) must hold on all control points so that $\underline{\underline{H}} \cdot \underline{G} = [U_\infty \tan\alpha]$ which can be solved for $\underline{G}$:

$$\underline{G} = \underline{\underline{H}}^{-1} [U_\infty \tan\alpha] \quad \text{Solution to the unpowered problem} \qquad (15)$$

The matrix $\underline{\underline{H}}^{-1}$ is referred to as the matrix of influence coefficients and plays an essential role in the following parts.

3. Vortex Model of the Wake

(a) General

We have seen that the difficulty of the problem arises not only from the nonlinearity of boundary condition (5), but also in the fact that the location of that boundary condition is unknown.

To obviate this difficulty, a number of investigators (Refs. 8, 2) have successfully used an iteration technique yielding a progressively better satisfaction of boundary conditions (3) and (5).

The wake is modelled by trapezoidal segments, (similar to the previous section), the position of which varies during the iteration. It must, however, be truncated after a certain downstream position. This truncation must be compatible with the boundary condition at downstream infinity mentioned previously.

(b) Representation of the Flow Field at Downstream Infinity:

The numerical scheme we are proposing involves the calculation of the downwash at arbitrary points in the field. Thus, it is a matter of practical need that we choose a representation of the flow field at downstream infinity so as to get a smooth distribution of downwash even in the last wake endpoints.

We do know that the far wake must consist of two parallel vortex sheets of vorticity $\pm\gamma_\infty = 1 - \sqrt{1+C_H}$, which is found by

applying the jump condition at $p = p_\infty$, i.e., where $u_j = U_\infty + \frac{1}{2}\gamma_\infty$. The separation of these sheets is a priori unknown otherwise. The direction is known: the far wake vortex sheets must lie along the freestream direction.

The velocity field induced by two line vortices, starting at a downstream distance x_o and separated by a distance h_∞ can then be directly computed using (2).

$$2\pi u_x = \gamma_\infty \left[\mathrm{Tan}^{-1} \left(\frac{x_o - x}{y - h_\infty}\right) - \mathrm{Tan}^{-1} \left(\frac{x_o - x}{y + h_\infty}\right) \right] \tag{16}$$

$$2\pi v_y = \gamma_\infty \ \mathrm{Log} \left[\frac{(x_o - x)^2 + (y - h_\infty)^2}{(x_o - x)^2 - (y - h_\infty)^2} \right]^{\frac{1}{2}} \tag{17}$$

where h_∞ varies during the iteration. This far wake model was also used by Shollenberger.

4. Description of the Iteration Procedure:

(a) Updating the Airfoil Vorticity:

We can conveniently separate the field components due to the wake and due to the airfoil:

$$\begin{aligned} v_y &= v_y^{(a)} + v_y^{(w)} \\ u_x &= u_x^{(a)} + u_x^{(w)} \end{aligned} \tag{18}$$

then, we may rewrite boundary condition (3) as

$$v_y^{(a)} - u_x^{(a)} \tan\alpha(x) = U_\infty \tan\alpha(x) + u_x^{(w)} \tan\alpha(x) - v_y^{(w)} \tag{19}$$

The field at the control points is expressed as: $\underline{\underline{H}} \cdot \underline{G}$, where $\underline{G}$ is to be determined. Then, the amount of vorticity imbedded in the

airfoil required to satisfy the boundary condition in the presence of the wake-induced velocity components will be

$$\underline{G} = \underline{\underline{H}}^{-1} \cdot [U_\infty \tan\alpha + u_x^{(w)} \tan\alpha - v_y^{(w)}] \tag{20}$$

$\underline{\underline{H}}^{-1}$ is independent of the iteration and is calculated once and for all for $C_H = 0$.

(b) Updating the Wake

(i) Updating the Position. To find the slope of the vortex sheet at the control point, we observe that if indeed this slope were actually known, then it would be continuous across the vortex sheet, i.e.:

$$\frac{u_{x1}}{v_{y1}} = \frac{u_{xo}}{v_{yo}} = \tan\alpha(x) \tag{21}$$

(1 and 0 referring to the velocities inside and outside the wake).

So that since $1 + \dfrac{u_{x1}}{v_{y1}} = 1 + \dfrac{u_{xo}}{v_{yo}}$

and $$\tan\alpha(x) = \frac{u_{xo}+u_{x1}}{v_{yo}+v_{y1}} = \frac{u_{xo}}{v_{yo}} \tag{22}$$

Now, we want to use the jump condition across the vortex so we must transform to a system parallel to the vortex.

$$u_x = u \cos\alpha(x) - v \sin\alpha(x)$$

$$v_y = u \sin\alpha(x) + v \cos\alpha(x)$$

for u_o and u_1

where

$$u_o = u_{other} - \tfrac{1}{2}\gamma(x)$$

$$u_1 = u_{other} + \tfrac{1}{2}\gamma(x)$$

so that

$$u_o + u_1 = 2\,u_{other}$$

$$v = v_{other} + v_{s.i.}$$

$$\tan\alpha(x) = \frac{2\,u_{other}\sin\alpha + (v_{other}+v_{si})\cos\alpha}{2\,u_{other}\cos\alpha - (v_{other}+v_{si})\sin\alpha} \tag{23}$$

If the boundary condition is exactly satisfied, then $v_N = v_{other} + v_{si}$, which represents the total velocity normal to the vortex sheet, will be zero, so that (23) is satisfied identically.

If the boundary condition is not exactly satisfied, then $v_N \neq 0$ and a better estimate of the slope can be found by using (23) as:

$$\tan\alpha^{(new)} = \frac{2u_{other}^{(new)} \cdot \sin\alpha^{(old)} + (v_{other}^{(new)} + v_{si}^{(new)}) \cdot \cos\alpha^{(old)}}{2u_{other}^{(new)} \cos\alpha^{(old)} - (v_{other}^{(new)} + v_{si}^{(new)}) \cdot \sin\alpha^{(old)}} \tag{24}$$

Having executed that for all the control points in the wake, we can find the new wake position by direct integration:

$$y_w(x) = y_{TE} + \int_{x_{TE}}^{x} \tan\alpha(x')dx' \tag{25}$$

(ii) Updating the Vorticity: The updating of the vorticity at the control points is readily obtained by using boundary condition (5). The vorticity at the endpoints is then obtained by averaging the vorticity between neighboring endpoints. The exceptions to this rule

are:

(1) at the trailing edge of the airfoil, the vorticity is linearly extrapolated from the first wake control point. The continuity of vorticity at this point complies with the Kutta condition for regular blowing.

(2) the vorticity of the two last wake endpoints is set to $\pm\gamma_\infty$.

5. Computation of the Aerodynamic Coefficients

(a) Forces

Definitions:

We will call "lift" any force component perpendicular to the freestream direction, and "thrust" any component parallel but opposite to the freestream direction (i.e., thrust is measured by negative numbers and drag by positive numbers).

(i) The leading edge suction term can be found explicitly by integrating the flat plate vorticity term around a lip of finite radius and then letting the radius go to zero. The leading edge suction is then

$$C_s = -2\pi \tilde{\Gamma}_f^{\alpha 2} \qquad \text{for each airfoil} \tag{26}$$

and acts tangentially to the leading edge element.

This thrust, of course, does not produce any moment about the leading edge.

(ii) The Pressure Integral Across the Camberline. This is the only place where the actual location of the actuator disk enters, since the Bernoulli equation involves explicitly the head of the flow.

For convenience, we assume that the actuator disk is located at the trailing edge of the system, so that the fluid is assumed to be at atmospheric head H_o up to that point. This certainly does not affect the value of the total lift on the system, since it depends only on the total amount of vorticity shed by the actuator disk, but will affect the distribution of lift between the two airfoils and the load. However, to represent these realistically would require detailed knowledge of the mixing zone, unavailable at the present time. To find the pressure difference acting between x_i and x_{i+1} on the element of the camberline, we apply the Bernoulli equation on its upper and lower side.

$$p_L - p_\infty = \tfrac{1}{2}\rho U_\infty^2 - \tfrac{1}{2}\rho\left[u_{other}(x) - u'\right]^2$$

$$p_u - p_\infty = \tfrac{1}{2}\rho U_\infty^2 - \tfrac{1}{2}\rho\left[u_{other}(x) + u'\right]^2 \qquad (27)$$

where $u' = -\tfrac{1}{2}\gamma(x)$; thus the load is $\Delta p = \tfrac{1}{2}\rho(4\, u_{other} u')$. (28)

The elementary normal force acting on the element is:

$$N_{ti} = \int_{x_i}^{x_{i+1}} \Delta p \, dx$$

$$= +\rho \int_{x_i}^{x_{i+1}} u_{other}(x)\gamma(x)dx$$

$u_{other}(x)$ is the contribution of all the other vortices in the field, and does not vary much over segment i. It is most convenient to compute the velocity at the control point between x_i and x_{i+1}. Thus, normalizing as usual:

$$\tilde{N}_{ti} = + 2\tilde{U}\,(x_i + \frac{\sigma_i}{2}) \cdot \int_{x_i}^{x_{i+1}} \tilde{\gamma}(x)\,dx$$

This component contributes both to the overall thrust and lift of the system. It is more convenient to refer this component to the mean chord coordinates. Let ε_i = slope of the camberline in these coordinates. Then:

$$\tilde{N}_i = \cos \varepsilon_i \, \tilde{N}_{ti}$$

$$\tilde{T}_i = -\sin \varepsilon_i \, \tilde{N}_{ti} \qquad (29)$$

Using the representation of the vorticity (10), we can integrate the vorticity term

$$\int_{x_i}^{x_{i+1}} \tilde{\gamma}(x)dx = \tilde{\Gamma}_f [(\theta_{i+1}-\theta_i)+(\sin\theta_{i+1}-\sin\theta_i)]$$

$$+ \tfrac{1}{2}[\tilde{\Gamma}_{i+1} + \tilde{\Gamma}_i] \cdot \Delta x_i \qquad (30)$$

where $\theta = \text{Arc}\cos(\frac{2x}{c} - 1)$.

Including the leading edge suction term, (26), the total normal and tangential referred to the airfoil mean line become:

$$\tilde{N} = -2\pi\,\tilde{\Gamma}_f^2 \sin\beta + \sum_{i=1}^{n} \tilde{N}_i$$

$$\tilde{T} = -2\pi\,\tilde{\Gamma}_f^2 \cos\beta + \sum_{i=1}^{n} \tilde{T}_i \qquad (31)$$

(β is the slope of the camberline at the leading edge $\beta = \varepsilon_1$.)

To obtain the lift and thrust coefficients we rotate to the freestream coordinates:

$$C_L = \tilde{N} \cdot \cos(\alpha+\beta) - \tilde{T} \sin(\alpha+\beta)$$

$$C_T = \tilde{N} \cdot \sin(\alpha+\beta) + \tilde{T} \cos(\alpha+\beta) \qquad (32)$$

(iii) The Pressure Integral on the Actuator Disk. The forces due to the actuator disk (for the case of uniform loading) (referring to Fig. 8) are simply its normal thrust referred to the thrust and lift directions defined previously:

$$C_{L_A} = C_H \cdot h \cdot \sin(\alpha+\delta)$$

$$C_{T_A} = -C_H \cdot h \cdot \cos(\alpha+\delta) \qquad (33)$$

So that finally we obtain the total lift and thrust coefficient acting on the system:

$$C_{L_{tot}} = C_{L_1} + C_{L_2} + C_{L_A}$$

$$C_{T_{tot}} = C_{T_1} + C_{T_2} + C_{T_A} \qquad (34)$$

It is these coefficients characteristic of the total vorticity in the field (airfoil + wake) that are significant in the comparison with jet-flap theory.

(b) Moments

We refer all our moments to the leading edge of the main airfoil. In this definition the nose thrust of the main airfoil does not contribute to the moment of the system, but the nose thrust of the shroud does.

(i) Main Airfoil. Referring to Fig. 8, the contribution of the ith element to the moment about the nose is

$$\tilde{M}_i = \int_{x_i}^{x_{i+1}} x d\tilde{N}_i - \int_{y_i}^{y_{i+1}} y d\tilde{T}_i \tag{35}$$

where

$$d\tilde{N}_i = \cos\varepsilon_i \cdot d\tilde{N}_{ti}$$

$$d\tilde{T}_i = -\sin\varepsilon_i \, d\tilde{N}_{ti} \tag{36}$$

and y is related to x by the local slope of the camberline: $y(x) = x\tan\varepsilon_i + y_i - x_i \tan\varepsilon_i$. Making the same approximation as in (a) concerning the velocity, we get, after some manipulation:

$$\tilde{M}^{(i)} = +2\tilde{U}(x_i + \tfrac{i}{2}) \cdot [\cos\varepsilon_i + \sin\varepsilon_i \tan\varepsilon_i] \cdot \int_{x_i}^{x_{i+1}} x\tilde{\gamma}(x)dx$$

$$- (y_i - x_i \tan\varepsilon_i)\, \tilde{T}^{(i)} \tag{37}$$

Writing the vorticity integral explicitly:

$$\int_{x_i}^{x_{i+1}} x\tilde{\gamma}(x)dx = \tfrac{1}{4}\tilde{\Gamma}_f[\theta_{i+1} - \theta_i - \tfrac{1}{2}(\sin 2\theta_{i+1} - \sin 2\theta_i)] +$$

$$+ \tfrac{1}{2}\tilde{\Gamma}_i (x_{i+1}^2 - x_i^2) + \frac{\tilde{\Gamma}_{i+1} - \tilde{\Gamma}_i}{x_{i+1} - x_i}\left[\tfrac{1}{3}x_{i+1}^3 + \tfrac{1}{6}x_i^3 - \tfrac{1}{2}x_i x_{i+1}\right] \tag{38}$$

The total moment acting about the nose due to the lower airfoil becomes:

$$C_{M_l} = \sum_{i=1}^{n} \tilde{M}^{(i)} \tag{39}$$

(ii) Moment Due to the Shroud

Moment due to the normal force on the shroud. We assume that the maximum camber of the shroud airfoil is small enough so that we may neglect the local slope in computing the moment about the leading edge of the shroud, i.e. (referring to Fig. 8)

$$M_1 = \int_{x_1}^{x_2} x' \cdot \left(\frac{dN}{dx'}\right) dx' \tag{40}$$

and then the moment transferred to the leading edge of the main airfoil becomes:

$$M_o = \int_{x_1}^{x_2} x dF_y - \int_{y_1}^{y_2} y dF_x \tag{41}$$

using

$$\tan\varepsilon_M = \frac{y_2 - y_1}{x_2 - x} \tag{42}$$

$$\begin{aligned} dF_y &= dN \cos\varepsilon_M \\ dF_x &= -dN \sin\varepsilon_M \end{aligned} \tag{43}$$

we finally get:

$$C_{M_2} = M_o(N) = M_1(N) + [x_1 \cdot \cos\varepsilon_M + y_1 \cdot \sin\varepsilon_M] \cdot |\tilde{N}| \tag{44}$$

where (x_1, y_1) is the position of the nose of the shroud in the main airfoil coordinates.

We must add to this the moment due to the leading edge suction, which is readily found to be

$$M_o(s_{LE}) = 2\pi\tilde{\Gamma}_f^2 \ [y_1 \cos\varepsilon_M - x_1 \sin\varepsilon_M] \tag{45}$$

(iii) Moment Due to Actuator. Referring to Fig. 8, the contribution to the moment due to the actuator is found to be independent of the position of the actuator and

$$C_{M_{act}} = C_H \, h.d \tag{46}$$

where d is the lever arm of the actuator. The total moment can be found by simply adding the various contributions:

$$C_{M_{tot}} = C_{M_1} + C_{M_2} + M_o(S_{le}) + C_{M_{act}} \tag{47}$$

6. Performance of Numerical Scheme

The numerical calculations were performed on the IBM/System 370 available at the CIT Computing Center.

45 segments were chosen to represent the camberline of the test configuration. The total computing time for the unpowered configuration, including the inversion of the influence coefficients matrix, was about 20 seconds.

The step size of the segments selected to represent the wake must be smaller than or equal to the exit height of the ejector, $\frac{h}{c}$. For a fixed downstream wake cutoff distance, low $\frac{h}{c}$ ratios translate into a larger number of segments to insure convergence, resulting in an increase of the required computing time. Thus, for a $\frac{h}{c} = 15\%$ and wake cutoff at 5 chords downstream, 50 segments were used.

The number of iterations required for a given accuracy in the aerodynamic coefficients appear to be directly proportional to C_H, and sensitive to a lesser degree to an increase in the angle of

attack and/or flap deflection.

For the case of high C_H and low $\frac{h}{c}$, the total amount of computing time for a complete set of iterations is about 2 minutes.

III. COMPARISON WITH JET-FLAP THEORY

In a well-known paper (Ref. 6), Spence developed a linearized theory for the two-dimensional potential flow about a single element jet-flap airfoil and computed the lift increment due to blowing in the form of lift derivatives tabulated versus the jet momentum coefficient of the primary C_μ. In the previous section, we proposed a numerical scheme to compute the lift coefficient on a multi-element airfoil, given the head change C_H. The purpose of this section is to establish a technique for the comparison between the lift increments obtained by the two different methods.

1. General Characteristics of the Computed Lift Curves

For a constant flap deflection, the functional dependence of the lift coefficient can be written as:

$$C_L = C_L(\alpha, C_H) \tag{48}$$

so that

$$C_L = C_L(\alpha = 0°, C_H=0) + \frac{\partial C_L}{\partial \alpha}\Big|_{C_H} \cdot \alpha + \frac{\partial C_L}{\partial C_H}\Big|_{\alpha} \cdot C_H \tag{49}$$

(neglecting cross-terms)

We may regroup

$$C_L(\alpha = 0°, C_H) = C_L(\alpha = 0°, C_H = 0) + \frac{\partial C_L}{\partial C_H} \cdot C_H \tag{50}$$

so that the lift increment due to angle of attack only becomes

$$\Delta C_L = \frac{\partial C_L}{\partial \alpha}\Big|_{C_H} \alpha$$

$$= C_L - C_L(\alpha = 0°, C_H) \tag{51}$$

40

The presence of a finite lift at zero angle of attack in the powered case results from the asymmetry in the lifting surfaces. In the early part of the work, some difficulty was encountered in the interpretation of the lift curves, because a finite lift at $\alpha = 0°$ results in lift derivatives (as computed directly from (48)) becoming infinite at that angle, thus precluding any meaningful comparison with Spence's theory.

Dr. H. J. Stewart recognized the similarity of this behavior with that of a wing equipped with suction-type boundary-layer control, of which he previously made the theory for a single element airfoil (Ref. 18). This theory will be repeated below, and affords a direct interpretation of the lift curves at $\alpha = 0°$.

Having established that, it will then be shown that the lift increment due to angle of attack only can be directly related to Spence's increment, having suitably related the head change C_H to the total momentum flowing in the wake.

2. Effect of a Sink on a Single-element Airfoil

The suction effect of a boundary layer control device can be represented by a sink on the upper side of the airfoil. (Fig. 10) The analysis of this effect was done in Ref. 18 and is repeated here, as it provides the theoretical background necessary to interpret the presence in our configuration of finite lift at $\alpha = 0°$. In the transformed plane, the combination of sources and sinks necessary to maintain the circle a streamline is also shown in Fig. 10. Let θ be the angle between the direction of the sinks and the rear stagnation point. Let the distance between the sinks go to zero. Then, the

horizontal velocity component generated by the sink of strength -2Q is cancelled by the velocity due to the source +Q at the origin. The net vertical velocity component is given by:

$$v_y = \frac{2Q}{2\pi(2R \sin\frac{\theta}{2})} \cos(\frac{\theta}{2}) \tag{52}$$

$$= \frac{Q}{2\pi R} \cot(\frac{\theta}{2}) \tag{53}$$

Thus, to maintain the stagnation point at the trailing edge, an extra amount $\Delta\Gamma_{ind}$ of vorticity at the center of the circle is necessary, directed counter-clockwise so that its induced velocity component exactly cancels (53):

$$\frac{\Delta\Gamma_{ind}}{2\pi R} = \frac{Q}{2\pi R} \cdot \cot(\frac{\theta}{2}) \Rightarrow \Delta\Gamma_{ind} = Q \cot(\frac{\theta}{2}) \tag{54}$$

The resulting lift increment is $\rho U_\infty \Delta\Gamma_{ind}$. The total lift becomes:

$$L = \pi\rho U_\infty^2 c\sin\alpha + \rho U_\infty \cdot Q \cot(\frac{\theta}{2}) \tag{55}$$

and in particular is nonzero as $\alpha = 0^\circ$.

3. Comparison with the Computed Lift Curves at $\alpha = 0^\circ$: the Actuator as a Sink

To relate this to our configuration, we must first estimate Q as a function of C_H. The strength of the sink is the difference in mass flux between the power-on and power-off configuration, which can be estimated as:

$$-Q = hU_\infty - hu_j$$

$$= hU_\infty \left[1 - (1 + C_H)^{\frac{1}{2}}\right] \tag{56}$$

Also, we recognize that the $\cot(\frac{\theta}{2})$ factor is valid only for a single element airfoil. For a multiple element airfoil, we expect that the factor should be somewhat different. In particular, if the two chords are equal, then the symmetry of the problem dictates that there can be no lift at $\alpha = 0^\circ$. Thus, the estimate of the lift increment becomes:

$$\Delta C_{L_{ind}} = 2k(\frac{c_u}{c}, \frac{h}{c}) \left[(1 + C_H)^{\frac{1}{2}} - 1\right] \tag{57}$$

where the factor $k(\frac{c_u}{c}, \frac{h}{c})$ must be determined for the particular geometry considered.

The lift slope computed numerically in Fig. 11 corresponds to a system having a chord ratio $\frac{c_u}{c} = 40\%$ and an ejector height $\frac{h}{c} = 15\%$. The numerical value of coefficient k was determined by a best fit of the curves $C_L(\alpha = 0^\circ, C_H)$ and $\Delta C_{L_{ind}}$, which was obtained for $k = .1625$. The agreement between the two curves validates the interpretation proposed for the mechanism of generation of lift at $\alpha = 0^\circ$.

4. Comparison of the Lift Increments Due to Angle of Attack with Spence's Theory

The lift increment due to angle of attack computed numerically by Spence in Ref. 6 can be approximated by

$$\Delta C_{L_{JF}} = 2\pi\left[1 + .151\ C_J^{\frac{1}{2}} + .219\ C_J\right]\alpha \qquad (58)$$

(no lift at $\alpha = 0°$)

where C_J is the momentum flowing in the powered wake. For a jet flap, this is just equal to the momentum of the primary $C_J = C_\mu$, as this model neglects any entrainment in that region. To relate $\Delta C_{L_{JF}}$ to the lift increments computed in our configuration, we must relate C_J to C_H.

a. Relation Between Head Change and Momentum Coefficient

Referring to Fig. 2, the total momentum flow in the far wake is:

$$M = p\ u_j^2\ h_\infty$$

where u_j is related to the head change by

$$p_\infty + \tfrac{1}{2}\rho U_\infty^2 + \Delta H = p_\infty + \tfrac{1}{2}\rho u_j^2$$

so that

$$\rho u_j^2 = \rho U_\infty^2 + 2\Delta H$$

and

$$M = h_\infty\left[\rho U_\infty^2 + 2\Delta H\right] \qquad (59)$$

For the type of geometries representative of an ejector-powered jet-flap, the exit height to chord ratio $\frac{h_s}{c}$ will be of the order of 10%. Under these conditions, the results of the numerical

scheme proposed in Section II show no appreciable slipstream contraction, i.e., $\frac{h_s}{h_\infty} \approx 1$. This allows us to neglect the pressure integral on the wake and identify (59) with the total momentum flow at the exit of the ejector:

$$M_s = h_s \left[\rho U_\infty^2 + 2\Delta H\right]$$

so that the jet coefficient that will be used in the comparison with Spence's theory will be

$$\begin{aligned} C_J &= \frac{M_s}{\frac{1}{2}\rho U_\infty^2 c} \\ &= 2\,\frac{h_s}{c} + 2 \cdot \frac{\Delta H}{\frac{1}{2}\rho U_\infty^2}\,\frac{h_s}{c} \\ &= 2\,\frac{h_s}{c}\left[1 + C_H\right] \end{aligned} \tag{60}$$

To relate C_J to the conventional primary jet momentum C_μ, we note that C_H is the force, i.e., change in momentum, exerted per unit height by the actuator disk on the pumped fluid, so that

$$C_\mu = \frac{h_s}{c} C_H \tag{61}$$

and

$$C_J = 2\,\frac{h_s}{c} + 2\,C_\mu \tag{62}$$

A further implication of this choice is clear when we consider the ejector at zero forward speed $U_\infty = 0$

so that (51) $\Rightarrow M_J = 2M_\mu$

and

$$\frac{M_J}{M_\mu} = 2$$

45

This ideal augmentation coefficient can be achieved only by an ideal mixing device (Ref. 21).

b. Comparison of the Lift Increments

We are now in a position to compare the lift increments due to angle of attack computed by the two methods. This has been done in Figures 11 and 12 by comparing the lift curve obtained numerically and the curve $C_L = C_L(\alpha = 0°, C_H) + \Delta C_{L_{JF}}$, where $C_L(\alpha = 0°, C_H)$ is also computed numerically, for the following configurations (the geometries are in Fig. 2-A):

Fig. 11. System of unflapped flat-plate airfoils, with height $\frac{h}{c} = 15\%$ and chord ratio $\frac{c_u}{c} = 40\%$

Fig. 12. System of flapped cambered sections corresponding to a configuration tested in the 10-foot tunnel at GALCIT and described in Ref. 34.

It is seen that for these widely different configurations the lift increments computed by both methods agree quite well. In addition, the distribution of lift between the two airfoils has been plotted in Figs. 15 and 16 for an actuator disk effectively located at the trailing edge of the system. Both lift slopes are negative, indicating the presence of the upper airfoil stagnation point on its upper surface. This again illustrates the sink effect of the actuator on the lifting surfaces.

5. Comparison of the Moment Curves

A similar comparison was made for the moment curves of the same configurations as above, the moment increment being also obtained from Ref. 6.

For the flat-plate system (Fig. 13), the curves have different slopes and cross for a value of C_H high enough.

For the cambered system (Fig. 14), the magnitude of the moment increment as well as the slopes agree with the moment increment computed from Ref. 6.

To the extent of this comparison, this indicates that the moment increment is sensitive to the particular geometry considered and cannot in general be reliably computed from the jet flap increment.

6. Conclusions

The method of superposition that has been just discussed allows a simple interpretation of the lift curves computed numerically in terms of analytical results for single-airfoil configurations. While it does not remove the need to compute numerically the lift at $\alpha = 0°$, it lends to the numerical solution a flexibility that is inherently lacking in this type of approach.

APPENDIX

A. The Trapezoidal Vorticity

1. Expression for the Flow Field

Let σ_i be the mesh size $\sigma_i = x_{i+1} - x_i$.

The trapezoidal vorticity is a linear distribution of vorticity between x_i and x_{i+1}.

$$\gamma(x) = \Gamma_i + (\Gamma_{i+1}-\Gamma_i) \cdot \frac{x}{\sigma_i} \tag{1-1}$$

We want to compute the induced velocity using the Biot Savart law:

$$dur = \frac{\gamma(x)dx}{2\pi r} \tag{1-2}$$

$$2\pi u_x = \int_o^\sigma \frac{-\gamma(x)\cdot y}{r^2}\, dx \tag{1-3}$$

$$2\pi u_y = \int_o^\sigma \frac{x'-x}{r^2}\, \gamma(x)dx \tag{1-4}$$

Carrying out the integration:

$$2\pi u_x = \Gamma_i \cdot \left[\mathrm{Tan}^{-1}\left(\frac{x-\sigma_i}{y}\right)-\mathrm{Tan}^{-1}\left(\frac{x}{y}\right)\right] +$$

$$+(\Gamma_{i+1}-\Gamma_i)\cdot\left\{\frac{y}{\sigma_i}\,\mathrm{Log}\left[\frac{x^2+y^2}{(\sigma_i-x)^2+y^2}\right]^{\frac{1}{2}} + \frac{x}{\sigma_i}\left[\mathrm{Tan}^{-1}\left(\frac{x-\sigma_i}{y}\right)-\mathrm{Tan}^{-1}\left(\frac{x}{y}\right)\right]\right. \tag{1-5}$$

$$2\pi u_y = \Gamma_i\,\mathrm{Log}\left[\frac{x^2+y^2}{(\sigma_i-x)^2+y^2}\right]^{\frac{1}{2}} +$$

$$+(\Gamma_{i+1}-\Gamma_i)\cdot\left\{-1+\frac{x}{\sigma_i}\,\mathrm{Log}\left[\frac{x^2+y^2}{(\sigma_i-x)^2+y^2}\right]^{\frac{1}{2}} - \frac{y}{\sigma_i}\left[\mathrm{Tan}^{-1}\left(\frac{x-\sigma_i}{y}\right)-\mathrm{Tan}^{-1}\left(\frac{x}{y}\right)\right]\right\} \tag{1-6}$$

2. Limit Forms of (1-5) and (1-6) as $y \to \pm 0$

(i) $x<0$ or $x > \sigma$ $\quad \mathrm{Tan}^{-1}\left(\frac{x-\sigma_i}{y}\right) - \mathrm{Tan}^{-1}\left(\frac{x}{y}\right) \to \pm\frac{\pi}{2} - \left(\pm\frac{\pi}{2}\right) = 0$ (1-7)

$$\therefore\ 2\pi u_x = 0$$

$$2\pi u_y = \Gamma_i \mathrm{Log}\left|\frac{x}{\sigma_i - x}\right| + (\Gamma_{i+1} - \Gamma_i)\left\{-1 + \frac{x}{\sigma_i}\mathrm{Log}\left|\frac{x}{\sigma_i - x}\right|\right\}$$

Same holds for $x > \sigma_i$

(ii) $0 < x < \sigma_i$

$$\mathrm{Tan}^{-1}\left(\frac{x}{y}\right) - \mathrm{Tan}^{-1}\left(\frac{x-\sigma_i}{y}\right) \to \pm\frac{\pi}{2} + \left(\pm\frac{\pi}{2}\right) = \pm\pi$$

So that $u_x(0< x < \sigma_i,\ y = \pm 0) = \pm\frac{1}{2}\gamma(x)$ (1-8)

(iii) Expression for the downwash

In computing the downwash, we require $u_x = 0$ so that

$$2\pi u_y = \Gamma_i \mathrm{Log}\left|\frac{x}{\sigma_i - x}\right| + (\Gamma_{i+1} - \Gamma_i)\cdot\left[-1 + \frac{x}{\sigma_i}\mathrm{Log}\left|\frac{x}{\sigma_i - x}\right|\right]$$

and in particular (1-9) evaluated at the midpoint yields:

$$u_y\left(x' = \frac{\sigma}{2},\ y' = 0\right) = -\frac{1}{2\pi}(\Gamma_{i+1} - \Gamma_i) \qquad (1\text{-}10)$$

3. Comment

It should not be concluded that the field at the end of these segments $x = \sigma$ is inherently singular, since the downwash is computed as $v = v_{si} + v_{other}$ although, should one need the downwash at that particular point to interface with a complete integral model of the turbulent flow outside the ejector additional numerical sophistication would be needed.

B. Field of the Leading Edge Singularity

The Kutta-Joukowsky flow about a lifting flat plate is represented by

$$w(z) = u - iv$$

$$= i\,\tilde{\Gamma}_f \left[1 - \sqrt{\frac{z-1}{z}}\right] \tag{1-11}$$

where $\tilde{\Gamma}_f =$ sinα for an isolated flat plate.

Using the angles in Fig. 5, this can be decomposed into real and imaginary parts

$$R^2 = (1-x)^2 + y^2$$

$$r^2 = x^2 + y^2 \tag{1-12}$$

Then

$$u = \tilde{\Gamma}_f \cdot \left[\frac{R^{\frac{1}{2}}}{r^{\frac{1}{2}}} \sin\gamma\right] \tag{1-13}$$

$y \geq 0$

$$v = \tilde{\Gamma}_f \left[1 - \frac{R^{\frac{1}{2}}}{r^{\frac{1}{2}}} \cos\gamma\right] \tag{1-14}$$

where $\gamma = \dfrac{\theta_2 - \theta_1}{2}$

The downwash on the chordline $y = 0$, $0 \leq x \leq 1$, is constant : $v = \tilde{\Gamma}_f$.

Outside this interval, on the line through the two branch points, we have

$$v = \tilde{\Gamma}_f \cdot \left[1 - \sqrt{\frac{x-1}{x}}\right], \quad x < 0 \quad \text{and} \quad x \geq 1$$

50

In addition, the vorticity distribution can be deduced from (11) and is,

$$\gamma_f(0 \leq x \leq 1) = 2\Gamma_f \cdot \sqrt{\frac{1-x}{x}} \qquad (1\text{-}15)$$

with the square root singularity at the leading edge.

The complex function (1-11) represents the leading edge singularity for any thin airfoil as well as for a flat plate, provided the branch cut is moved to coincide with the camberline. In the particular scheme we used for the numerical solution, the branch cut was not moved, so that the contribution of the leading edge singularity to the total downwash on its own airfoil, given in equation (11), is just $\tilde{\Gamma}_f$, and the vorticity is (1-15). These two results are linearized approximations. The nonlinear results could have been incorporated at a slight increase in the complexity of the calculation. A consistency check was made by computing the velocity components directly from the computed vorticity distribution equation (15), and they satisfied the imposed boundary condition within three significant digits. Thus, in this particular example, this approximation was well justified.

REFERENCES

1. Herold, Alan C., A Two-dimensional, Iterative Solution for the Jet Flap, NASA CR-2190.
2. Chaplin, H. R., A Method for the Numerical Calculation of Slipstream Contraction of a Shrouded Impulse Disk in the Static Case, DTMB Rept. 1857, June 1964.
3. Greenberg, Michael D., Powers, Stephen R., Non-Linear Actuator Disk Theory and Flow Field Calculations, Including Non Uniform Loading, NASA CR-1672.
4. von Karman, Th., Burgers, J. M., Aerodynamic Theory, Durand, ed., Vol. II, Perfect Fluids, Section 10.
5. Spence, D. A., The Lift Coefficient of a Thin, Jet Flapped Wing, Proc. Royal Soc. A 238, 1956.
6. Spence, D. A., Some Simple Results for 2-D Jet Flap Aerofoils., Aero Quarterly, Nov. 1958.
7. Wygnanski, I., Newman, B. G., The Effect of Jet Entrainment on Lift and Moment for a Thin Airfoil with Blowing, Aero Quarterly, May 1964.
8. Shollenberger, Carl A., An Investigation of a 2-D Propulsive System, Calif. Inst. of Technology, Ph. D. Thesis, 1971.
9. Weissinger, Johannes, Maas, Dieter, Theory of the Ducted Propeller - A Review. Article in 7th Symposium on Naval Hydrodynamics, Aug. 25-30, 1968.
10. Yen, K. T., On the Thrust Hypothesis for the Jet Flap, Including Jet-Mixing Effects, Journal of the Aerospace Sciences, Aug. 1960.

REFERENCES (Cont'd)

11. Stratford, B. S., Early Thoughts on the Jet Flap, Aero Quarterly 7, 1956.

12. Levinsky, E. S., et al., Lifting Theory for V/STOL Aircraft in Transition and Cruise I., J. of Aircraft, Vol. 6, No. 6.

13. Spence, D. A., The Lift Coefficient of a Thin Jet-Flapped Wing. II. A Solution of the Integro-differential Equation for the Slope of the Jet., Proc. Roy. Soc., Series A 261.

14. Stratford, B. S., Mixing and the Jet Flap, Aero Quarterly, Vol. VII, May 1956.

15. Stratford, B. S., A Further Discussion on the Mixing and the Jet Flap,

16. Lissaman, P. B. S., A Linear Solution for the Jet Flap in Ground Effect, Ph. D. Thesis, Calif. Inst. of Technology, 1965.

17. Lopez, M. L., Shen, C. C., Recent Developments in Jet Flap Theory and Its Application to STOL Aerodynamic Analysis, AIAA Paper 71-578.

18. Stewart, H. J., Private Communication.

19. Quinn, Brian, A Wind Tunnel Investigation of the Forces Acting on an Ejector in Flight, ARL Rept. 70-0141.

20. Fancher, R. B., Why Ejectors for Aircraft Propulsion-Lift Systems and Where We Stand, ARL Rept. 71-0140.

21. von Karman, T., Theoretical Remarks on Thrust Augmentation. Reissner Anniversary Volume, J. W. Edwards, 1949.

REFERENCES (Cont'd)

22. Steady Flow Ejector Research Program. Final Report Contract Nonr-3067(00), Dec. 1960.

23. Curtet, Roger, Thèse, Faculté des Sciences de l'Université de Grenoble, Nov. 1958, Publ. Sc. and Tech au Min de l'Air, No. 106.

24. Rose, James R., Ph. D. Thesis, Calif. Inst. of Technology, An Analysis of the 2-D, Incompressible Jet Ejector, 1969.

25. Hill, P. G., Turbulent Jets in Ducted Streams, JFM 22, 1965.

26. Koenig, David G., Corsiglia, Victor R., Aerodynamic Characteristics of a Large Scale Model with an Unswept Wing and Augmented Jet Flap, NASA TN D-4610, 1968.

27. Cook, A. M., Aiken, T. N., Low Speed Aerodynamic Characteristics of a Large Scale STOL Transport Model with an Augmented Jet Flap, NASA TM X62017, 1971.

28. Flight International, Boeing's AMST Proposal, 8 Feb. 1973, p. 210.

29. Perry, D. H., A Review of Some Published Data on the External-Flow Jet-Augmented Flap, Aeronautical Research Council Current Papers, CP No. 1194, London, 1972.

30. Lachmann, G. V., ed., Boundary Layer and Flow Control, Vol. I, Pergamon Press, London, 1961.

31. McCormack, Barnes W., Jr., Aerodynamics of V/STOL Flight, Academic Press, New York, 1967.

32. Harris, G. L. and Lissaman, P. B. S., The Mechanics of Ejector Thrust Augmentation, CIT Ae TR 67-1, 1967.

REFERENCES (Cont'd)

33. Newman, B. G., The Prediction of Turbulent Jets and Wall Jets, Canadian Aeronautics and Space Journal, October 1969.

34. GALCIT Report 926 (to be published).

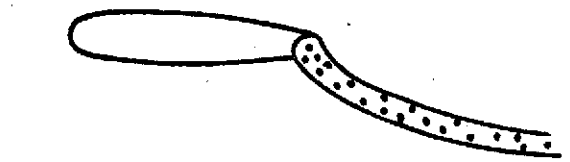

Conventional Jet Flap

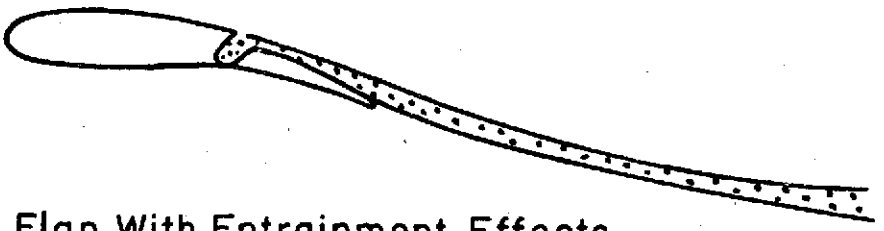

Jet Flap With Entrainment Effects

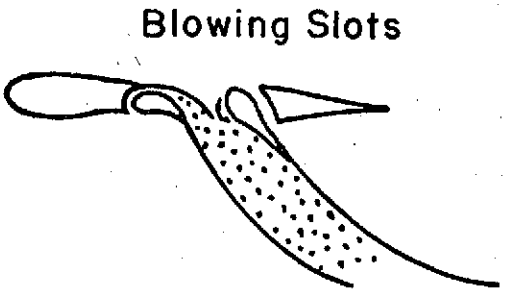

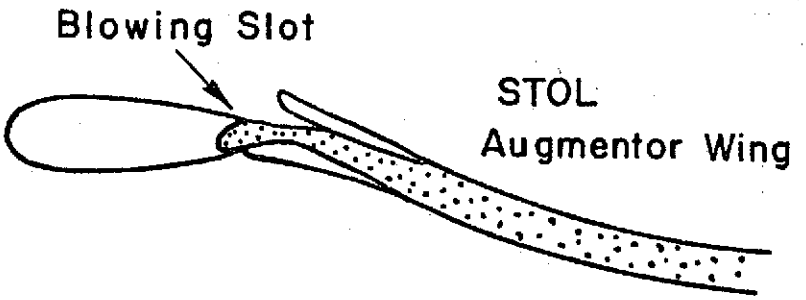

(Ejector Powered
Jet Flap)

FIG. I POWERED LIFTING SYSTEMS

56

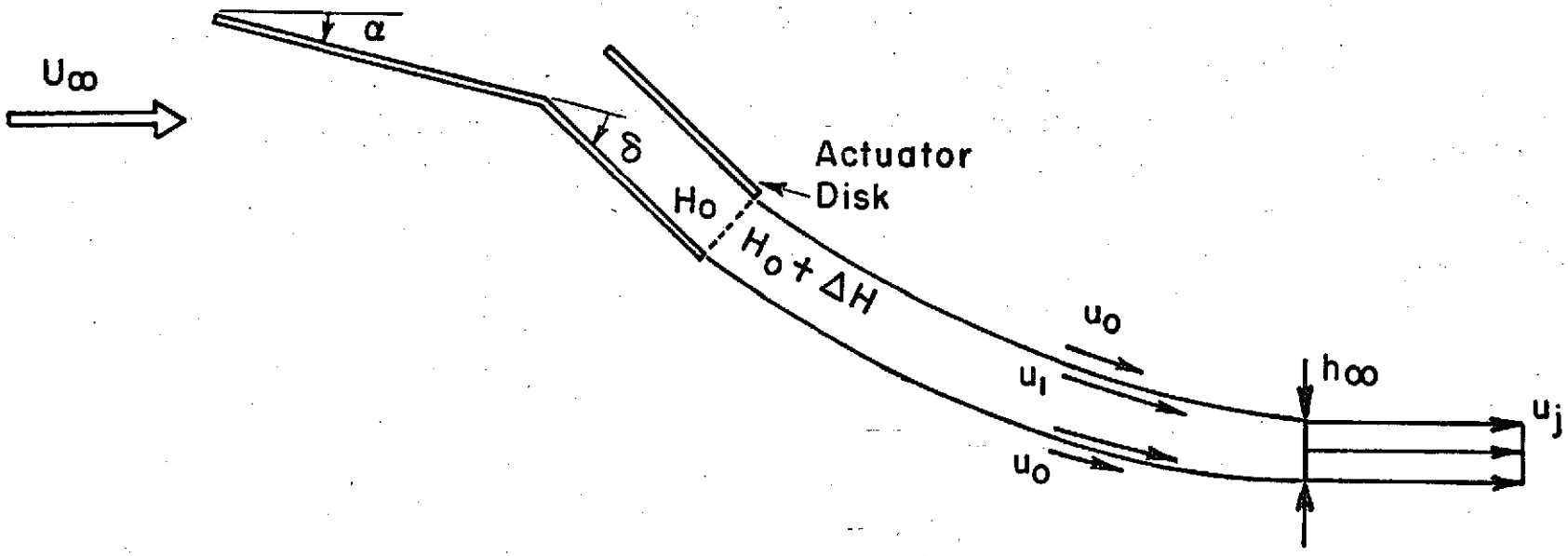

FIG. 2 POTENTIAL FLOW PROBLEM: BASIC GEOMETRY

57

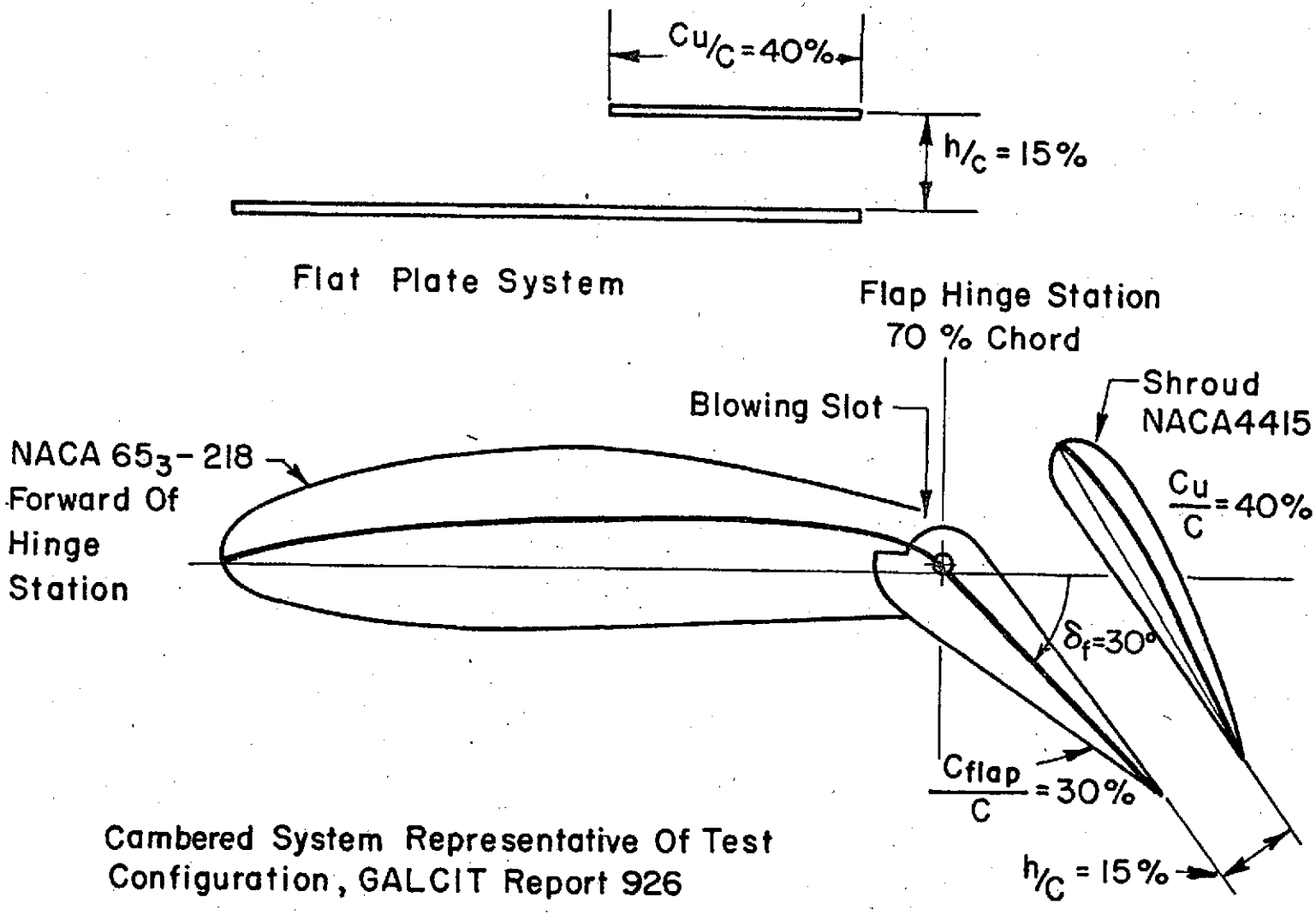

FIG. 2-a SPECIFIC GEOMETRIES USED IN SECTION III

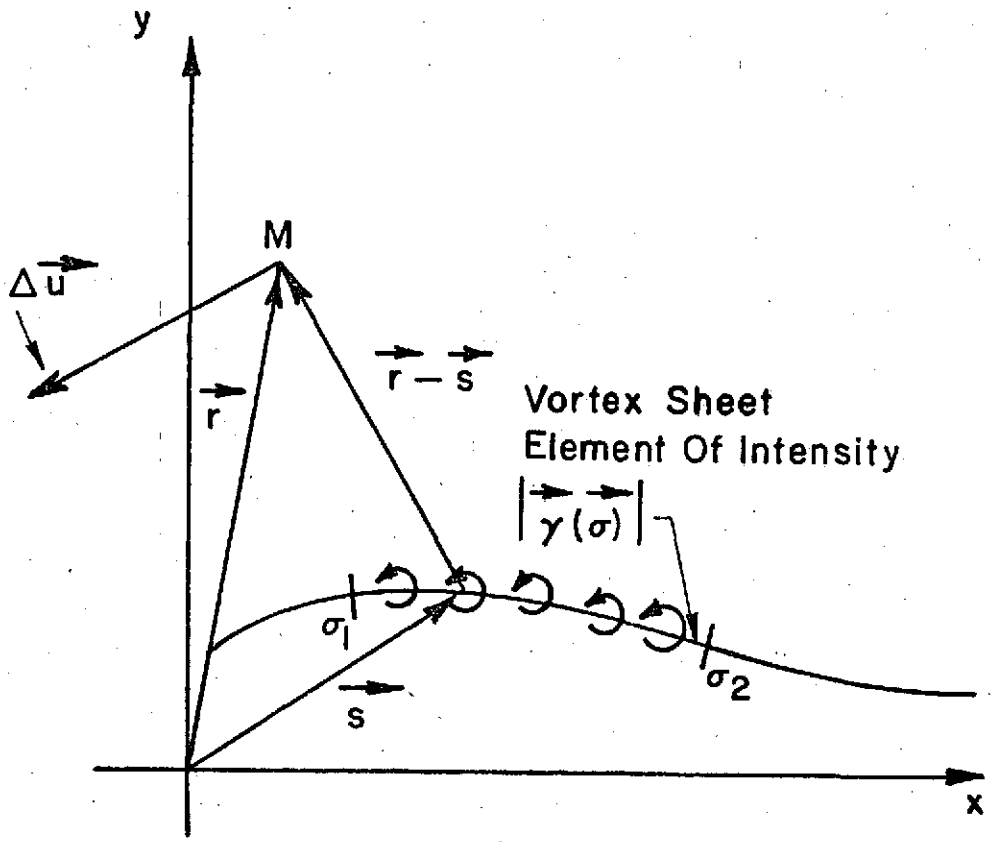

FIG. 3 POISSON SOLUTION TO $\nabla^2 \underline{u} = 0$

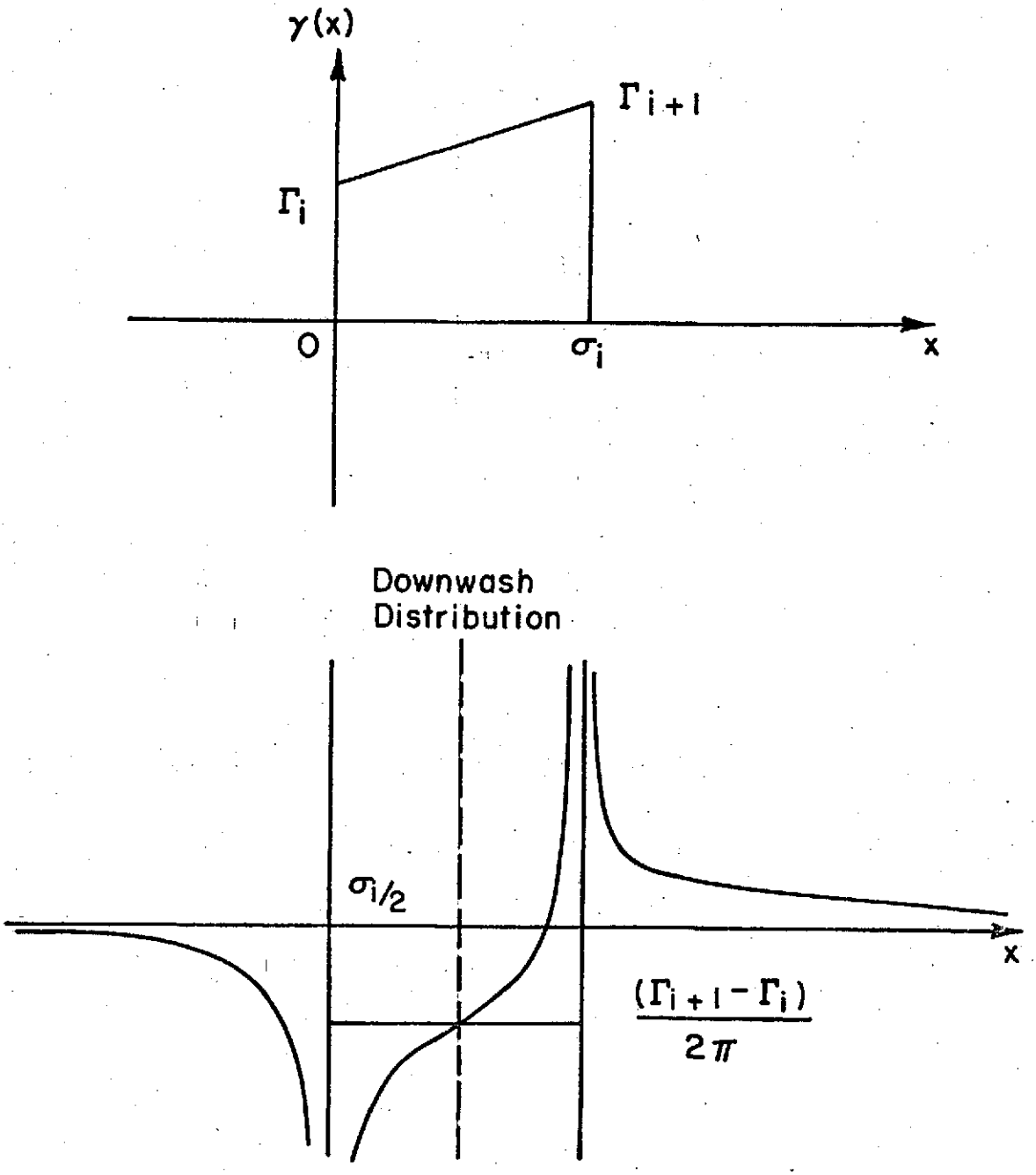

FIG. 4 DOWNWASH OF THE TRAPEZOIDAL VORTICITY

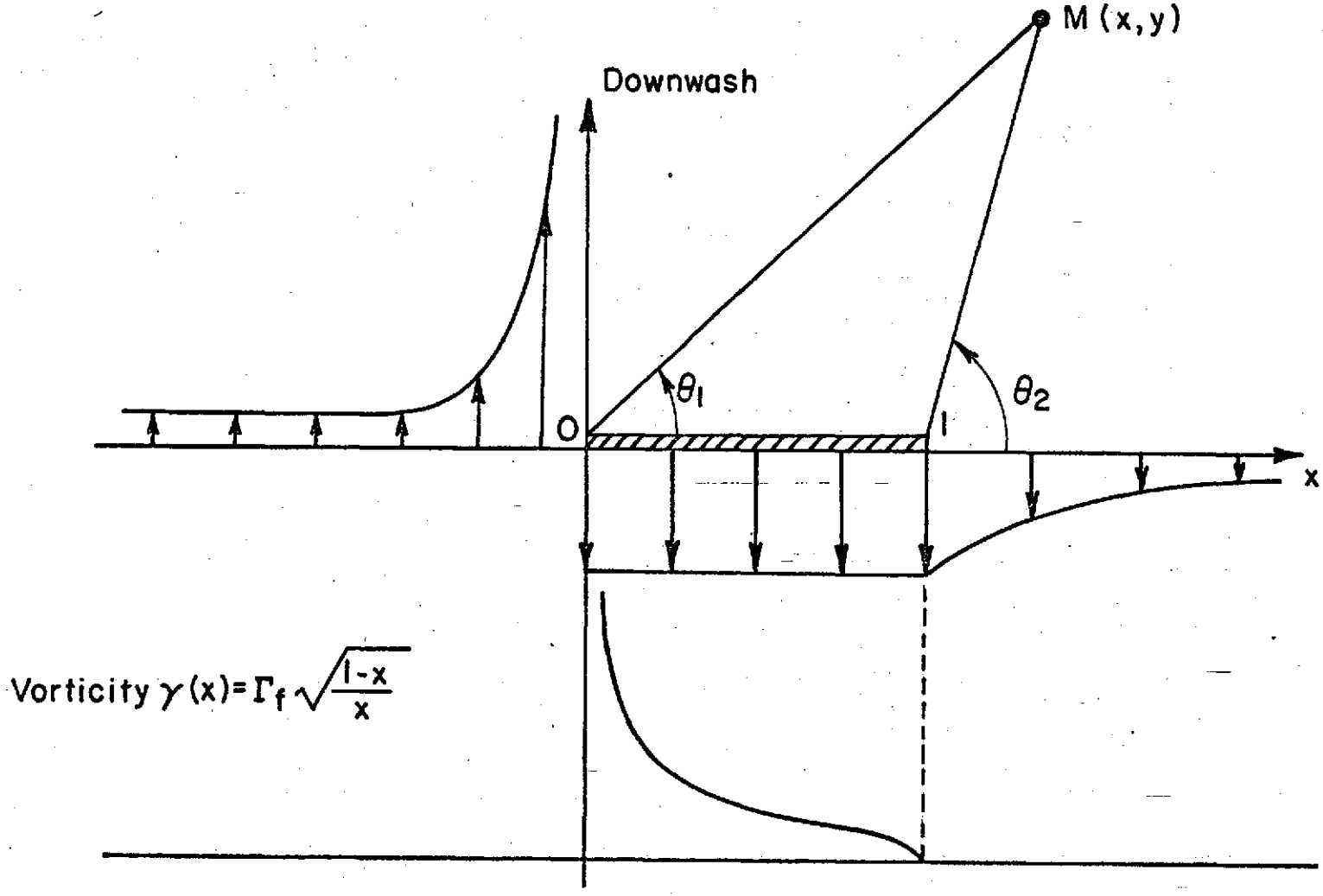

FIG. 5 DOWNWASH FIELD OF NOSE SINGULARITY

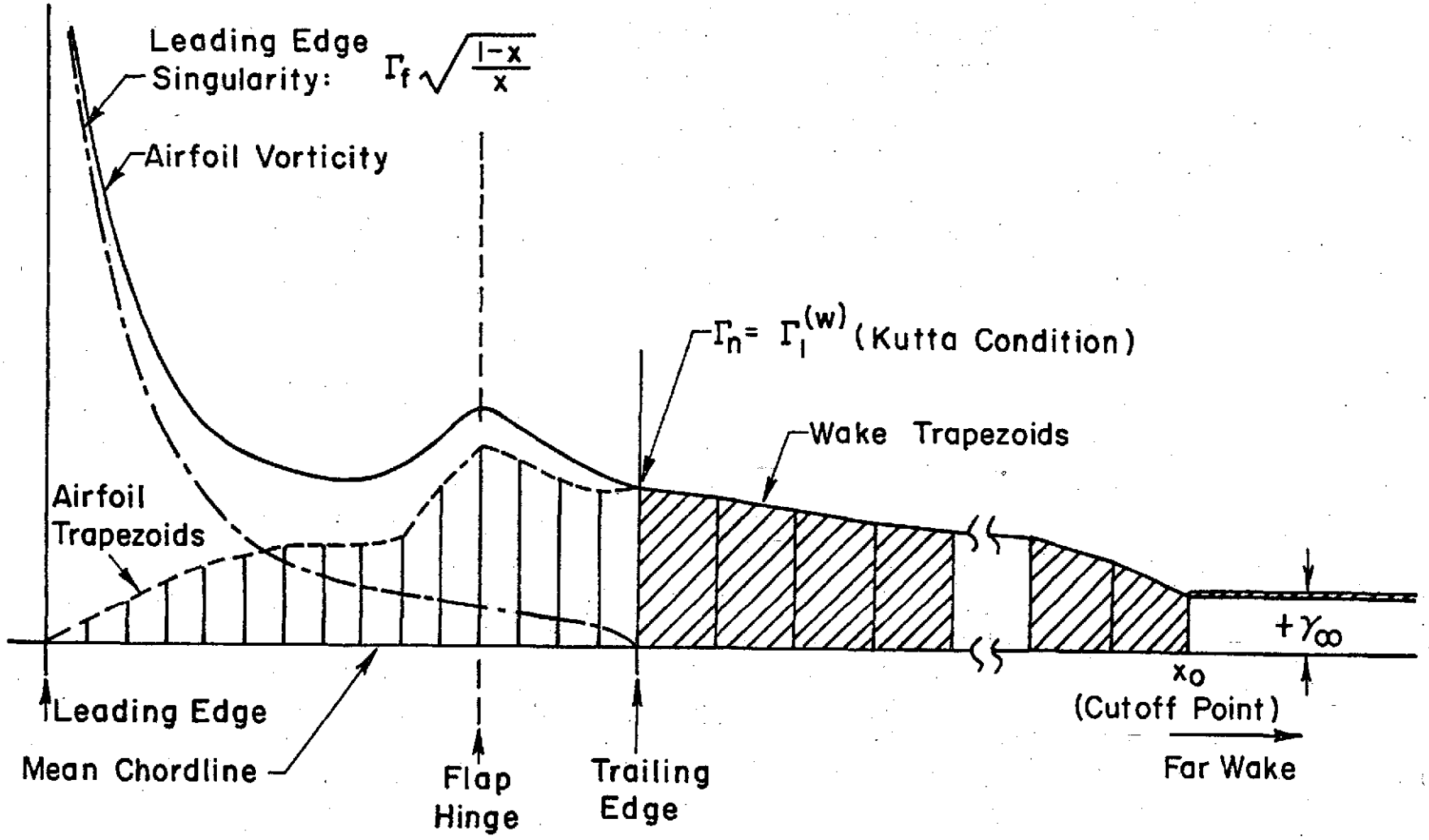

FIG. 6 NUMERICAL REPRESENTATION OF THE VORTICITY (LOWER AIRFOIL)

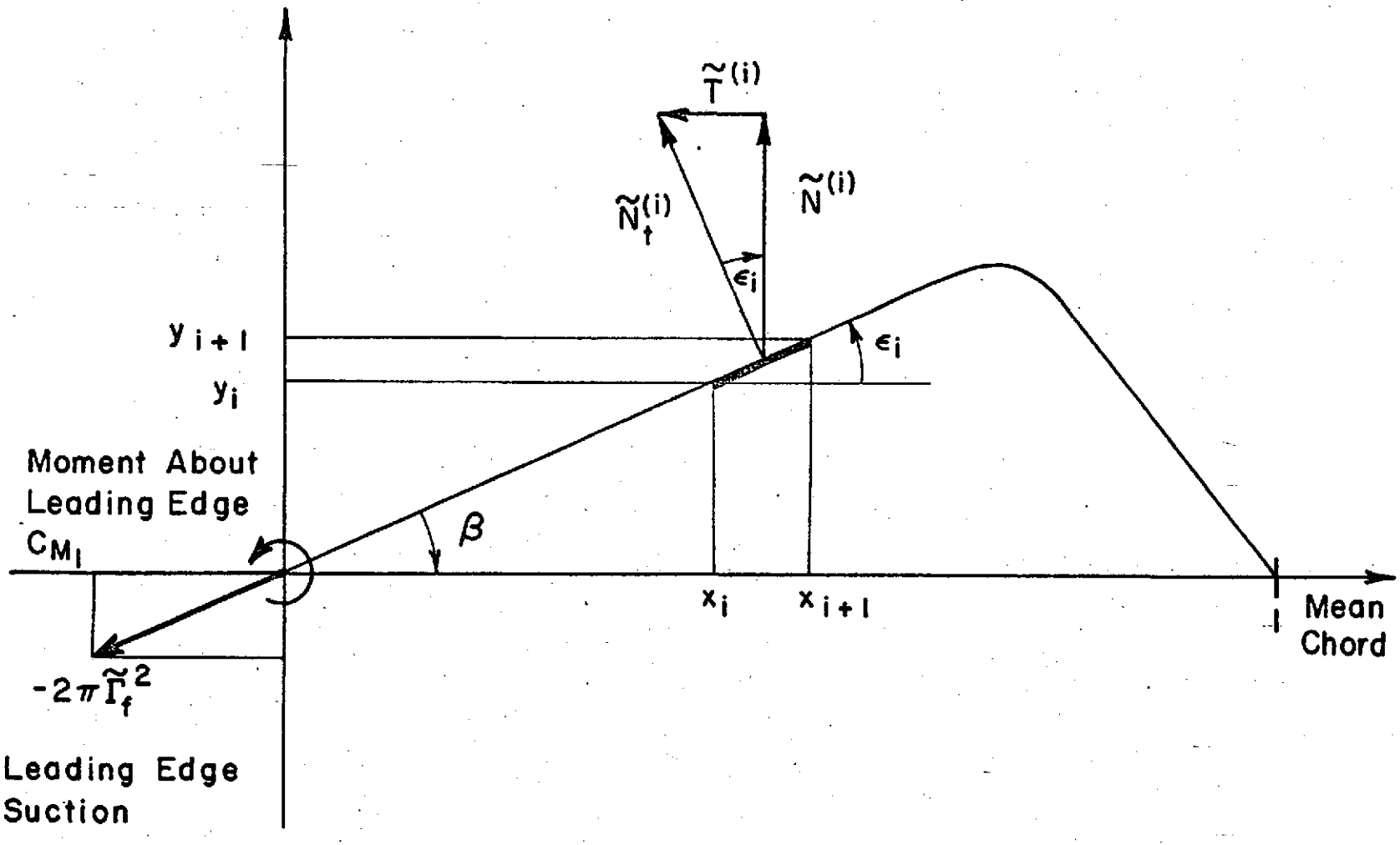

FIG. 7 FORCES/MOMENTS ACTING ON MAIN AIRFOIL

63

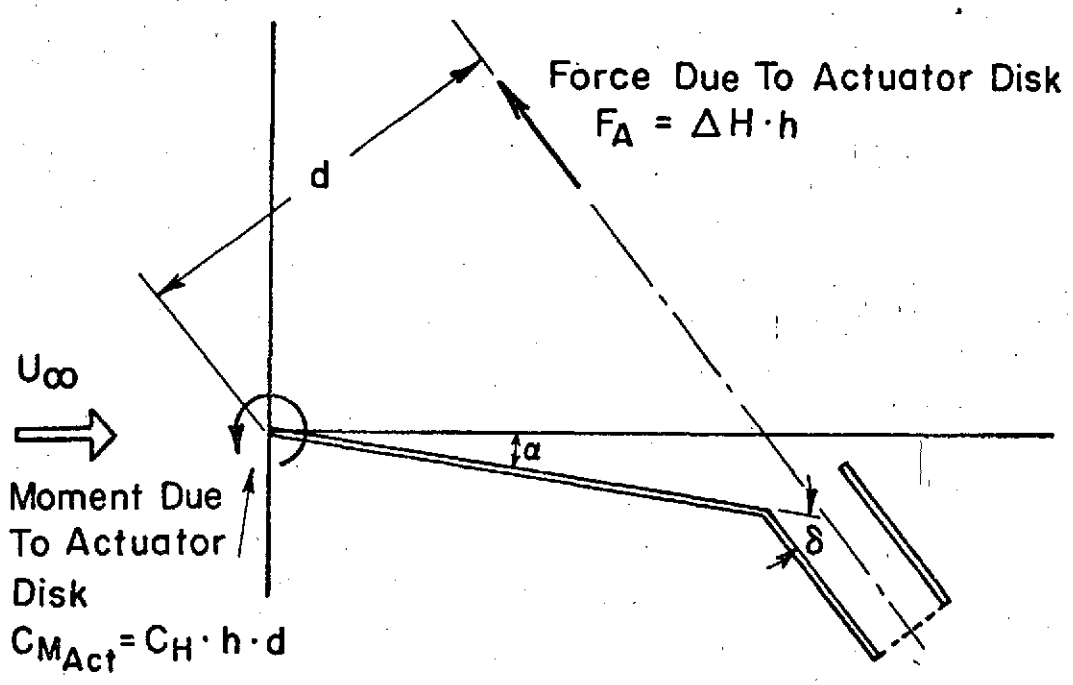

(a) Force And Moment System Due To Actuator Disk

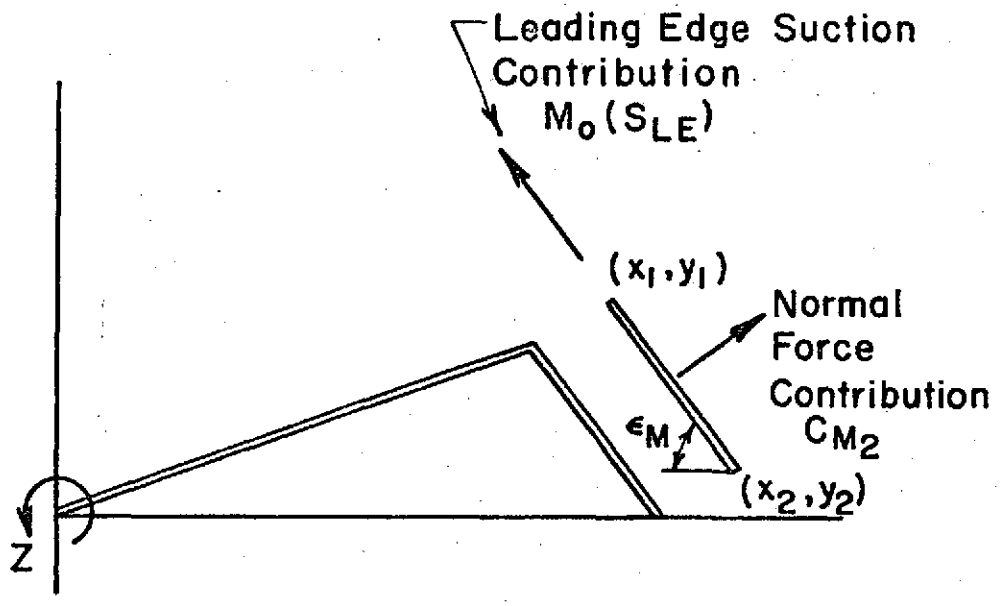

(b) Moment System Due To Upper Airfoil

FIG. 8

64

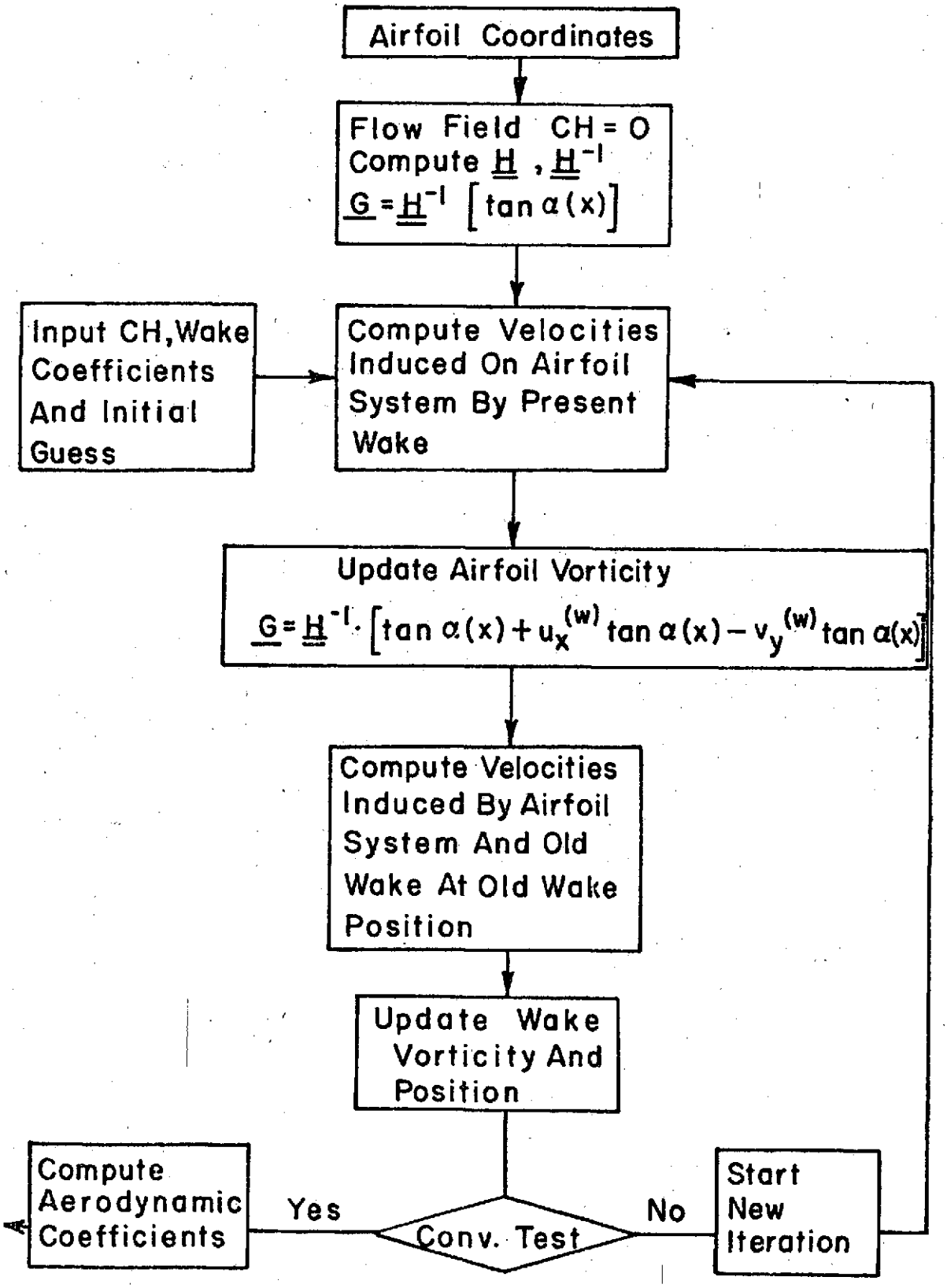

FIG. 9 POTENTIAL FLOW PROGRAM FLOW CHART

65

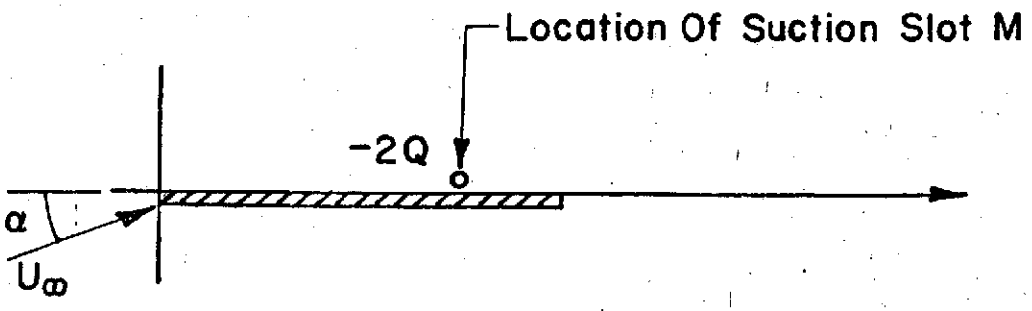

FLAT PLATE AIRFOIL WITH SUCTION SLOT

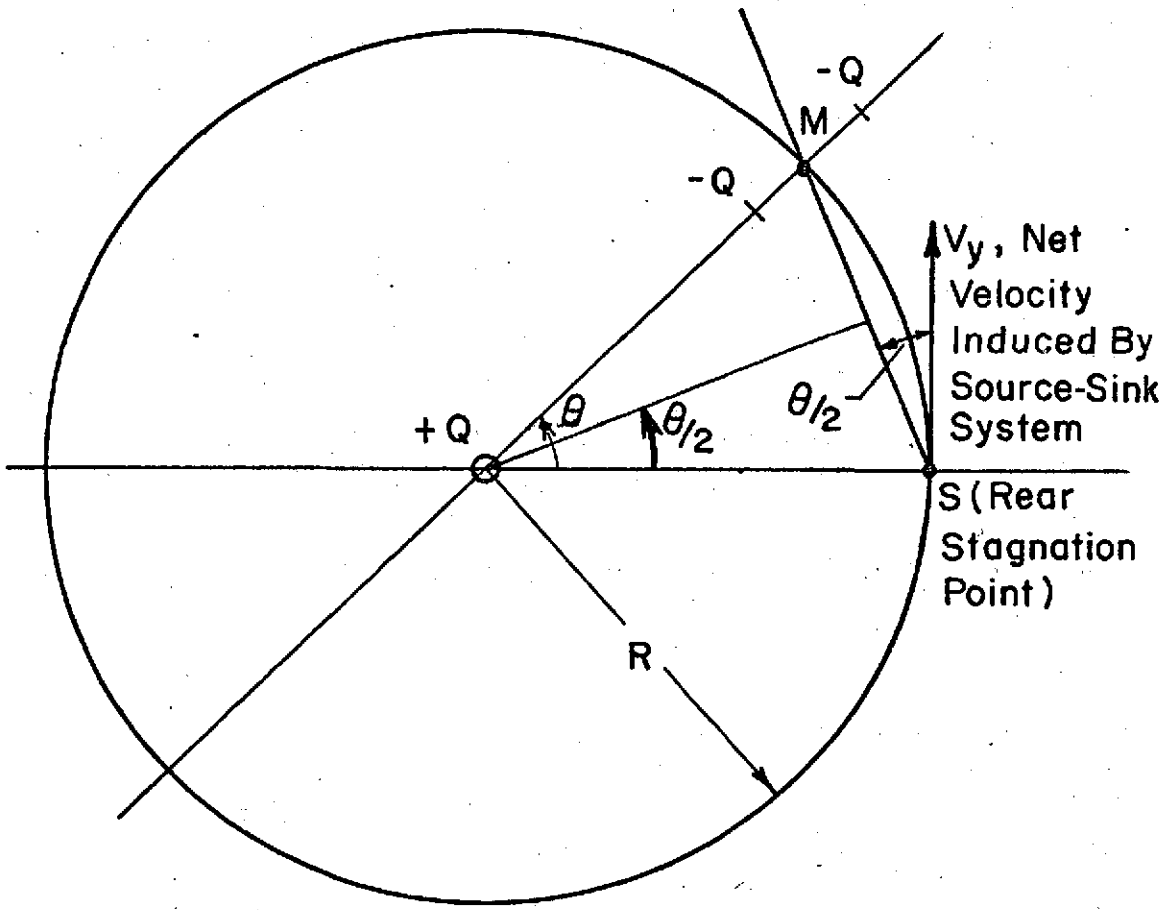

TRANSFORMED FLAT PLATE
AND SINK - SOURCE SYSTEM

FIG. 10 EFFECT OF A SINK ON A FLAT PLATE AIRFOIL

66

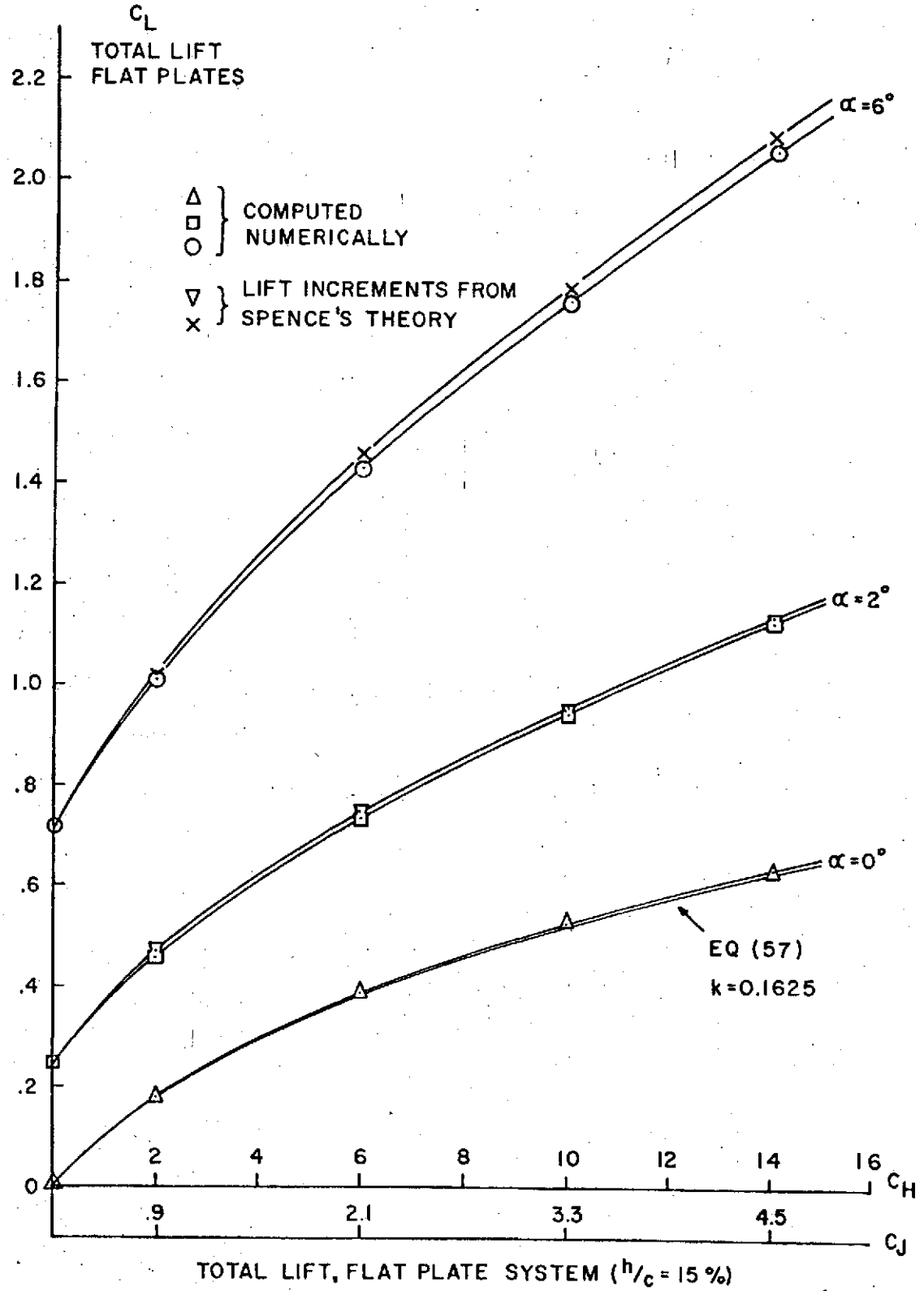

TOTAL LIFT, FLAT PLATE SYSTEM ($^h/_c$ = 15 %)

FIG. 11

67

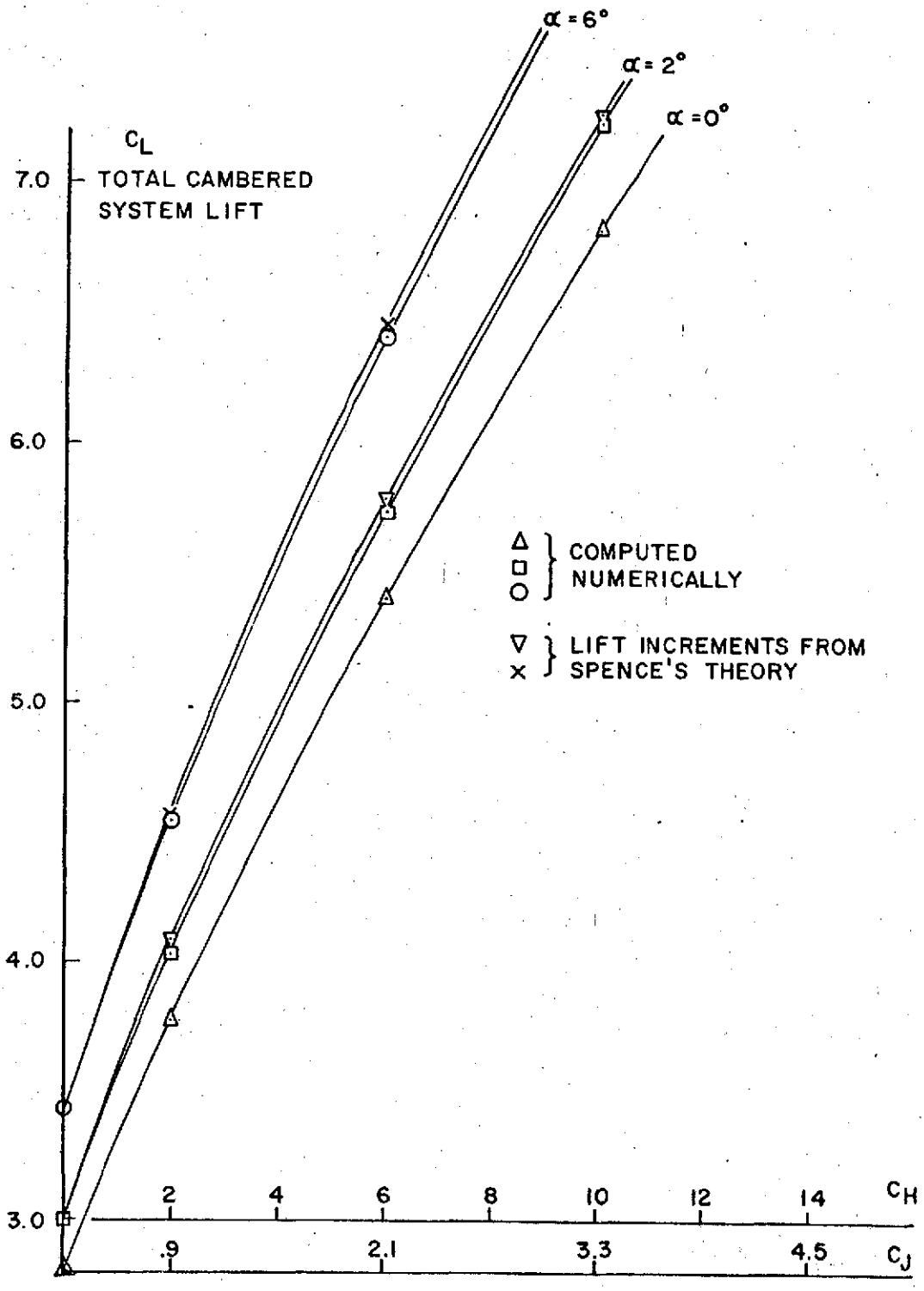

TOTAL LIFT, CAMBERED SYSTEM (h/c=15%)

FIG. 12

68

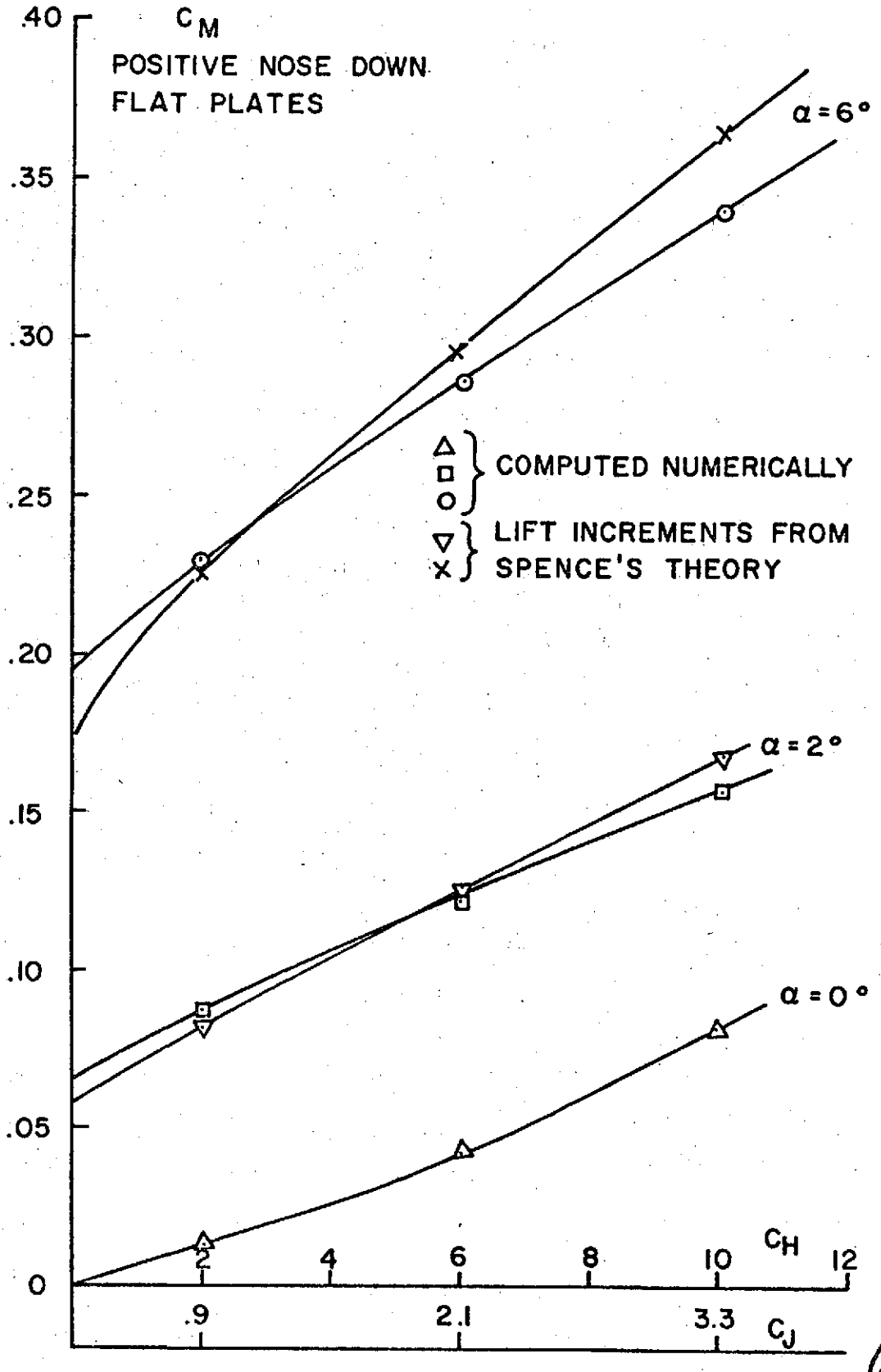

TOTAL MOMENT, FLAT PLATES
FIG. 13

69

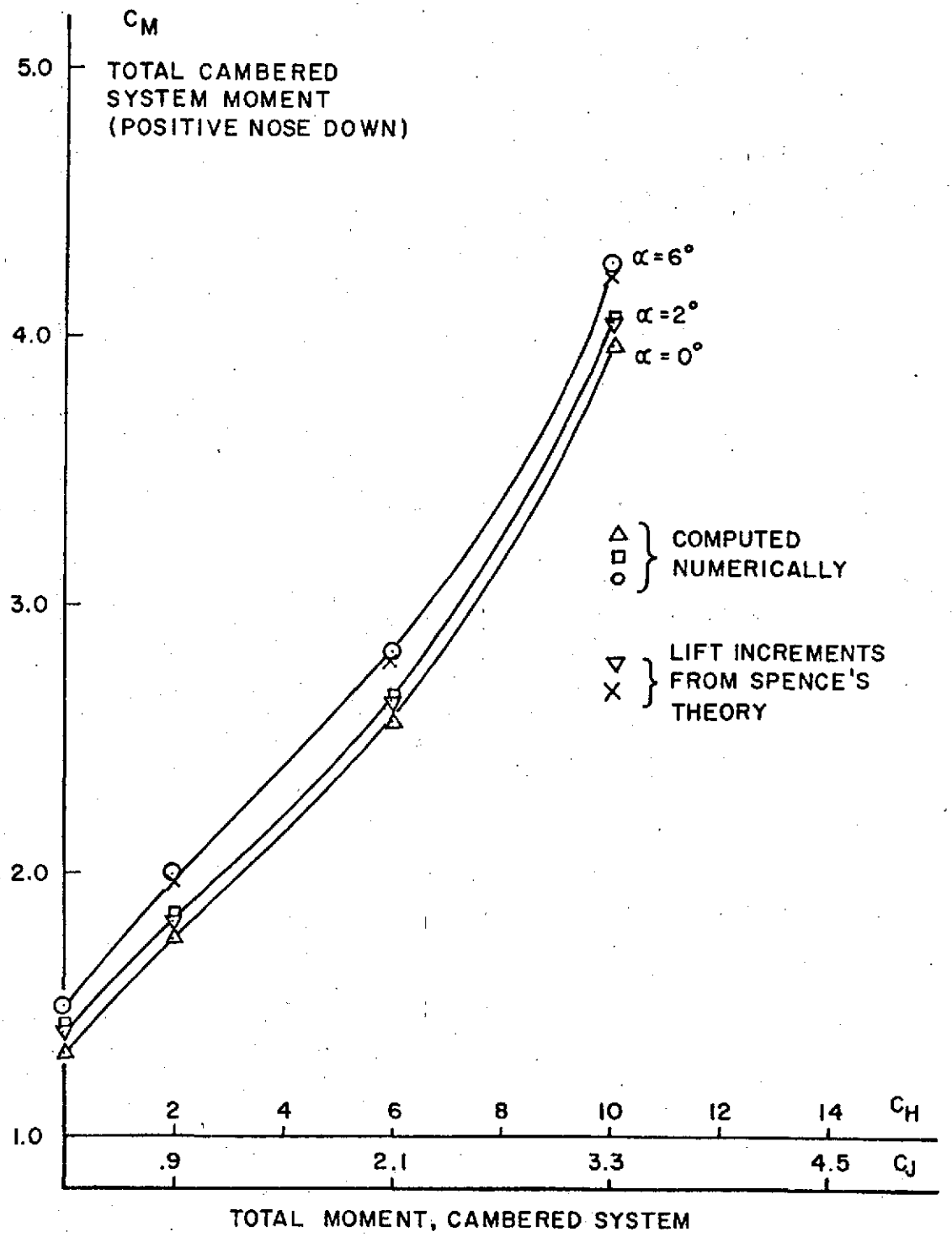

TOTAL MOMENT, CAMBERED SYSTEM

FIG. 14

70

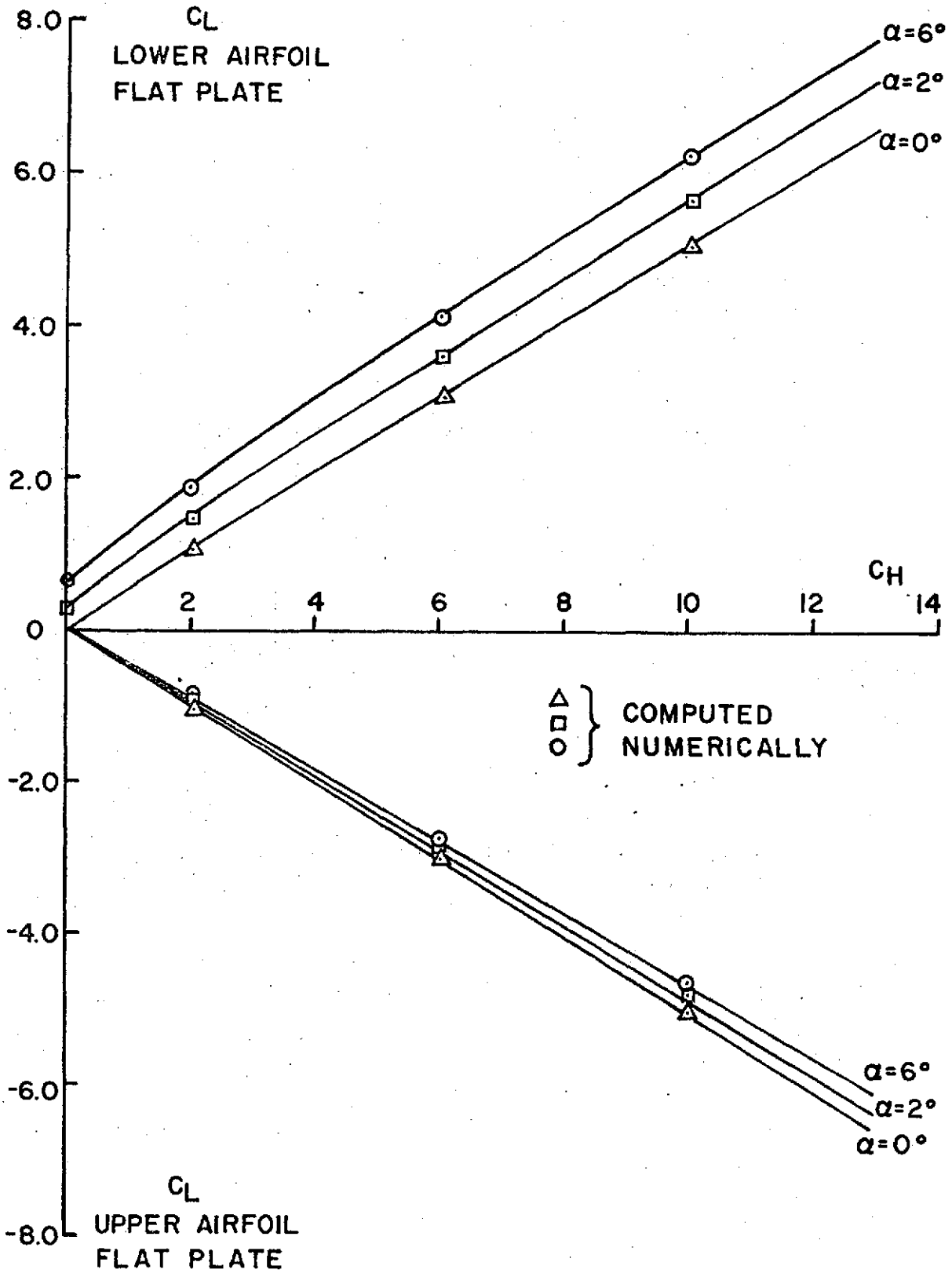

LIFT DISTRIBUTION, FLAT PLATES (ACTUATOR DISK AT TRAILING EDGE

FIG. 15.

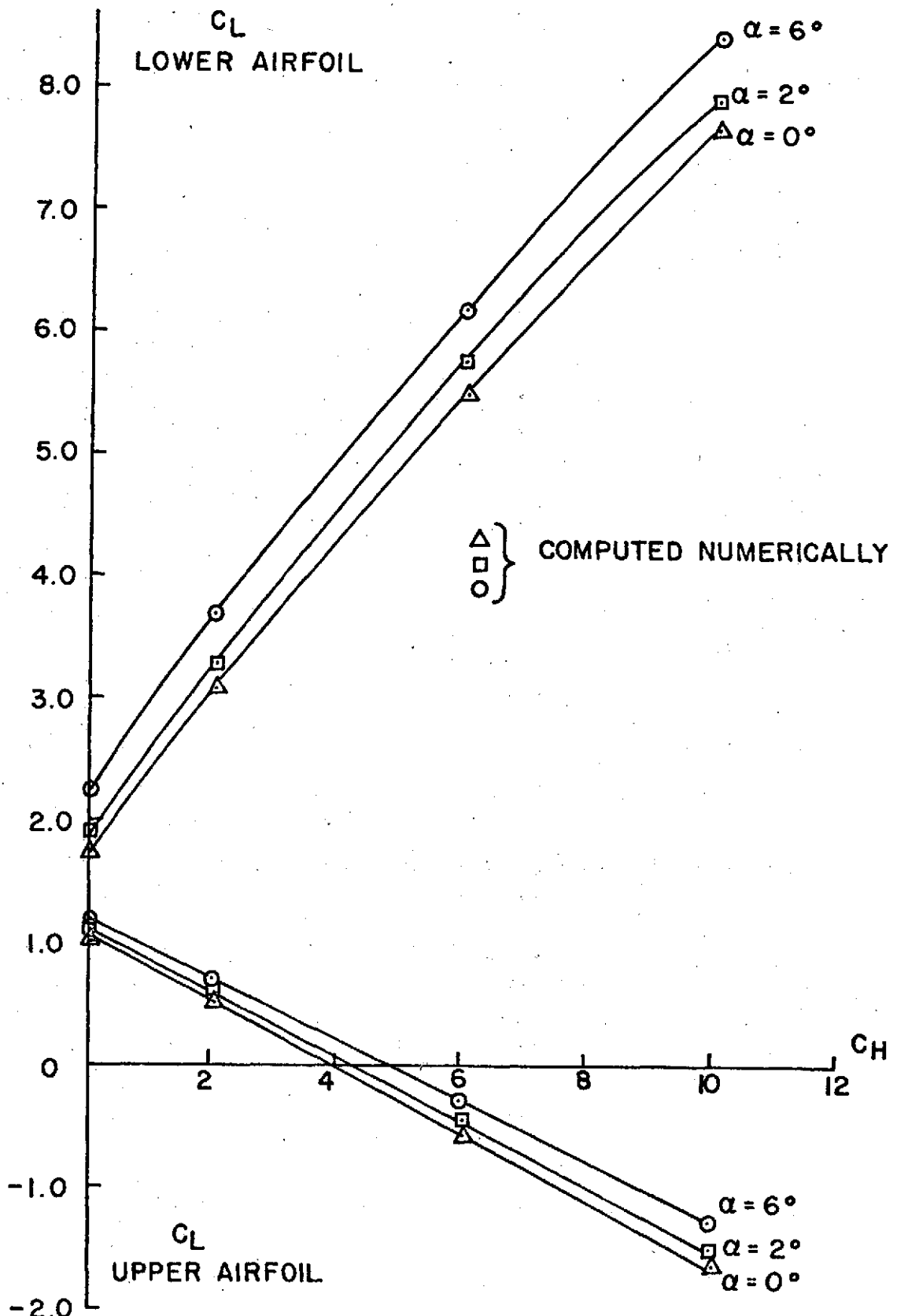

LIFT DISRIBUTION, CAMBERED SYSTEM ACTUATOR DISK AT TRAILING EDGE

FIG. 16

72

PART III

EXPERIMENTAL

GUGGENHEIM AERONAUTICAL LABORATORY

CALIFORNIA INSTITUTE OF TECHNOLOGY

10-Foot Wind Tunnel

REPORT ON LOW-SPEED WIND TUNNEL TESTS OF A QUASI-TWO DIMENSIONAL EJECTOR-AUGMENTED JET FLAP AIRFOIL

William H. Bettes

Prepared for NASA Ames Research Center

William H. Bettes
Director, 10-ft Wind Tunnel

Copy ___

H. J. Stewart
Professor of Aeronautics

Pasadena, California

August 1, 1974

74

TABLE OF CONTENTS

INDEX OF RUNS

Run No.	Model Configuration	Test	q, lb/ft^2	α_g, deg.	Q_e, ft^3/sec	C_j	h/c_s	G_{TE}, in.
1	Basic	SP	0	0	21.45	∞	0.225	1.60
2	"	"	2.25	Vary	"	1.45	"	"
3	"	"	3.0	"	"	1.09	"	"
4	"	"	5.0	"	"	0.65	"	"
5	"	"	10.0	"	"	0.33	"	"
6	"	TP	0	0	"	∞	"	"
7	"	"	2.25	Vary	"	1.45	"	"
8	"	"	10.0	"	"	0.33	"	"
9	"	SP	2.25	"	0	0.00	"	"
10	"	"	3.0	"	"	"	"	"
11	"	"	5.0	"	"	"	"	"
12	"	"	10.0	"	"	"	"	"
13	" + Rake	RP	0	0	21.45	∞	"	"
14	" + "	"	2.25	Vary	"	1.45	"	"
15	" + "	"	3.0	"	"	1.09	"	"
16	" + "	"	5.0	"	"	0.65	"	"
17	" + "	"	10.0	"	"	0.33	"	"
18	" + "	"	2.25	"	0	0	"	"
19	" + "	"	3.0	"	"	"	"	"
20	" + "	"	5.0	"	"	"	"	"
21	" + "	"	10.0	"	"	"	"	"
22	" + "	"	0	0	21.45	∞	0.270	2.05
23	" + "	"	2.25	Vary	"	1.45	"	"
24	" + "	"	3.0	"	"	1.09	"	"
25	" + "	"	5.0	"	"	0.65	"	"
26	" + "	"	10.0	"	"	0.33	"	"
27	" + "	"	2.25	"	0	0	"	"
28	" + "	"	3.0	"	"	"	"	"
29	" + "	"	5.0	"	"	"	"	"
30	" + "	"	10.0	"	"	"	"	"

INDEX OF RUNS

Run No.	Model Configuration	Test	q, lb/ft^2	α_g, deg.	Q_e, ft^3/sec	C_j	h/c_s	G_{TE}, in.
31	Basic	SP	0	0	21.45	∞	0.270	2.05
32	"	"	2.25	Vary	"	1.45	"	"
33	"	"	3.0	"	"	1.09	"	"
34	"	"	5.0	"	"	0.65	"	"
35	"	"	10.0	"	"	0.33	"	"
36	"	"	2.25	"	0	0	"	"
37	"	"	3.0	"	"	"	"	"
38	"	"	5.0	"	"	"	"	"
39	"	"	10.0	"	"	"	"	"
40	"	"	2.25	"	"	"	0.180	1.15
41	"	"	3.0	"	"	"	"	"
42	"	"	5.0	"	"	"	"	"
43	"	"	10.0	"	"	"	"	"
44	"	"	0	0	21.45	∞	"	"
45	"	"	2.25	Vary	"	1.45	"	"
46	"	"	3.0	"	"	1.09	"	"
47	"	"	5.0	"	"	0.66	"	"
48	"	"	10.0	"	"	0.33	"	"
49	" + Rake	RP	0	0	"	∞	"	"
50	" + "	"	2.25	Vary	"	1.45	"	"
51	" + "	"	3.0	"	"	1.09	"	"
52	" + "	"	5.0	"	"	0.66	"	"
53	" + "	"	10.0	"	"	0.33	"	"
54	" + "	"	2.25	"	0	0	"	"
55	" + "	"	3.0	"	"	"	"	"
56	" + "	"	5.0	"	"	"	"	"
57	" + "	"	10.0	"	"	"	"	"

INDEX OF FIGURES

I. General

II. Experimental

TABLE I

A. Nomenclature

Definition of Tests

RP = Test where pressures from a total head rake were recorded photographically from a 100-tube multimanometer board.

SP = Test where pressures from flush model surface orifices were recorded photographically from a 100-tube multimanometer board.

TP = Test where the behavior of tufts, attached to the model surface, was recorded by still photography.

Definition of Angular Measurements

α_g, (ALPHA) = Geometrical angle of attack of the wing chord plane (with δ_F=0) relative to a horizontal plane through the wind tunnel axis.

δ_f = Angle of flap deflection relative to the wing chord plane. ($\delta_f = 30^o$ for these tests)

δ_s = Angle of deflection of the shroud relative to the wing chord plane. ($\delta_s = 32^o$ for these tests)

Angular displacements about spanwise axes are positive when the nose is raised, trailing edge lowered.

Definition of Geometrical Parameters

(see Table II-A and Fig. 2 for dimensions)

b = Model span (measured inside end plates)

c = Wing (design) chord

c' = Wing chord with $\delta_f = 30^o$

c_f = Flap chord

c_s = Shroud chord

G_{TE} = Distance between flap trailing edge and shroud trailing edge measured normal to the flap chord plane.

TABLE I(Cont'd)

h =	Distance between flap and shroud chord lines measured normal to the flap chord line at 0.25 c_s.
x =	Distance along chord line with x = 0 at surface leading edge.
δ =	Height of the auxiliary air blowing slot measured at the slot exit.
C_L =	Centerline.
H_L =	Hingeline.
I. D. =	Inside diameter.
T. E. =	Trailing edge.

Definition of Airflow Parameters

In the following the "equivalent free air stream" conditions are defined by the pressure, density and temperature which an observer at rest at infinity would measure if the model were moving with a uniform velocity V through an infinite fluid at rest at infinity.

P =	Static pressure of the equivalent free airstream
Q_e =	Volume flow through the auxiliary air supply system
q =	Dynamic pressure of the equivalent free airstream
R =	Reynolds number = $\frac{\rho V c}{\mu}$
V =	Velocity of the equivalent free airstream
V_j =	Velocity of the auxiliary air at the jet exit
ρ =	Mass density of air in the equivalent free airstream
ρ_j =	Mass density of the auxiliary air at the jet exit
μ =	Absolute viscosity of air

80

TABLE I(Cont'd)

Definition of Coefficients

C_D = Pressure drag coefficient (wind axes) determined from surface pressure integrals as follows:

$C_D = C_C \cos \alpha_g + C_N \sin \alpha_g$ where C_N and C_C are normal force coefficients and chord force coefficients respectively, and

$$C_N = \frac{\text{normal force}}{qc'}$$

$$= \frac{1}{c'} \left[\int_{\text{wing}} \frac{\Delta P}{q} dc + \int_{\text{flap}} \frac{\Delta P}{q} dc_f \cos \delta_f + \int_{\text{shroud}} \frac{\Delta P}{q} dc_s \cos \delta_s \right]$$

where ΔP is the difference in pressure between the upper and lower surface. Note that C_D does not include skin friction drag. C_C is found similarly by integrating parallel with the local chord. C_D is positive in the direction of the relative wind.

C_{D_T} = "Total" drag coefficient determined from

$C_{D_T} = C_D - C_\mu \cos(\alpha_g + \delta_f)$

C_L = Lift coefficient (wind axes) determined from surface pressure integrals as follows:

$C_L = C_N \cos \alpha_g - C_C \sin \alpha_g$

See definition of C_D for C_N and C_C. C_L is positive up, normal to the direction of the relative wind.

C_{L_T} = Total lift coefficient determined from

$C_{L_T} = C_L + C_\mu \sin (\alpha_g + \delta_f)$

C_{p_m} = Pressure coefficient = $\frac{P_m - P}{q}$ where P_m is the pressure recorded at model or rake orifice m.

C_j = Auxiliary air jet momentum coefficient

$$= \frac{\rho_j V_j^2 \delta}{qc}$$

81

TABLE I(Cont'd)

C_μ = Jet momentum reaction coefficient

= $- C_j$

Definition of Corrections to the Observed Data

The only corrections applied during the present tests were those to account for the solid blocking of the model and the solid plus wake blocking of the model support system and auxiliary air supply hoses. The wind tunnel airstream velocity settings have been corrected for the increased velocity due to an effective decrease in tunnel test section area. This correction is given by the following formula in terms of the tunnel airstream setting parameter q:

$$q = q_u (1 + 2 \epsilon)$$

where ϵ is the blockage factor dependent on model, model support and air hose shapes and volumes and on tunnel test section shape and cross-sectional area; q_u is the dynamic pressure of the airstream in the clear tunnel (no model).

B. Model Configuration Notation

Basic = Quasi-two dimensional model of an ejector-augmented jet flap airfoil system. The airfoil system consisted of a main wing, a flap with the wing-flap gap sealed and set at $\delta_f = 30^\circ$ for these tests, and a shroud set at $\delta_s = 32^\circ$. The model incorporated static pressure orifices at center span and elliptical end plates with major axis of 42 inches and minor axis of 20 inches. Model span between end plates was 36 inches. See Fig. 2 for model cross-sectional detail and static pressure orifice locations and Photo Pages 4 and 5 for overall views.

Rake = Thirteen tube total head rake installed on the model by attachment of a streamlined rake support tube

TABLE I(Cont'd)

to the end plates. The rake was installed with the total head tubes facing upstream into the region between the flap and shroud. The rake was adjusted to place rake orifice number 1 (see Fig. 4) in a plane with the flap chord and 0.35 inches downstream of the flap trailing edge. The leading portion of the total head tubes were flattened such that the height of the tube opening was 0.04 inch and the tubes were spaced 0.20 inches apart. See Fig. 4 and Photo Page 5.

TABLE II

A. Model Dimensional Data

	Wing & Flap	Shroud	Ejector
b, inches	36.0	36.0	36.0
c, "	24.0	--	--
c', "	26.0	--	--
c_f, "	9.28	--	--
c_s, "	--	10.0	--
δ, "	--	--	0.09
Supply hose I. D., inches	--	--	2.37
Plennum I. D., "	--	--	2.50
Airfoil Section	NACA 65_3-218	NACA 4415	--

B. Reynolds Number vs. Dynamic Pressure of the Airstream

q, lb/ft^2	R x 10^{-6}
2.25	0.50
3.0	0.58
5.0	0.75
10.0	1.05

The above table was computed assuming the following wind tunnel airstream conditions: Temperature = 32°C; barometric pressure = 742 mm Hg.; and water vapor pressure = 12 mm Hg. The Reynolds numbers are based on the wing design chord, c.

TABLE III

CHORDWISE LOCATION OF STATIC PRESSURE ORIFICES

Main Wing

Orifice no., m	Surface	x, % c
1	upper	0.388
2	"	0.625
3	"	1.110
4	"	2.340
5	"	4.819
6	"	7.311
7	"	9.809
8	"	14.818
9	"	19.835
10	"	24.858
11	"	29.884
12	"	34.912
13	"	39.942
14	"	44.972
15	"	55.026
16	"	60.047
17	"	65.063
18	"	70.073
19	lower	0.612
20	"	0.875
21	"	1.390
22	"	2.660
23	"	5.181
24	"	7.689
25	"	10.191
26	"	15.182
27	"	20.165
28	"	25.142
29	"	30.116

TABLE III(Cont'd)

Main Wing(cont'd)

Orifice no., m	Surface	x, % c
30	lower	35.088
31	"	40.058
32	"	45.028
33	"	54.974
34	"	59.953
35	"	64.937

Flap

Orifice no., m	Surface	x, % c_f
36	upper	13.793
37	"	24.569
38	"	35.345
39	"	46.121
40	"	56.897
41	"	67.672
42	"	89.224
43	lower	13.793
44	"	24.569
45	"	35.345
46	"	46.121
47	"	56.897
48	"	67.672
49	"	78.448
50	"	89.224

TABLE III(Cont'd)

Shroud

Orifice no., m	Surface	x, $\%c_s$
51	upper	1.250
52	"	2.500
53	"	5.000
54	"	7.500
55	"	10.000
56	"	15.000
57	"	20.000
58	"	25.000
59	"	30.000
60	"	40.000
61	"	50.000
62	"	60.000
63	"	70.000
64	"	80.000
65	"	90.000
66	lower	1.250
67	"	2.500
68	"	5.000
69	"	7.500
70	"	10.000
71	"	15.000
72	"	20.000
73	"	25.000
74	"	30.000
75	"	40.000
76	"	50.000
77	"	60.000
78	"	70.000
79	"	90.000

87

TABLE IV

TABULATED SURFACE PRESSURE COEFFICIENTS

TABULATED PRESSURE COEFFICIENTS

RUN 2, Q = 2.25 LB./FTSQ

ORIFICE NO.	CP VALUES AT ALPHA ANGLE SETTINGS 0	3	6	9
1	-1.332	-1.737	-3.541	-4.382
2	-0.907	-1.891	-3.618	-4.294
3	-0.768	-1.809	-3.289	-3.867
4	-1.642	-1.655	-2.842	-3.376
5	-1.611	-1.408	-2.133	-2.387
6	-1.636	-1.358	-1.994	-2.102
7	-0.140	-1.313	-1.989	-2.036
8	0.107	-1.281	-1.881	-1.886
9	-1.731	-1.386	-1.994	-1.886
10	-1.788	-1.363	-1.912	-1.886
11	-1.921	-1.399	-1.912	-1.863
12	-2.130	-1.500	-1.994	-1.886
13	-2.308	-1.554	-1.994	-1.938
14	-2.409	-1.586	-2.107	-1.966
15	-2.726	-1.737	-2.215	-2.046
16	-2.967	-1.960	-2.472	-2.195
17	-3.937	-2.634	-3.176	-2.739
18	-7.613	-5.327	-6.245	-5.591
19	1.000	0.851	0.594	-0.041
20	1.000	0.940	0.811	0.465
21	0.923	1.000	0.919	0.822
22	0.744	0.940	1.000	0.970
23	0.616	0.851	0.973	1.000

TABULATED PRESSURE COEFFICIENTS

RUN 2, Q = 2.25 LB./FTSQ

ORIFICE NO.	CP VALUES AT ALPHA ANGLE SETTINGS 0	3	6	9
24	0.513	0.700	0.838	0.941
25	0.462	0.550	0.784	0.822
26	0.360	0.491	0.703	0.703
27	0.283	0.401	0.622	0.613
28	0.257	0.401	0.568	0.554
29	0.232	0.340	0.514	0.494
30	0.155	0.251	0.487	0.406
31	0.232	0.251	0.514	0.406
32	0.232	0.311	0.460	0.435
33	0.411	0.401	0.514	0.465
34	0.488	0.550	0.649	0.584
35	0.693	0.700	0.784	0.703
36	-11.568	-8.121	-8.892	-8.345
37	-8.519	-6.052	-7.057	-6.246
38	-6.054	-4.202	-4.950	-4.429
39	-4.456	-3.031	-3.629	-3.324
40	-2.935	-1.914	-3.007	-2.303
41	-2.371	-1.609	-1.912	-1.661
42	-2.339	-1.486	-1.763	-1.544
43	0.769	0.790	0.784	0.822
44	0.744	0.700	0.730	0.791
45	0.642	0.641	0.649	0.613
46	0.616	0.611	0.622	0.584

TABULATED PRESSURE COEFFICIENTS

RUN 2, Q = 2.25 LB./FTSQ

ORIFICE NO.	CP VALUES AT ALPHA ANGLE SETTINGS 0	3	6	9
47	0.616	0.550	0.568	0.554
48	0.616	0.550	0.568	0.554
49	0.539	0.460	0.487	0.435
50	0.488	0.430	0.460	0.406
51	-0.672	-0.465	-0.673	-0.837
52	-1.611	-1.162	-1.516	-1.530
53	-2.403	-1.686	-2.107	-2.046
54	-2.796	-1.800	-2.472	-2.378
55	-2.967	-2.110	-2.616	-2.504
56	-2.967	-2.060	-2.616	-2.467
57	-2.999	-2.010	-2.503	-2.387
58	-2.701	-1.832	-2.246	-2.097
59	-2.492	-1.809	-2.220	-2.097
60	-2.308	-1.158	-1.886	-1.825
61	-1.984	-1.313	-1.547	-1.427
62	-1.186	-1.035	-1.321	-1.221
63	-1.370	-0.834	-1.012	-0.973
64	-1.091	-0.720	-0.786	-0.842
65	-0.882	-0.511	-0.699	-0.711
66	-7.822	-5.551	-6.127	-5.375
67	-11.397	-8.093	-9.159	-8.101
68	-14.275	-10.189	-11.617	-10.424
69	-17.152	-12.308	-13.981	-12.602

TABULATED PRESSURE COEFFICIENTS

RUN 2, Q = 2.25 LB./FTSQ

ORIFICE NO.	CP VALUES AT ALPHA ANGLE SETTINGS 0	3	6	9
70	-18.192	-13.033	-14.875	-13.398
71	-18.483	-13.220	-15.019	-13.501
72	-16.563	-11.866	-13.570	-11.838
73	-12.855	-9.068	-10.419	-9.295
74	-11.048	-7.792	-8.913	-7.993
75	-8.171	-5.751	-6.636	-5.961
76	-6.054	-4.202	-4.847	-4.326
77	-4.697	-3.208	-3.711	-3.324
78	-3.956	-2.657	-3.089	-2.762
79	-3.106	-2.037	-2.446	-2.149

TABULATED PRESSURE COEFFICIENTS

RUN 3, Q = 3.00 LB./FTSQ

ORIFICE NO.	CP VALUES AT ALPHA ANGLE SETTINGS 0	3	6	9
1	-1.012	-1.733	-3.286	-4.589
2	-1.325	-1.886	-3.358	-4.610
3	-1.304	-1.749	-3.037	-4.195
4	-1.268	-1.556	-2.622	-3.569
5	-1.208	-1.375	-2.073	-2.532
6	-1.208	-1.238	-1.865	-2.263
7	-1.208	-1.222	-1.793	-2.152
8	-1.190	-1.123	-1.703	-1.959
9	-1.382	-1.244	-1.848	-1.997
10	-1.443	-1.260	-1.789	-1.993
11	-1.461	-1.257	-1.772	-1.907
12	-1.617	-1.394	-1.807	-1.979
13	-1.624	-1.459	-1.886	-1.997
14	-1.713	-1.462	-1.941	-2.056
15	-1.831	-1.528	-1.941	-2.076
16	-1.909	-1.615	-2.017	-2.132
17	-2.375	-2.051	-2.470	-2.546
18	-4.349	-3.677	-4.402	-4.364
19	1.000	0.910	0.588	0.097
20	1.000	0.982	0.785	0.515
21	0.941	1.000	1.000	0.861
22	0.803	0.838	0.981	1.000
23	0.645	0.766	0.823	0.969

TABULATED PRESSURE COEFFICIENTS

RUN 3, Q = 3.00 LB./FTSQ

ORIFICE NO.	CP VALUES AT ALPHA ANGLE SETTINGS 0	3	6	9
24	0.486	0.657	0.804	0.896
25	0.428	0.568	0.706	0.824
26	0.368	0.460	0.588	0.661
27	0.289	0.405	0.510	0.551
28	0.269	0.369	0.451	0.515
29	0.230	0.333	0.412	0.461
30	0.190	0.315	0.392	0.442
31	0.230	0.315	0.392	0.442
32	0.289	0.369	0.412	0.461
33	0.428	0.460	0.549	0.551
34	0.565	0.585	0.588	0.606
35	0.664	0.640	0.726	0.733
36	-6.523	-5.567	-6.338	-6.296
37	-4.769	-4.069	-4.627	-4.665
38	-3.310	-2.801	-3.324	-3.286
39	-2.435	-2.029	-2.339	-2.422
40	-1.539	-1.307	-1.544	-1.520
41	-1.151	-0.864	-1.223	-0.953
42	-1.151	-0.864	-1.147	-1.112
43	0.744	0.802	0.785	0.824
44	0.684	0.766	0.765	0.806
45	0.645	0.730	0.706	0.733
46	0.585	0.585	0.687	0.642

TABULATED PRESSURE COEFFICIENTS

RUN 3, Q = 3.00 LB./FTSQ

ORIFICE NO.	CP VALUES AT ALPHA ANGLE SETTINGS 0	3	6	9
47	0.526	0.585	0.687	0.624
48	0.526	0.549	0.628	0.606
49	0.486	0.477	0.569	0.588
50	0.466	0.477	0.549	0.551
51	-1.446	-1.173	-1.523	-1.734
52	-2.008	-1.802	-2.187	-2.284
53	-2.435	-2.141	-1.973	-2.698
54	-2.709	-2.387	-2.830	-2.944
55	-2.766	-2.362	-2.882	-3.020
56	-2.688	-2.331	-2.792	-2.882
57	-2.535	-2.213	-2.622	-2.681
58	-2.240	-1.973	-2.308	-2.387
59	-2.183	-1.836	-2.297	-2.280
60	-1.791	-1.515	-1.810	-1.852
61	-1.443	-1.238	-1.471	-1.527
62	-1.151	-1.036	-1.223	-1.223
63	-0.959	-0.796	-0.929	-0.956
64	-0.742	-0.575	-0.725	-0.749
65	-0.564	-0.419	-0.552	-0.562
66	-3.058	-2.518	-2.792	-2.681
67	-5.530	-4.732	-5.346	-5.328
68	-7.515	-6.539	-7.312	-7.274
69	-9.404	-8.139	-9.255	-9.168

TABULATED PRESSURE COEFFICIENTS

RUN 3, Q = 3.00 LB./FTSQ

ORIFICE NO.	CP VALUES AT ALPHA ANGLE SETTINGS 0	3	6	9
70	-10.144	-8.856	-9.980	-9.866
71	-10.357	-9.011	-10.132	-10.074
72	-9.290	-8.055	-9.061	-8.995
73	-7.106	-6.096	-6.953	-6.839
74	-6.074	-5.243	-5.951	-5.902
75	-4.459	-3.848	-4.399	-4.364
76	-3.236	-2.755	-3.151	-3.117
77	-2.435	-2.038	-2.311	-2.284
78	-1.969	-1.621	-1.941	-1.841
79	-1.482	-1.170	-1.444	-1.375

TABULATED PRESSURE COEFFICIENTS

RUN 4, Q = 5.00 LB./FTSQ

ORIFICE NO.	CP VALUES AT ALPHA ANGLE SETTINGS 0	3	6	9
1	-1.011	-1.763	-3.275	-4.602
2	-1.295	-1.980	-3.359	-4.598
3	-1.359	-1.923	-3.047	-4.181
4	-1.347	-1.745	-2.686	-3.467
5	-1.359	-1.468	-2.120	-2.549
6	-1.258	-1.367	-1.934	-2.241
7	-1.232	-1.189	-1.798	-2.161
8	-1.307	-1.311	-1.739	-1.874
9	-1.421	-1.435	-1.805	-1.983
10	-1.452	-1.421	-1.787	-1.948
11	-1.525	-1.458	-1.739	-1.890
12	-1.582	-1.483	-1.739	-1.905
13	-1.707	-1.532	-1.798	-1.929
14	-1.710	-1.549	-1.796	-1.992
15	-1.712	-1.524	-1.776	-1.840
16	-1.762	-1.499	-1.739	-1.831
17	-1.892	-1.648	-1.956	-1.961
18	-3.068	-2.722	-2.958	-3.001
19	0.958	0.903	0.587	0.141
20	0.944	0.945	0.791	0.521
21	0.880	0.959	0.929	0.808
22	0.672	0.802	0.929	0.914
23	0.504	0.690	0.780	0.888

TABULATED PRESSURE COEFFICIENTS

RUN 4, $\overset{0}{Q}$ = 5.00 LB./FTSQ

ORIFICE NO.	CP VALUES AT ALPHA ANGLE SETTINGS 0	3	6	9
24	0.364	0.552	0.683	0.808
25	0.310	0.474	0.611	0.732
26	0.220	0.339	0.445	0.617
27	0.163	0.294	0.394	0.521
28	0.089	0.317	0.348	0.460
29	0.104	0.269	0.287	0.376
30	0.104	0.226	0.289	0.356
31	0.104	0.236	0.284	0.365
32	0.168	0.259	0.313	0.352
33	0.362	0.418	0.407	0.487
34	0.466	0.509	0.539	0.569
35	0.608	0.655	0.635	0.662
36	-4.470	-3.844	-4.154	-4.146
37	-3.251	-2.829	-3.087	-3.087
38	-2.311	-1.945	-2.182	-2.170
39	-1.480	-1.381	-1.524	-1.568
40	-0.997	-0.803	-0.987	-0.963
41	-0.647	-0.565	-0.625	-0.618
42	-0.597	-0.623	-0.735	-0.681
43	0.674	0.699	0.670	0.747
44	0.620	0.655	0.629	0.667
45	0.544	0.542	0.539	0.628
46	0.492	0.542	0.519	0.569

TABULATED PRESSURE COEFFICIENTS

RUN 4, Q = 5.00 LB./FTSQ

ORIFICE NO.	CP VALUES AT ALPHA ANGLE SETTINGS 0	3	6	9
47	0.440	0.478	0.534	0.528
48	0.414	0.484	0.491	0.484
49	0.414	0.422	0.442	0.473
50	0.402	0.395	0.449	0.450
51	-2.541	-2.340	-2.688	-2.766
52	-3.016	-2.670	-3.069	-3.135
53	-3.265	-2.885	-3.227	-3.363
54	-3.409	-3.036	-3.376	-3.469
55	-3.421	-3.007	-3.370	-3.422
56	-3.173	-2.782	-3.131	-3.181
57	-2.969	-2.588	-2.890	-2.907
58	-2.593	-2.226	-2.519	-2.460
59	-2.306	-2.044	-2.304	-2.245
60	-1.944	-1.718	-1.956	-1.890
61	-1.546	-1.336	-1.522	-1.508
62	-1.232	-1.063	-1.186	-1.187
63	-0.919	-0.826	-0.866	-0.950
64	-0.675	-0.576	-0.623	-0.733
65	-0.505	-0.386	-0.432	-0.488
66	-0.794	-0.656	-0.682	-0.713
67	-2.903	-2.478	-2.710	-2.673
68	-4.626	-4.003	-4.343	-4.307
69	-6.136	-5.349	-5.831	-5.782

TABULATED PRESSURE COEFFICIENTS

RUN 4, Q = 5.00 LB./FTSQ

ORIFICE NO.	CP VALUES AT ALPHA ANGLE SETTINGS 0	3	6	9
70	-6.700	-5.880	-6.333	-6.340
71	-7.010	-6.138	-6.610	-6.559
72	-6.259	-5.438	-5.862	-5.830
73	-4.844	-4.217	-4.545	-4.491
74	-4.120	-3.596	-3.865	-3.860
75	-3.045	-2.635	-2.866	-2.827
76	-2.138	-1.821	-2.050	-1.979
77	-1.527	-1.301	-1.452	-1.423
78	-1.113	-0.972	-1.090	-1.093
79	-0.765	-0.706	-0.695	-0.748

TABULATED PRESSURE COEFFICIENTS

RUN 5, Q = 10.00 LB./FTSQ

ORIFICE NO.	CP VALUES AT ALPHA ANGLE SETTINGS 0	3	6	9
1	-0.486	-1.356	-2.516	-3.807
2	-0.819	-1.563	-2.727	-3.866
3	-0.858	-1.594	-2.601	-3.503
4	-0.915	-1.465	-2.152	-2.870
5	-0.907	-1.284	-1.762	-2.159
6	-0.946	-1.241	-1.612	-1.944
7	-0.982	-1.157	-1.534	-1.823
8	-1.025	-1.217	-1.476	-1.706
9	-1.182	-1.344	-1.553	-1.745
10	-1.221	-1.350	-1.552	-1.701
11	-1.248	-1.375	-1.473	-1.655
12	-1.307	-1.399	-1.552	-1.662
13	-1.375	-1.457	-1.583	-1.669
14	-1.402	-1.455	-1.588	-1.644
15	-1.338	-1.356	-1.442	-1.503
16	-1.276	-1.289	-1.375	-1.416
17	-1.270	-1.288	-1.364	-1.410
18	-1.751	-1.753	-1.813	-1.869
19	0.950	1.000	0.826	0.459
20	0.888	1.013	0.941	0.734
21	0.765	0.941	0.995	0.924
22	0.579	0.801	0.937	0.966
23	0.419	0.641	0.771	0.388

TABULATED PRESSURE COEFFICIENTS

RUN 5, Q = 10.00 LB./FTSQ

ORIFICE NO.	CP VALUES AT ALPHA ANGLE SETTINGS 0	3	6	9
24	0.327	0.507	0.656	0.777
25	0.271	0.423	0.589	0.695
26	0.178	0.319	0.455	0.571
27	0.142	0.265	0.388	0.478
28	0.126	0.240	0.332	0.426
29	0.120	0.216	0.298	0.384
30	0.130	0.192	0.292	0.366
31	0.129	0.216	0.288	0.343
32	0.166	0.240	0.292	0.366
33	0.351	0.415	0.431	0.477
34	0.480	0.515	0.533	0.583
35	0.616	0.641	0.656	0.683
36	-2.725	-2.722	-2.795	-2.763
37	-2.091	-2.097	-2.150	-2.154
38	-1.491	-1.542	-1.612	-1.639
39	-1.106	-1.160	-1.243	-1.257
40	-0.705	-0.736	-0.779	-0.788
41	-0.479	-0.533	-0.582	-0.578
42	-0.312	-0.389	-0.388	-0.457
43	0.702	0.710	0.731	0.759
44	0.640	0.649	0.661	0.689
45	0.579	0.588	0.601	0.613
46	0.536	0.524	0.558	0.560

TABULATED PRESSURE COEFFICIENTS

RUN 5, Q = 10.00 LB./FTSQ

ORIFICE NO.	CP VALUES AT ALPHA ANGLE SETTINGS 0	3	6	9
47	0.481	0.496	0.084	0.531
48	0.449	0.478	0.485	0.512
49	0.449	0.447	0.480	0.497
50	0.450	0.447	0.466	0.463
51	-3.158	-3.251	-3.340	-3.315
52	-3.239	-3.344	-3.434	-3.398
53	-3.263	-3.325	-3.408	-3.386
54	-3.260	-3.320	-3.394	-3.346
55	-3.158	-3.246	-3.292	-3.244
56	-2.879	-2.918	-2.971	-2.934
57	-2.621	-2.644	-2.661	-2.442
58	-2.189	-2.191	-2.211	-2.149
59	-1.986	-1.984	-1.995	-1.915
60	-1.641	-1.594	-1.580	-1.504
61	-1.194	-1.143	-1.079	-0.911
62	-0.852	-0.704	-0.631	-0.489
63	-0.511	-0.424	-0.412	-0.407
64	-0.326	-0.336	-0.388	-0.396
65	-0.272	-0.300	-0.370	-0.405
66	0.407	0.386	0.382	0.293
67	-0.954	-0.965	-1.006	-1.017
68	-2.181	-2.210	-2.280	-2.249
69	-3.269	-3.290	-3.371	-3.362

TABULATED PRESSURE COEFFICIENTS

RUN 5, Q = 10.00 LB./FTSQ

ORIFICE NO.	CP VALUES AT ALPHA ANGLE SETTINGS 0	3	6	9
70	-3.731	-3.753	-3.824	-3.802
71	-4.021	-4.027	-4.099	-4.069
72	-3.598	-3.578	-3.680	-3.638
73	-2.879	-2.890	-2.966	-2.940
74	-2.451	-2.467	-2.517	-2.518
75	-1.856	-1.878	-1.946	-1.930
76	-1.327	-1.374	-1.417	-1.457
77	-0.952	-0.997	-1.030	-1.058
78	-0.697	-0.729	-0.781	-0.786
79	-0.345	-0.399	-0.454	-0.452

TABULATED PRESSURE COEFFICIENTS

RUN 9, Q = 2.25 LB./FTSQ

ORIFICE NO.	CP VALUES AT ALPHA ANGLE SETTINGS 0	3	6	9
1	-0.403	-1.079	-1.778	-3.085
2	-0.740	-1.293	-1.902	0.113
3	-0.800	-1.233	-1.761	-2.946
4	-0.850	-1.130	-1.534	-2.490
5	-0.875	-1.056	-1.290	-1.984
6	-0.870	-0.976	-1.196	-1.632
7	-0.875	-0.976	-1.175	-1.468
8	-0.875	-0.976	-0.742	-1.379
9	-1.016	-1.004	-1.106	-1.488
10	-1.121	-1.004	-1.098	-1.389
11	-1.096	-0.976	-1.063	-1.320
12	-1.121	-0.990	-1.020	-1.295
13	-1.121	-0.990	-1.059	-1.171
14	-1.096	-0.976	-0.939	-1.186
15	-0.955	-0.827	-0.717	-0.863
16	-0.980	-0.646	-0.610	-0.670
17	-0.378	-0.338	-0.353	-0.452
18	-0.243	-0.166	-0.250	-0.427
19	0.957	0.957	0.831	0.746
20	0.872	0.957	0.951	0.873
21	0.760	0.908	1.000	1.000
22	0.563	0.716	0.902	0.975
23	0.423	0.595	0.709	0.873

TABULATED PRESSURE COEFFICIENTS

RUN 9, Q = 2.25 LB./FTSQ

ORIFICE NO.	CP VALUES AT ALPHA ANGLE SETTINGS 0	3	6	9
24	0.254	0.475	0.636	0.772
25	0.114	0.403	0.539	0.620
26	0.029	0.354	0.346	0.493
27	0.029	0.234	0.273	0.417
28	0.001	0.186	0.225	0.366
29	-0.027	0.114	0.177	0.316
30	-0.027	0.114	0.177	0.239
31	0.029	0.114	0.177	0.290
32	0.114	0.186	0.225	0.290
33	0.114	0.234	0.322	0.366
34	0.395	0.403	0.394	0.417
35	0.563	0.523	0.588	0.746
36	-0.870	-0.823	-0.588	-0.536
37	-0.459	-0.422	-0.284	-0.422
38	-0.378	-0.315	-0.284	-0.348
39	-0.283	-0.189	-0.160	-0.268
40	-0.157	-0.087	-0.165	-0.239
41	-0.132	-0.059	-0.096	-0.239
42	-0.107	-0.008	-0.023	-0.154
43	0.760	0.716	0.733	0.746
44	0.676	0.668	0.709	0.696
45	0.535	0.595	0.588	0.620
46	0.451	0.499	0.515	0.518

TABULATED PRESSURE COEFFICIENTS

RUN 9, Q = 2.25 LB./FTSQ

ORIFICE NO.	CP VALUES AT ALPHA ANGLE SETTINGS 0	3	6	9
47	0.395	0.475	0.467	0.493
48	0.395	0.475	0.467	0.442
49	0.254	0.306	0.346	0.290
50	0.114	0.234	0.298	0.239
51	-4.312	-4.036	-3.729	-4.444
52	-3.841	-3.543	-3.220	-3.769
53	-3.454	-3.151	-2.856	-3.358
54	-3.193	-2.858	-2.493	-3.115
55	-3.043	-2.583	-2.415	-2.906
56	-2.817	-2.504	-2.000	-2.222
57	-2.029	-1.717	-1.406	-1.622
58	-1.557	-1.233	-1.055	-1.131
59	-1.231	-0.953	-0.396	-0.675
60	-0.679	-0.413	-0.314	-0.348
61	-0.378	-0.189	-0.169	-0.343
62	-0.348	-0.194	-0.263	-0.348
63	-0.343	-0.199	-0.306	-0.348
64	-0.343	-0.199	-0.233	-0.308
65	-0.348	-0.199	-0.302	-0.338
66	0.967	0.849	0.854	0.956
67	0.665	0.677	0.580	0.624
68	0.224	0.286	0.255	0.168
69	-0.243	-0.180	-0.169	-0.239

TABULATED PRESSURE COEFFICIENTS

RUN 9, Q = 2.25 LB./FTSQ

ORIFICE NO.	CP VALUES AT ALPHA ANGLE SETTINGS 0	3	6	9
70	-0.489	-0.422	-0.332	-0.452
71	-0.815	-0.725	-0.567	-0.645
72	-0.719	-0.683	-0.524	-0.541
73	-0.574	-0.520	-0.426	-0.427
74	-0.469	0.090	-0.327	-0.338
75	-0.268	-0.217	-0.190	-0.343
76	-0.223	-0.110	-0.165	-0.323
77	-0.132	-0.059	-0.096	-0.248
78	-0.127	-0.087	-0.058	-0.244
79	-0.022	-0.050	-0.079	-0.080

TABULATED PRESSURE COEFFICIENTS

RUN 10, Q = 3.00 LB./FTSQ

ORIFICE NO.	C_p VALUES AT ALPHA ANGLE SETTINGS 0	3	6	9
1	-0.307	0.035	-1.979	-2.864
2	-0.533	-1.388	-2.124	-2.974
3	-0.626	-1.356	-1.992	-2.648
4	-0.660	-1.270	-1.711	-2.292
5	-0.698	-1.155	-1.484	-1.781
6	-0.698	-1.290	-1.383	-1.534
7	-0.756	-1.075	-1.230	-1.445
8	-0.732	-1.023	-1.142	-1.346
9	-0.893	-1.155	-1.115	-1.363
10	-0.897	-1.155	-1.217	-1.325
11	-0.890	-1.100	-1.196	-1.212
12	-0.921	-1.096	-1.162	-1.195
13	-0.910	-1.096	-1.162	-1.123
14	-0.886	-1.020	-1.068	-1.082
15	-0.807	-0.909	-0.807	-0.759
16	-0.698	-0.617	-0.664	-0.499
17	-0.033	-0.374	-0.431	-0.423
18	-0.156	-0.222	-0.288	-0.262
19	0.843	0.943	0.879	0.635
20	0.825	1.000	1.000	0.850
21	0.734	0.923	1.000	0.957
22	0.590	0.770	0.879	1.000
23	0.445	0.598	0.738	0.828

TABULATED PRESSURE COEFFICIENTS

RUN 10, Q = 3.CC LB./FTSQ

ORIFICE NO.	CP VALUES AT ALPHA ANGLE SETTINGS 0	3	6	9
24	0.282	0.483	0.617	0.678
25	0.174	0.387	0.516	0.613
26	0.146	0.292	0.396	0.441
27	0.101	0.215	0.274	0.334
28	0.101	0.196	0.234	0.269
29	0.101	0.100	0.174	0.226
30	0.101	0.100	0.134	0.097
31	0.101	0.148	0.174	0.140
32	0.146	0.215	0.234	0.226
33	0.155	0.234	0.275	0.200
34	0.445	0.483	0.335	0.355
35	0.499	0.579	0.597	0.635
36	-0.811	-0.971	-0.695	-0.410
37	-0.382	-0.520	-0.454	-0.314
38	-0.303	-0.374	-0.373	-0.255
39	-0.214	-0.222	-0.268	-0.190
40	-0.139	-0.166	-0.160	-0.183
41	-0.074	-0.090	-0.122	-0.183
42	-0.005	-0.069	-0.051	-0.087
43	0.680	0.713	0.718	0.678
44	0.654	0.617	0.617	0.592
45	0.499	0.502	0.496	0.463
46	0.427	0.407	0.436	0.377

TABULATED PRESSURE COEFFICIENTS

RUN 10, Q = 3.00 LB./FTSQ

ORIFICE NO.	CP VALUES AT ALPHA ANGLE SETTINGS 0	3	6	9
47	0.391	0.387	0.396	0.312
48	0.336	0.349	0.355	0.269
49	0.300	0.234	0.234	0.097
50	0.264	0.215	0.134	0.054
51	-3.893	-4.039	-3.913	-3.896
52	0.084	-3.602	-3.432	-3.409
53	-3.049	-3.164	-3.025	-2.971
54	-2.806	-2.963	-2.792	-2.741
55	-1.610	-2.786	-2.697	-2.590
56	-2.288	-2.314	-2.036	-1.808
57	-1.658	-1.707	-1.535	-1.270
58	-1.263	-1.270	-0.973	-0.742
59	-0.982	-0.923	-0.610	-0.410
60	-0.362	-0.357	-0.322	-0.255
61	-0.249	-0.298	-0.309	-0.293
62	-0.252	-0.295	-0.309	-0.266
63	-0.303	-0.357	-0.363	-0.314
64	-0.303	-0.353	-0.363	-0.314
65	-0.300	-0.374	-0.322	-0.259
66	0.931	0.875	0.890	0.944
67	0.687	0.698	0.694	0.728
68	0.218	0.268	0.209	0.255
69	-0.231	-0.180	-0.214	-0.183

TABULATED PRESSURE COEFFICIENTS

RUN 10, Q = 3.00 LB./FTSQ

ORIFICE NO.	CP VALUES AT ALPHA ANGLE SETTINGS 0	3	6	9
70	-0.513	-0.471	-0.434	-0.389
71	-0.763	-0.766	-0.705	-0.537
72	-0.670	-0.728	-0.627	-0.471
73	-0.540	-0.642	-0.549	-0.386
74	-0.447	-0.569	-0.444	-0.255
75	-0.231	-0.298	-0.309	-0.283
76	-0.139	-0.187	-0.217	-0.183
77	-0.077	-0.069	-0.143	-0.108
78	-0.005	-0.090	-0.139	-0.087
79	-0.005	-0.052	-0.048	-0.015

TABULATED PRESSURE COEFFICIENTS

RUN 11, Q = 5.CC LB./FTSQ

ORIFICE NO.	CP VALUES AT ALPHA ANGLE SETTINGS 0	3	6	9
1	-0.311	-0.969	-2.024	-3.122
2	-0.619	-1.217	-2.208	-3.219
3	-0.689	-1.227	-2.044	-2.914
4	-0.726	-1.159	-1.820	-2.504
5	-0.761	-1.048	-1.542	-1.873
6	-0.774	-1.005	-1.407	-1.718
7	-0.820	-1.005	-1.360	-1.620
8	-0.857	-0.988	-1.284	-1.523
9	-0.999	-1.097	-1.324	-1.558
10	-1.002	-1.052	-1.299	-1.463
11	-1.015	-1.052	-1.250	-1.381
12	-1.050	-1.052	-1.250	-1.377
13	-1.059	-1.052	-1.239	-1.330
14	-0.997	-1.005	-1.189	-1.233
15	-0.875	-0.898	-0.869	-0.918
16	-0.678	-0.575	-0.709	-0.743
17	-0.368	-0.351	-0.476	-0.493
18	-0.186	-0.174	-0.328	-0.409
19	0.936	1.006	0.911	0.648
20	0.793	0.959	0.958	0.840
21	0.686	0.887	0.958	0.944
22	0.518	0.754	0.861	0.900
23	0.398	0.570	0.677	0.780

TABULATED PRESSURE COEFFICIENTS

RUN 11, Q = 5.00 LB./FTSQ

ORIFICE NO.	CP VALUES AT ALPHA ANGLE SETTINGS 0	3	6	9
24	0.256	0.461	0.567	0.648
25	0.194	0.374	0.444	0.574
26	0.138	0.269	0.370	0.466
27	0.076	0.209	0.285	0.380
28	0.076	0.164	0.211	0.295
29	0.041	0.151	0.168	0.236
30	0.041	0.134	0.141	0.222
31	0.081	0.151	0.163	0.233
32	0.122	0.164	0.175	0.233
33	0.197	0.211	0.211	0.315
34	0.411	0.434	0.433	0.453
35	0.566	0.572	0.554	0.572
36	-1.013	-0.947	-0.857	-0.646
37	-0.523	-0.560	-0.581	-0.480
38	-0.357	-0.400	-0.478	-0.420
39	-0.252	-0.257	-0.377	-0.336
40	-0.140	-0.176	-0.317	-0.276
41	-0.127	-0.107	-0.245	-0.249
42	-0.031	-0.071	-0.133	-0.183
43	0.649	0.517	0.677	0.659
44	0.577	0.572	0.579	0.561
45	0.470	0.461	0.480	0.466
46	0.402	0.387	0.383	0.380

TABULATED PRESSURE COEFFICIENTS

RUN 11, Q = 5.00 LB./FTSQ

ORIFICE NO.	CP VALUES AT ALPHA ANGLE SETTINGS 0	3	6	9
47	0.354	0.376	0.334	0.331
48	0.297	0.314	0.285	0.269
49	0.242	0.222	0.197	0.224
50	0.183	0.175	0.101	0.083
51	-3.958	-3.872	-4.072	-4.043
52	-3.468	-3.371	-3.559	-3.472
53	-3.083	-2.982	-3.153	-3.013
54	-2.843	-2.760	-2.892	-2.830
55	-2.707	-2.598	-2.711	-2.557
56	-2.062	-1.894	-1.876	-1.716
57	-1.599	-1.403	-1.286	-1.027
58	-1.096	-0.808	-0.622	-0.482
59	-0.586	-0.479	-0.454	-0.431
60	-0.357	-0.327	-0.429	-0.431
61	-0.359	-0.315	-0.454	-0.431
62	-0.357	-0.353	-0.463	-0.469
63	-0.400	-0.345	-0.476	-0.449
64	-0.403	-0.351	-0.460	-0.480
65	-0.365	-0.357	-0.427	-0.420
66	0.951	1.006	0.976	0.975
67	0.704	0.711	0.688	0.725
68	0.242	0.265	0.211	0.187
69	-0.258	-0.257	-0.303	-0.263

TABULATED PRESSURE COEFFICIENTS

RUN 11, Q = 5.00 LB./FTSQ

ORIFICE NO.	CP VALUES AT ALPHA ANGLE SETTINGS 0	3	6	9
70	-0.556	-0.481	-0.512	-0.469
71	-0.919	-0.855	-0.795	-0.655
72	-0.868	-0.819	-0.770	-0.637
73	-0.678	-0.661	-0.685	-0.540
74	-0.617	-0.575	-0.604	-0.469
75	-0.319	-0.351	-0.447	-0.407
76	-0.195	-0.246	-0.303	-0.311
77	-0.138	-0.150	-0.243	-0.243
78	-0.114	-0.094	-0.191	-0.201
79	-0.083	-0.035	-0.119	-0.159

TABULATED PRESSURE COEFFICIENTS

RUN 12. Q = 10.00 LB./FTSQ

ORIFICE NO.	CP VALUES AT ALPHA ANGLE SETTINGS 0	3	6	9
1	-0.061	-0.933	-1.749	-2.839
2	-0.444	-1.230	-1.972	-2.985
3	-0.540	-1.211	-1.856	-2.704
4	-0.609	-1.170	-1.676	-2.346
5	-0.662	-1.065	-1.388	-1.753
6	-0.686	-0.971	-1.284	-1.601
7	-0.741	-1.027	-1.219	-1.507
8	-0.801	-1.039	-1.158	-1.392
9	-0.921	-1.126	-1.199	-1.344
10	-0.948	-1.126	-1.192	-1.357
11	-0.933	-1.115	-1.138	-1.298
12	-0.975	-1.119	0.078	-1.274
13	-0.999	-1.126	-1.115	-1.238
14	-0.959	-1.088	-1.115	-1.167
15	-0.836	-0.908	-0.790	-0.851
16	-0.542	-0.628	-0.589	-0.673
17	-0.330	-0.386	-0.388	-0.442
18	-0.188	-0.227	-0.274	-0.326
19	0.875	0.978	0.925	0.714
20	0.752	0.970	0.983	0.886
21	0.634	0.869	0.979	0.995
22	0.458	0.697	0.843	0.918
23	0.326	0.532	0.689	0.792

TABULATED PRESSURE COEFFICIENTS

RUN 12, Q = 10.00 LB./FTSQ

ORIFICE NO.	CP VALUES AT ALPHA ANGLE SETTINGS 0	3	6	9
24	0.236	0.408	0.552	0.649
25	0.176	0.327	0.469	0.572
26	0.109	0.228	0.351	0.454
27	0.057	0.172	0.283	0.376
28	0.043	0.140	0.248	0.292
29	0.026	0.116	0.184	0.252
30	0.026	0.140	0.174	0.215
31	0.043	0.107	0.174	0.215
32	0.080	0.141	0.184	0.240
33	0.266	0.240	0.280	0.292
34	0.388	0.438	0.460	0.456
35	0.555	0.557	0.576	0.573
36	-1.071	-1.134	-0.831	-0.690
37	-0.710	-0.778	-0.596	-0.541
38	-0.444	-0.524	-0.460	-0.440
39	-0.312	-0.356	-0.359	-0.356
40	-0.215	-0.268	-0.270	-0.297
41	-0.144	-0.188	-0.216	-0.237
42	-0.059	-0.086	-0.111	-0.141
43	0.639	0.675	0.688	0.687
44	0.556	0.557	0.599	0.573
45	0.445	0.476	0.498	0.471
46	0.375	0.383	0.404	0.393

TABULATED PRESSURE COEFFICIENTS

RUN 12, Q = 10.00 LB./FTSQ

ORIFICE NO.	CP VALUES AT ALPHA ANGLE SETTINGS 0	3	6	9
47	0.321	0.339	0.356	0.340
48	0.266	0.290	0.280	0.268
49	0.201	0.240	0.208	0.210
50	0.134	0.136	0.108	0.107
51	-3.765	-3.882	-3.682	-3.765
52	-3.283	-3.391	-3.209	-3.256
53	-2.940	-3.006	-2.831	-2.876
54	-2.673	-2.683	-2.399	-2.454
55	-2.469	-2.434	-2.204	-2.151
56	-1.801	-1.702	-1.488	-1.405
57	-1.180	-0.983	-0.696	-0.599
58	-0.602	-0.486	-0.361	-0.410
59	-0.439	-0.442	-0.418	-0.393
60	-0.415	-0.442	-0.395	-0.416
61	-0.415	-0.443	-0.418	-0.434
62	-0.439	-0.467	-0.442	-0.464
63	-0.463	-0.499	-0.465	-0.488
64	-0.444	-0.476	-0.460	-0.481
65	-0.415	-0.436	-0.412	-0.434
66	0.953	1.003	0.966	0.966
67	0.712	0.735	0.711	0.702
68	0.205	0.203	0.203	0.215
69	-0.330	-0.337	-0.270	-0.257

TABULATED PRESSURE COEFFICIENTS

RUN 12, Q = 10.00 LB./FTSQ

ORIFICE NO.	CP VALUES AT ALPHA ANGLE SETTINGS 0	3	6	9
70	-0.590	-0.622	-0.519	-0.482
71	-0.801	-1.019	-0.820	-0.762
72	-0.988	-0.942	-0.809	-0.714
73	-0.843	-0.878	-0.696	-0.607
74	-0.716	-0.747	-0.618	-0.550
75	-0.415	-0.468	-0.477	-0.441
76	-0.300	-0.312	-0.347	-0.333
77	-0.186	-0.213	-0.235	-0.251
78	-0.156	-0.157	-0.190	-0.213
79	-0.095	-0.101	-0.134	-0.142

TABULATED PRESSURE COEFFICIENTS

RUN 32, Q = 2.25 LB./FTSQ

ORIFICE NO.	CP VALUES AT ALPHA ANGLE SETTINGS 0	3	6	9
1	-1.101	-2.269	-3.788	-4.856
2	-1.412	-2.415	-3.870	-4.781
3	-1.463	-2.291	-3.519	-4.247
4	-1.330	-2.016	-3.114	-3.762
5	-1.279	-1.790	-2.435	-2.605
6	-1.284	-1.590	-2.204	-2.438
7	-1.206	-1.564	-2.165	-2.226
8	-1.284	-1.510	-2.030	-2.076
9	-1.412	-1.617	-2.136	-2.221
10	-1.261	-1.714	-2.083	-2.076
11	-1.550	-1.688	-2.059	-2.076
12	-1.563	-1.812	-2.165	-1.974
13	-1.692	-1.812	-2.189	-2.102
14	-1.792	-1.879	-2.189	-2.076
15	-1.820	-1.892	-2.218	-2.067
16	-1.953	-2.140	-2.435	-2.221
17	-2.415	-2.491	-2.815	-2.645
18	-3.937	-3.986	-3.755	-3.987
19	0.908	0.882	0.606	0.114
20	1.000	0.957	0.803	0.468
21	0.977	0.981	0.926	0.801
22	0.794	0.882	1.000	0.979
23	0.680	0.857	0.951	0.934

TABULATED PRESSURE COEFFICIENTS

RUN 32, Q = 2.25 LB./FTSQ

ORIFICE NO.	CP VALUES AT ALPHA ANGLE SETTINGS 0	3	6	9
24	0.588	0.733	0.827	0.890
25	0.497	0.634	0.754	0.801
26	0.405	0.560	0.655	0.735
27	0.359	0.485	0.556	0.668
28	0.337	0.386	0.507	0.602
29	0.337	0.361	0.482	0.557
30	0.337	0.361	0.482	0.535
31	0.337	0.386	0.482	0.535
32	0.359	0.411	0.507	0.557
33	0.497	0.585	0.581	0.646
34	0.611	0.609	0.680	0.668
35	0.680	0.733	0.729	0.646
36	-1.715	-1.763	-2.030	-1.877
37	-1.307	-1.315	-1.457	-1.356
38	-0.817	-0.796	-0.970	-0.849
39	-0.326	-0.414	-0.455	-0.421
40	0.109	0.060	0.032	-0.001
41	0.008	0.109	-0.021	0.087
42	-0.400	-0.588	-0.807	-0.372
43	0.771	0.783	0.803	0.713
44	0.703	0.733	0.803	0.779
45	0.565	0.684	0.729	0.757
46	0.565	0.609	0.729	0.668

TABULATED PRESSURE COEFFICIENTS

RUN 32, Q = 2.25 LB./FTSQ

ORIFICE CP VALUES AT ALPHA ANGLE SETTINGS

NO.	0	3	6	9
47	0.520	0.585	0.680	0.624
48	0.520	0.560	0.680	0.624
49	0.451	0.560	0.581	0.557
50	0.474	0.485	0.581	0.513
51	-1.490	-1.666	-1.972	-1.952
52	-2.109	-2.291	-2.546	-2.513
53	-2.622	-2.637	-2.989	-2.870
54	-2.800	-2.837	-3.350	-3.117
55	-2.828	-2.939	-3.374	-3.069
56	-2.777	-2.837	-3.225	-3.069
57	-2.594	-2.615	-3.032	-2.844
58	-2.260	-2.384	-2.685	-2.473
59	-2.154	-2.389	-2.627	-2.473
60	-1.847	-2.012	-2.204	-1.979
61	-1.563	-1.595	-1.784	-1.727
62	-1.229	-1.315	-1.457	-1.356
63	-1.101	-1.045	-1.264	-1.180
64	-0.830	-0.889	-1.052	-0.963
65	-0.345	-0.690	-0.744	-0.756
66	-1.953	-1.941	-2.030	-1.851
67	-3.904	-3.813	-4.063	-3.638
68	-5.096	-5.038	-5.392	-4.953
69	-5.897	-5.836	-6.284	-5.774

TABULATED PRESSURE COEFFICIENTS

RUN 32, Q = 2.25 LB./FTSQ

ORIFICE NO.	CP VALUES AT ALPHA ANGLE SETTINGS 0	3	6	9
70	-6.182	-6.710	-6.529	-6.176
71	-6.337	-6.187	-6.447	-5.902
72	-5.448	-5.362	-5.826	-5.430
73	-4.170	-4.088	-4.549	-4.207
74	-3.552	-3.467	-2.868	-3.519
75	-2.516	-2.491	-2.786	-2.623
76	-1.705	-1.785	-2.011	-1.864
77	-1.206	-1.240	-1.457	-1.281
78	-0.844	-0.916	-0.970	-1.008
79	-0.606	-0.663	-0.705	-0.637

TABULATED PRESSURE COEFFICIENTS

RUN 33, Q = 3.00 LB./FTSQ

ORIFICE NO.	CP VALUES AT ALPHA ANGLE SETTINGS 0	3	6	9
1	-0.923	-1.983	-3.343	-4.858
2	-1.204	-2.170	-3.401	-4.858
3	-1.051	-2.095	-3.098	-4.518
4	-1.117	-1.800	-2.681	-3.661
5	-1.029	-1.616	-1.976	-2.561
6	-1.011	-1.412	-1.942	-2.291
7	-1.029	-1.429	-1.717	-2.200
8	-1.104	-1.356	-1.660	-2.035
9	-1.219	-1.468	-1.754	-2.028
10	-1.291	-1.406	-1.734	-1.970
11	-1.310	-1.668	-1.717	-1.950
12	-1.378	-1.560	-1.848	-1.603
13	-1.484	-1.632	-1.841	-1.886
14	-1.434	-1.652	-1.848	-1.913
15	-1.484	-1.652	-1.848	-1.913
16	-1.571	-1.471	-1.942	-2.048
17	-1.886	-2.059	-1.929	-2.304
18	-2.870	-3.093	-3.343	-3.421
19	0.970	0.889	0.587	0.082
20	0.970	0.963	0.737	0.479
21	0.895	1.000	0.962	0.800
22	0.687	0.908	1.000	0.989
23	0.592	0.760	0.887	0.932

TABULATED PRESSURE COEFFICIENTS

RUN 33, Q = 3.00 LB./FTSQ

ORIFICE NO.	CP VALUES AT ALPHA ANGLE SETTINGS			
	0	3	6	9
24	0.479	0.630	0.775	0.838
25	0.385	0.575	0.682	0.800
26	0.309	0.427	0.549	0.611
27	0.290	0.390	0.512	0.573
28	0.233	0.353	0.436	0.536
29	0.233	0.335	0.418	0.479
30	0.196	0.335	0.380	0.403
31	0.233	0.335	0.399	0.441
32	0.252	0.353	0.418	0.422
33	0.460	0.520	0.548	0.573
34	0.573	0.593	0.624	0.630
35	0.668	0.686	0.718	0.744
36	-1.497	-1.616	-1.670	-1.724
37	-1.029	-1.153	-1.206	-1.292
38	-0.662	-0.766	-0.863	-0.871
39	-0.326	-0.414	-0.453	-0.567
40	0.092	-0.040	-0.050	-0.128
41	0.039	-0.063	0.024	-0.054
42	-0.241	-0.132	-0.222	-0.321
43	0.744	0.741	0.775	0.762
44	0.687	0.723	0.756	0.744
45	0.611	0.612	0.831	0.668
46	0.555	0.557	0.606	0.611

TABULATED PRESSURE COEFFICIENTS

RUN 33, Q = 3.CO LB./FTSQ

ORIFICE NO.	CP VALUES AT ALPHA ANGLE SETTINGS 0	3	6	9
47	0.536	0.538	0.587	0.573
48	0.498	0.520	0.568	0.573
49	0.403	0.446	0.530	0.517
50	0.422	0.409	0.474	0.460
51	-1.802	-1.983	-2.191	-2.446
52	-2.238	-2.446	-2.624	-2.787
53	-2.518	-2.725	-2.984	-3.111
54	-2.692	-2.945	-3.155	-3.259
55	-2.605	-2.909	-3.078	-3.279
56	-2.079	-2.761	-2.984	-3.053
57	-2.325	-2.594	-2.681	-2.787
58	-2.110	-2.298	-2.433	-2.564
59	-1.992	-2.095	-2.191	-2.291
60	-1.658	-1.780	-1.868	-1.950
61	-1.325	-1.392	-1.525	-1.613
62	-1.098	-1.189	-1.243	-1.289
63	-0.839	-0.989	-0.941	-1.016
64	-0.662	-0.766	-0.732	-0.813
65	-0.475	-0.526	-0.544	-0.253
66	-0.836	-0.874	-0.863	-0.813
67	-2.309	-2.446	-2.547	-2.561
68	-3.430	-3.628	-3.720	-3.796
69	-4.302	-4.406	-4.573	-4.629

TABULATED PRESSURE COEFFICIENTS

RUN 33, Q = 3.CO LB./FTSQ

ORIFICE NO.	CP VALUES AT ALPHA ANGLE SETTINGS 0	3	6	9
70	-4.707	-4.626	-4.798	-5.125
71	-4.729	-4.780	-4.819	-5.108
72	-3.938	-4.216	-4.345	-4.366
73	-3.128	-3.352	-3.495	-3.509
74	-2.518	-2.778	-2.849	-2.939
75	-1.904	-1.983	-2.113	-2.142
76	-1.325	-1.392	-1.509	-1.515
77	-0.905	-0.949	-1.055	-1.056
78	-0.640	-0.690	-0.712	-0.719
79	-0.397	-0.414	-0.433	-0.469

TABULATED PRESSURE COEFFICIENTS

RUN 34, Q = 5.00 LB./FTSQ

ORIFICE NO.	CP VALUES AT ALPHA ANGLE SETTINGS 0	3	6	9
1	-0.810	-1.888	-3.136	-4.694
2	-1.098	-2.134	-3.192	-4.637
3	-1.112	-2.044	-2.998	-4.239
4	-1.112	-1.779	-2.486	-3.526
5	-1.033	-1.535	-1.975	-2.584
6	-1.039	-1.381	-1.779	-2.342
7	-1.043	-1.467	-1.689	-2.233
8	-1.082	-1.429	-1.621	-2.048
9	-1.226	-1.523	-1.681	-2.074
10	-1.256	-1.562	-1.681	-2.014
11	-1.285	-1.523	-1.650	-1.980
12	-1.356	-1.619	-1.687	-1.967
13	-1.416	-1.665	-1.734	-1.967
14	-1.485	-1.677	-1.734	-1.965
15	-1.437	-1.640	-1.623	-1.874
16	-1.437	-1.650	-1.642	-1.833
17	-1.639	-1.759	-1.794	-2.001
18	-2.326	-2.545	-2.526	-3.084
19	0.973	0.849	0.667	0.147
20	0.912	0.913	0.832	0.487
21	0.843	0.951	0.936	0.842
22	0.683	0.809	0.936	0.915
23	0.541	0.636	0.797	0.853

TABULATED PRESSURE COEFFICIENTS

RUN 34, Q = 5.00 LB./FTSQ

ORIFICE NO.	CP VALUES AT ALPHA ANGLE SETTINGS			
	0	3	6	9
24	0.444	0.517	0.710	0.798
25	0.379	0.469	0.624	0.710
26	0.276	0.363	0.509	0.555
27	0.237	0.269	0.402	0.474
28	0.181	0.244	0.359	0.415
29	0.175	0.187	0.346	0.364
30	0.175	0.231	0.299	0.353
31	0.219	0.204	0.309	0.353
32	0.237	0.246	0.346	0.362
33	0.424	0.409	0.447	0.477
34	0.503	0.471	0.509	0.542
35	0.641	0.619	0.614	0.655
36	-1.627	-1.756	-1.746	-1.829
37	-1.157	-1.312	-1.276	-1.395
38	-0.891	-0.962	-1.035	-1.093
39	-0.590	-0.751	-0.751	-0.808
40	-0.239	-0.430	-0.433	-0.510
41	-0.204	-0.292	-0.277	-0.298
42	-0.166	-0.236	-0.233	-0.279
43	0.695	0.636	0.698	0.723
44	0.663	0.619	0.640	0.674
45	0.604	0.517	0.575	0.591
46	0.505	0.502	0.554	0.555

TABULATED PRESSURE COEFFICIENTS

RUN 34, Q = 5.00 LB./FTSQ

ORIFICE NO.	CP VALUES AT ALPHA ANGLE SETTINGS 0	3	6	9
47	0.539	0.469	0.544	0.523
48	0.495	0.469	0.509	0.506
49	0.460	0.409	0.461	0.483
50	0.460	0.409	0.464	0.468
51	-2.531	-2.839	-2.902	-3.329
52	-2.803	-3.262	-3.192	-3.390
53	-2.947	-3.133	-3.245	-3.520
54	-3.078	-3.029	-3.342	-3.607
55	-3.080	-2.968	-3.274	-3.509
56	-2.835	-2.887	-3.237	-3.329
57	-2.460	-2.733	-2.756	-3.022
58	-2.166	-2.368	-2.340	-2.514
59	-1.943	-2.128	-2.141	-2.278
60	-1.639	-1.771	-1.787	-1.882
61	-1.250	-1.423	-1.376	-1.474
62	-0.991	-1.066	-1.039	-1.140
63	-0.691	-0.812	-0.741	-0.761
64	-0.407	-0.547	-0.505	-0.510
65	-0.284	-0.315	-0.336	-0.364
66	0.055	-0.061	0.007	0.032
67	-1.333	-1.433	-1.368	-1.476
68	-1.935	-2.468	-2.390	-2.576
69	-3.040	-3.235	-3.227	-3.341

TABULATED PRESSURE COEFFICIENTS

RUN 34, Q = 5.CO LB./FTSQ

ORIFICE NO.	CP VALUES AT ALPHA ANGLE SETTINGS 0	3	6	9
70	-3.285	-3.463	-3.451	-3.629
71	-3.465	-3.671	-3.611	-3.786
72	-3.082	-3.275	-3.247	-3.461
73	-2.610	-2.758	-2.719	-3.165
74	-2.118	-2.313	-2.246	-2.372
75	-1.605	-1.759	-1.736	-1.833
76	-1.181	-1.314	-1.319	-1.427
77	-0.837	-0.962	-0.969	-1.061
78	-0.585	-0.739	-0.698	-0.793
79	-0.247	-0.386	-0.361	-0.457

TABULATED PRESSURE COEFFICIENTS

RUN 35, Q = 10.00 LB./FTSQ

ORIFICE NO.	CP VALUES AT ALPHA ANGLE SETTINGS 0	3	6	9
1	-0.574	-1.550	-2.430	-3.904
2	-0.889	-1.684	-2.644	-3.926
3	-0.945	-1.634	-2.441	-3.585
4	-0.969	-1.555	-2.070	-2.935
5	-0.962	-1.310	-1.688	-2.208
6	-0.991	-1.265	-1.560	-2.013
7	-1.036	-1.257	-1.486	-1.880
8	-1.070	-1.216	-1.485	-1.759
9	-1.234	-1.532	-1.531	-1.783
10	-1.285	-1.509	-1.493	-1.741
11	-1.296	-1.526	-1.479	-1.688
12	-1.372	-1.503	-1.503	-1.682
13	-1.617	-1.509	-1.527	-1.700
14	-1.501	-1.505	-1.532	-1.682
15	-1.383	-1.406	-1.461	-1.528
16	-1.345	-1.283	-1.346	-1.458
17	-1.352	-1.288	-1.456	-1.434
18	-1.727	-1.685	-1.705	-1.794
19	0.947	0.960	0.822	0.469
20	0.861	0.960	0.919	0.728
21	0.739	0.936	0.971	0.923
22	0.560	0.783	0.908	0.959
23	0.392	0.640	0.780	0.871

TABULATED PRESSURE COEFFICIENTS

RUN 35, Q = 10.00 LB./FTSQ

ORIFICE NO.	CP VALUES AT ALPHA ANGLE SETTINGS 0	3	6	9
24	0.303	0.519	0.658	0.776
25	0.244	0.430	0.561	0.693
26	0.151	0.347	0.461	0.552
27	0.104	0.246	0.374	0.480
28	0.097	0.246	0.329	0.427
29	0.085	0.210	0.293	0.391
30	0.073	0.210	0.293	0.363
31	0.086	0.229	0.288	0.342
32	0.127	0.234	0.295	0.362
33	0.348	0.407	0.429	0.498
34	0.460	0.514	0.548	0.552
35	0.590	0.644	0.664	0.688
36	-1.426	-1.532	-1.358	-1.405
37	-1.119	-1.062	-1.068	-1.144
38	-0.890	-0.860	-0.876	-0.955
39	-0.710	-0.657	-0.679	-0.782
40	-0.461	-0.467	-0.489	-0.547
41	-0.346	-0.318	-0.372	-0.441
42	-0.216	-0.218	-0.280	-0.376
43	0.689	0.733	0.740	0.753
44	0.634	0.668	0.688	0.693
45	0.559	0.591	0.589	0.611
46	0.498	0.549	0.553	0.581

TABULATED PRESSURE COEFFICIENTS

RUN 35, Q = 10.00 LB./FTSQ

ORIFICE NO.	CP VALUES AT ALPHA ANGLE SETTINGS 0	3	6	9
47	0.472	0.490	0.530	0.539
48	0.435	0.478	0.508	0.508
49	0.422	0.432	0.478	0.483
50	0.403	0.432	0.467	0.496
51	-3.511	-3.490	-3.495	-3.651
52	-3.484	-3.465	-3.471	-3.609
53	-3.444	-3.382	-3.368	-3.477
54	-3.379	-3.323	-3.293	-3.420
55	-3.269	-3.233	-3.194	-3.295
56	-2.962	-2.914	-2.881	-2.928
57	-2.658	-2.562	-2.518	-2.551
58	-2.160	-2.122	-2.047	-2.057
59	-1.952	-1.895	-1.838	-1.824
60	-1.569	-1.473	-1.346	-1.287
61	-1.126	-0.943	-0.760	-0.612
62	-0.674	-0.530	-0.442	-0.478
63	-0.428	-0.397	-0.442	-0.501
64	-0.370	-0.401	-0.437	-0.535
65	-0.346	-0.383	-0.437	-0.517
66	0.675	0.706	0.688	0.676
67	-0.353	-0.319	-0.349	-0.346
68	-1.247	-1.205	-1.195	-1.270
69	-1.907	-1.866	-1.868	-1.965

TABULATED PRESSURE COEFFICIENTS

RUN 35, Q = 10.00 LB./FTSQ

ORIFICE NO.	CP VALUES AT ALPHA ANGLE SETTINGS 0	3	6	9
70	-2.161	-2.115	-2.100	-2.185
71	-2.390	-2.347	-2.349	-2.426
72	-2.190	-2.145	-2.129	-2.226
73	-1.912	-1.871	-1.869	-1.942
74	-1.604	-1.622	-1.590	-1.635
75	-1.273	-1.254	-1.236	-1.303
76	-0.969	-0.956	-0.975	-1.020
77	-0.724	-0.735	-0.743	-0.795
78	-0.549	-0.569	-0.610	-0.666
79	-0.328	-0.342	-0.390	-0.447

TABULATED PRESSURE COEFFICIENTS

RUN 36, Q = 2.25 LB./FTSQ

ORIFICE NO.	CP VALUES AT ALPHA ANGLE SETTINGS 0	3	6	9
1	-0.344	-1.223	-2.361	-3.258
2	-0.625	-1.451	-2.470	-3.398
3	-0.757	-1.405	-2.246	-3.034
4	-0.757	-1.302	-2.051	-2.525
5	-0.807	-1.219	-1.822	-2.156
6	-0.884	-1.195	-1.647	-1.877
7	-0.856	-1.163	-1.463	-1.762
8	-0.856	-1.088	-1.458	-1.488
9	-0.988	-1.223	-1.488	-1.687
10	-0.911	-1.219	-1.428	-1.597
11	-0.983	-1.163	-1.373	-1.488
12	-1.060	-1.195	-1.343	-1.373
13	-1.033	-1.116	-1.343	-1.318
14	-0.983	-1.116	-1.203	-1.318
15	-0.829	-1.028	-0.949	-0.914
16	-0.829	-0.720	-0.759	-0.729
17	-0.448	-0.403	-0.470	-0.590
18	-0.349	-0.329	-0.420	-0.475
19	1.000	1.000	0.895	0.712
20	0.892	1.000	0.966	0.880
21	0.785	0.949	0.966	1.000
22	0.596	0.822	1.000	1.000
23	0.381	0.619	0.752	0.856

TABULATED PRESSURE COEFFICIENTS

RUN 36, Q = 2.25 LB./FTSQ

ORIFICE NO.	CP VALUES AT ALPHA ANGLE SETTINGS 0	3	6	9
24	0.301	0.518	0.612	0.760
25	0.247	0.392	0.585	0.712
26	0.112	0.290	0.466	0.520
27	0.112	0.239	0.395	0.473
28	0.112	0.214	0.324	0.352
29	0.112	0.113	0.300	0.352
30	0.112	0.113	0.252	0.328
31	0.112	0.188	0.300	0.328
32	0.112	0.239	0.324	0.376
33	0.274	0.315	0.395	0.449
34	0.462	0.467	0.490	0.449
35	0.623	0.619	0.657	0.640
36	-0.757	-0.879	-0.734	-0.475
37	-0.448	-0.594	-0.590	-0.390
38	-0.349	-0.441	-0.475	-0.360
39	-0.217	-0.245	-0.306	-0.330
40	-0.167	-0.143	-0.276	-0.310
41	-0.118	-0.101	-0.196	-0.306
42	-0.077	-0.063	-0.196	-0.196
43	0.731	0.671	0.752	0.712
44	0.650	0.619	0.704	0.689
45	0.515	0.544	0.585	0.640
46	0.435	0.467	0.514	0.592

TABULATED PRESSURE COEFFICIENTS

RUN 36, Q = 2.25 LB./FTSQ

ORIFICE NO.	CP VALUES AT ALPHA ANGLE SETTINGS 0	3	6	9
47	0.409	0.392	0.443	0.544
48	0.381	0.341	0.347	0.376
49	0.301	0.265	0.347	0.328
50	0.247	0.113	0.252	0.161
51	-4.301	-4.474	-4.860	-4.765
52	-3.685	-3.952	-4.356	-4.131
53	-3.308	-3.449	-3.767	-3.653
54	-3.055	-3.245	-3.513	-3.423
55	-2.900	-3.049	-3.303	-3.059
56	-2.411	-2.457	-2.356	-2.161
57	-1.804	-1.857	-1.737	-1.463
58	-1.418	-1.326	-1.203	-0.899
59	-1.033	-1.088	-0.789	-0.645
60	-0.548	-0.566	-0.415	-0.475
61	-0.448	-0.459	-0.425	-0.500
62	-0.408	-0.455	-0.425	-0.475
63	-0.448	-0.483	-0.475	-0.585
64	-0.421	-0.459	-0.560	-0.530
65	-0.349	-0.473	-0.445	-0.525
66	0.753	0.929	0.952	0.767
67	0.626	0.826	0.787	0.732
68	0.345	0.449	0.393	0.448
69	-0.195	-0.012	-0.021	0.034

TABULATED PRESSURE COEFFICIENTS

RUN 36, Q = 2.25 LB./FTSQ

ORIFICE NO.	CP VALUES AT ALPHA ANGLE SETTINGS 0	3	6	9
70	-0.353	-0.194	-0.166	-0.196
71	-0.507	-0.594	-0.590	-0.340
72	-0.526	-0.590	-0.590	-0.540
73	-0.448	-0.487	-0.445	-0.475
74	-0.349	-0.459	-0.420	-0.360
75	-0.299	-0.376	-0.415	-0.330
76	-0.217	-0.329	-0.415	-0.221
77	-0.190	-0.133	-0.196	-0.186
78	-0.118	-0.143	-0.156	-0.221
79	-0.050	-0.012	-0.051	-0.166

TABULATED PRESSURE COEFFICIENTS

RUN 37, Q = 3.00 LB./FTSQ

ORIFICE NO.	CP VALUES AT ALPHA ANGLE SETTINGS 0	3	6	9
1	-0.314	-0.996	-2.093	-2.794
2	-0.559	-1.257	-2.316	-2.921
3	-0.698	-1.224	-2.154	-2.312
4	-0.657	-1.145	-1.888	-2.232
5	-0.732	-1.049	-1.725	-1.783
6	-0.756	-0.996	-1.542	-1.549
7	-0.742	0.085	-1.502	-1.482
8	-0.810	-0.917	-1.322	-1.311
9	-0.926	-0.996	-1.462	-1.378
10	-0.926	-0.996	-1.362	-1.311
11	-0.946	-0.996	-1.362	-1.275
12	-0.263	-1.079	-1.322	-1.218
13	-0.889	-1.049	-1.322	-1.141
14	-0.889	-0.976	-1.239	-1.084
15	-0.793	-0.828	-0.933	-0.783
16	-0.732	-0.568	-0.774	-0.595
17	-0.331	-0.400	-0.569	-0.481
18	-0.314	-0.271	-0.468	-0.388
19	0.951	0.954	0.860	0.713
20	0.874	1.000	0.940	0.897
21	0.739	0.954	1.000	1.000
22	0.546	0.818	0.960	1.000
23	0.430	0.593	0.721	0.877

TABULATED PRESSURE COEFFICIENTS

RUN 37, Q = 3.00 LB./FTSQ

ORIFICE CP VALUES AT ALPHA ANGLE SETTINGS

NO.	0	3	6	9
24	0.275	0.479	0.562	0.774
25	0.198	0.434	0.463	0.611
26	0.159	0.275	0.343	0.549
27	0.198	0.208	0.264	0.427
28	0.178	0.162	0.244	0.305
29	0.101	0.094	0.205	0.284
30	0.101	0.094	0.184	0.243
31	0.217	0.162	0.205	0.305
32	0.217	0.185	0.224	0.305
33	0.256	0.253	0.284	0.366
34	0.507	0.479	0.403	0.467
35	0.623	0.660	0.523	0.652
36	-0.793	-0.736	-0.670	-0.471
37	-0.463	-0.548	-0.591	-0.388
38	-0.314	-0.308	-0.486	-0.331
39	-0.276	-0.215	-0.392	-0.294
40	-0.181	-0.139	-0.338	-0.237
41	-0.100	-0.087	-0.306	-0.294
42	-0.045	-0.067	-0.209	-0.180
43	0.700	0.728	0.742	0.734
44	0.681	0.705	0.622	0.713
45	0.546	0.615	0.582	0.611
46	0.468	0.501	0.443	0.467

TABULATED PRESSURE COEFFICIENTS

RUN 37, Q = 3.00 LB./FTSQ

ORIFICE NO.	CP VALUES AT ALPHA ANGLE SETTINGS 0	3	6	9
47	0.410	0.434	0.403	0.427
48	0.391	0.343	0.383	0.366
49	0.294	0.321	0.284	0.324
50	0.236	0.253	0.224	0.202
51	-4.181	-4.061	-4.467	-4.046
52	-3.704	-3.504	-3.775	-3.403
53	-3.170	-3.115	-3.311	-3.049
54	-3.014	-2.875	-3.148	-2.878
55	-2.817	-2.763	-2.965	-2.386
56	-2.211	-2.071	-2.071	-1.646
57	-1.691	-1.517	-1.462	-1.084
58	-1.212	-0.924	-0.832	-0.632
59	-0.810	-0.568	-0.591	-0.481
60	-0.389	-0.380	-0.475	-0.445
61	-0.382	-0.380	-0.526	-0.438
62	-0.331	-0.364	-0.551	-0.381
63	-0.409	-0.383	-0.547	-0.481
64	-0.389	-0.380	-0.468	-0.481
65	-0.389	-0.403	-0.472	-0.461
66	0.812	0.843	0.894	0.817
67	0.700	0.767	0.832	0.781
68	0.349	0.414	0.465	0.443
69	-0.018	0.025	0.000	0.084

TABULATED PRESSURE COEFFICIENTS

RUN 37, Q = 3.00 LB./FTSQ

ORIFICE NO.	CP VALUES AT ALPHA ANGLE SETTINGS 0	3	6	9
70	-0.181	-0.179	-0.162	-0.160
71	-0.599	-0.472	-0.468	-0.498
72	-0.562	-0.551	-0.569	0.011
73	-0.542	-0.456	-0.468	-0.401
74	-0.355	-0.413	-0.464	-0.361
75	-0.331	-0.288	-0.407	-0.314
76	-0.256	-0.219	-0.346	-0.294
77	-0.181	-0.083	-0.184	-0.294
78	-0.103	-0.047	-0.162	-0.237
79	-0.083	-0.050	-0.101	-0.160

TABULATED PRESSURE COEFFICIENTS

RUN 38, Q = 5.00 LB./FTSQ

ORIFICE NO.	CP VALUES AT ALPHA ANGLE SETTINGS 0	3	6	9
1	-0.288	-1.056	-2.003	-3.117
2	-0.551	-1.327	-2.217	-3.255
3	-0.595	-1.246	-2.075	-2.943
4	-0.654	-1.185	-1.786	-2.506
5	-0.699	-1.113	-1.513	-1.879
6	-0.699	-1.066	-1.413	-1.707
7	-0.746	-1.018	-1.322	-1.596
8	-0.778	-1.018	-1.201	-1.503
9	-0.882	-1.106	-1.285	-1.518
10	-0.904	-1.079	-1.239	-1.423
11	-0.914	-1.066	-1.188	-1.372
12	-0.939	-1.066	-1.177	-1.319
13	-0.932	-1.066	-1.143	-1.270
14	-0.882	-1.056	-1.082	-1.182
15	-0.790	-0.888	-0.829	-0.845
16	-0.573	-0.601	-0.664	-0.646
17	-0.343	-0.435	-0.450	-0.471
18	-0.242	-0.325	-0.354	-0.347
19	0.902	0.949	0.877	0.725
20	0.811	0.985	0.983	0.876
21	0.709	0.900	0.936	0.958
22	0.526	0.710	0.838	0.765
23	0.388	0.532	0.709	0.831

TABULATED PRESSURE COEFFICIENTS

RUN 38, Q = 5.00 LB./FTSQ

ORIFICE NO.	CP VALUES AT ALPHA ANGLE SETTINGS 0	3	6	9
24	0.297	0.411	0.541	0.707
25	0.228	0.352	0.423	0.625
26	0.146	0.244	0.291	0.481
27	0.089	0.185	0.232	0.411
28	0.079	0.138	0.183	0.340
29	0.087	0.100	0.172	0.298
30	0.057	0.123	0.136	0.264
31	0.057	0.127	0.170	0.264
32	0.089	0.149	0.136	0.264
33	0.195	0.185	0.229	0.326
34	0.433	0.460	0.408	0.464
35	0.526	0.542	0.541	0.592
36	-0.780	-0.814	-0.689	-0.571
37	-0.585	-0.673	-0.604	-0.471
38	-0.378	-0.435	-0.496	-0.396
39	-0.217	-0.298	-0.352	-0.318
40	-0.128	-0.220	-0.282	-0.247
41	-0.081	-0.148	-0.244	-0.236
42	-0.006	-0.029	-0.138	-0.121
43	0.618	0.638	0.637	0.707
44	0.571	0.549	0.535	0.614
45	0.433	0.460	0.425	0.501
46	0.374	0.398	0.397	0.439

TABULATED PRESSURE COEFFICIENTS

RUN 38, Q = 5.00 LB./FTSQ

ORIFICE NO.	CP VALUES AT ALPHA ANGLE SETTINGS 0	3	6	9
47	0.329	0.352	0.297	0.362
48	0.284	0.293	0.242	0.291
49	0.215	0.244	0.195	0.227
50	0.152	0.185	0.123	0.140
51	-4.030	-4.180	-3.819	-4.103
52	-3.344	-3.475	-3.437	-3.529
53	-2.974	-3.058	-3.006	-3.104
54	-2.736	-2.831	-2.766	-2.668
55	-2.541	-2.546	-2.325	-2.170
56	-1.832	-1.735	-1.559	-1.456
57	-1.286	-1.102	-0.810	-0.646
58	-0.658	-0.529	-0.445	-0.471
59	-0.437	-0.446	-0.426	-0.458
60	-0.368	-0.400	-0.426	-0.422
61	-0.402	-0.383	-0.437	-0.440
62	-0.390	-0.433	-0.486	-0.471
63	-0.425	-0.423	-0.486	-0.509
64	-0.402	-0.425	-0.486	-0.509
65	-0.410	-0.423	-0.447	-0.458
66	0.926	0.985	0.947	0.913
67	0.754	0.841	0.830	0.889
68	0.388	0.401	0.423	0.477
69	-0.002	-0.012	0.017	0.078

TABULATED PRESSURE COEFFICIENTS

RUN 38, Q = 5.CO LB./FTSQ

ORIFICE NO.	CP VALUES AT ALPHA ANGLE SETTINGS 0	3	6	9
70	-0.230	-0.232	-0.197	-0.121
71	-0.504	-0.537	-0.496	-0.420
72	-0.595	-0.613	-0.556	-0.471
73	-0.551	-0.575	-0.545	-0.471
74	-0.490	-0.507	-0.496	-0.422
75	-0.380	-0.374	-0.390	-0.347
76	-0.274	-0.279	-0.305	-0.296
77	-0.091	-0.135	-0.246	-0.234
78	-0.059	-0.050	-0.138	-0.172
79	-0.059	-0.029	-0.127	-0.121

TABULATED PRESSURE COEFFICIENTS

RUN 39, Q = 10.00 LB./FTSQ

ORIFICE NO.	CP VALUES AT ALPHA ANGLE SETTINGS 0	3	6	9
1	-0.129	-0.782	-1.775	-2.765
2	-0.457	-1.069	-2.022	-2.922
3	-0.556	-1.051	-1.903	-2.640
4	-0.655	-1.011	-1.668	-2.256
5	-0.680	-0.934	-1.421	-1.706
6	-0.730	-0.906	-1.300	-1.535
7	-0.761	-0.905	-1.228	-1.458
8	-0.829	-0.911	-1.171	-1.345
9	-0.957	-1.022	-1.232	-1.380
10	-0.984	-1.039	-1.210	-1.322
11	-0.984	-0.993	-1.155	-1.251
12	-1.009	-1.016	-1.150	-1.202
13	-1.030	-1.020	-1.144	-1.197
14	-1.002	-0.969	-1.059	-1.099
15	-0.859	-0.776	-0.794	-0.784
16	-0.569	-0.535	-0.626	-0.607
17	-0.389	-0.354	-0.439	-0.423
18	-0.285	-0.260	-0.331	-0.341
19	0.903	0.977	0.939	0.761
20	0.754	0.952	0.975	0.912
21	0.643	0.870	0.962	0.988
22	0.445	0.682	0.837	0.947
23	0.333	0.507	0.661	0.794

TABULATED PRESSURE COEFFICIENTS

RUN 39, Q = 10.00 LB./FTSQ

ORIFICE NO.	CP VALUES AT ALPHA ANGLE SETTINGS 0	3	6	9
24	0.224	0.391	0.541	0.676
25	0.173	0.326	0.463	0.593
26	0.093	0.226	0.331	0.462
27	0.056	0.173	0.262	0.362
28	0.030	0.136	0.223	0.315
29	0.030	0.115	0.180	0.255
30	0.030	0.115	0.175	0.221
31	0.050	0.138	0.157	0.220
32	0.086	0.150	0.198	0.243
33	0.260	0.262	0.266	0.315
34	0.408	0.432	0.440	0.476
35	0.544	0.560	0.571	0.586
36	-0.891	-0.811	-0.712	-0.596
37	-0.780	-0.693	-0.607	-0.507
38	-0.501	-0.453	-0.475	-0.420
39	-0.309	-0.271	-0.375	-0.335
40	-0.192	-0.172	-0.271	-0.271
41	-0.130	-0.090	-0.198	-0.221
42	0.012	-0.006	-0.102	-0.111
43	0.650	0.675	0.680	0.699
44	0.551	0.554	0.578	0.592
45	0.451	0.484	0.463	0.491
46	0.383	0.402	0.392	0.409

TABULATED PRESSURE COEFFICIENTS

RUN 39, Q = 10.00 LB./FTSQ

ORIFICE NO.	CP VALUES AT ALPHA ANGLE SETTINGS 0	3	6	9
47	0.331	0.343	0.331	0.338
48	0.279	0.296	0.276	0.283
49	0.224	0.232	0.223	0.219
50	0.154	0.185	0.150	0.118
51	-3.955	-3.694	-3.828	-3.800
52	-3.403	-3.167	-3.250	-3.220
53	-3.001	-2.781	-2.847	-2.789
54	-2.679	-2.429	-2.426	-2.302
55	-2.370	-2.100	-2.077	-2.038
56	-1.659	-1.421	-1.311	-1.169
57	-0.914	-0.657	-0.540	-0.501
58	-0.475	-0.388	-0.416	-0.419
59	-0.464	-0.404	-0.445	-0.437
60	-0.452	-0.393	-0.445	-0.437
61	-0.457	-0.401	-0.445	-0.448
62	-0.483	-0.413	-0.470	-0.471
63	-0.501	-0.435	-0.500	-0.488
64	-0.500	-0.435	-0.481	-0.478
65	-0.461	-0.394	-0.442	-0.425
66	0.978	0.977	0.958	0.994
67	0.810	0.801	0.789	0.817
68	0.383	0.391	0.374	0.409
69	-0.046	-0.025	-0.018	0.002

TABULATED PRESSURE COEFFICIENTS

RUN 39, Q = 10.00 LB./FTSQ

ORIFICE NO.	CP VALUES AT ALPHA ANGLE SETTINGS 0	3	6	9
70	-0.260	-0.237	-0.228	-0.199
71	-0.631	-0.559	-0.554	-0.478
72	-0.722	-0.647	-0.632	-0.548
73	-0.706	-0.627	-0.601	-0.507
74	-0.631	-0.559	-0.559	-0.478
75	-0.489	-0.413	-0.458	-0.407
76	-0.285	-0.266	-0.369	-0.330
77	-0.155	-0.125	-0.223	-0.235
78	-0.173	-0.090	-0.168	-0.199
79	-0.086	-0.061	-0.138	-0.159

TABULATED PRESSURE COEFFICIENTS

RUN 40, Q = 2.25 LB./FTSQ

ORIFICE CP VALUES AT ALPHA ANGLE SETTINGS

NO.	0	3	6	9
1	-0.261	-0.988	-1.887	-2.626
2	-0.570	-1.192	-2.042	-2.677
3	-0.673	-1.137	-1.914	-2.390
4	-0.701	-1.115	-1.655	-2.032
5	-0.725	-0.961	-1.372	-1.653
6	-0.744	-0.961	-1.272	-1.429
7	-0.809	-0.933	-1.244	-1.353
8	-0.790	-0.911	-1.162	-1.248
9	-0.959	-1.010	-1.199	-1.248
10	-0.992	-1.010	-1.172	-1.176
11	-0.992	-0.929	-1.117	-1.109
12	-0.992	-0.979	-1.067	-1.067
13	-0.992	-0.988	-1.039	-1.105
14	-1.006	-0.961	-1.012	-0.949
15	-0.833	-0.807	-0.716	-0.679
16	-0.804	-0.553	-0.556	-0.536
17	-0.252	-0.181	-0.310	-0.321
18	0.039	0.009	-0.142	-0.300
19	1.000	0.946	0.891	0.685
20	0.809	1.000	0.973	0.868
21	0.672	0.864	1.000	0.974
22	0.509	0.755	0.864	1.000
23	0.399	0.537	0.702	0.816

TABULATED PRESSURE COEFFICIENTS

RUN 40, Q = 2.25 LB./FTSQ

ORIFICE NO.	CP VALUES AT ALPHA ANGLE SETTINGS 0	3	6	9
24	0.236	0.375	0.648	0.763
25	0.208	0.375	0.491	0.659
26	0.100	0.211	0.349	0.500
27	0.100	0.103	0.268	0.396
28	0.100	0.103	0.241	0.316
29	0.045	0.103	0.214	0.290
30	0.072	0.103	0.187	0.264
31	0.100	0.211	0.268	0.264
32	0.100	0.103	0.295	0.290
33	0.236	0.211	0.295	0.316
34	0.536	0.429	0.377	0.316
35	0.563	0.565	0.675	0.605
36	-0.861	-0.784	-0.657	-0.536
37	-0.463	-0.448	-0.374	-0.418
38	-0.434	-0.322	0.113	-0.359
39	-0.360	-0.195	-0.192	-0.253
40	-0.252	-0.145	-0.142	-0.232
41	-0.200	-0.095	-0.146	-0.228
42	-0.121	0.009	-0.041	-0.131
43	0.699	0.647	0.756	0.632
44	0.699	0.592	0.729	0.685
45	0.591	0.510	0.567	0.527
46	0.482	0.429	0.458	0.448

TABULATED PRESSURE COEFFICIENTS

RUN 40, Q = 2.25 LB./FTSQ

ORIFICE NO.	CP VALUES AT ALPHA ANGLE SETTINGS 0	3	6	9
47	0.427	0.320	0.427	0.396
48	0.399	0.320	0.377	0.316
49	0.317	0.266	0.295	0.264
50	0.263	0.157	0.241	0.185
51	-4.041	-3.870	-3.951	-3.646
52	-2.659	-3.358	-3.454	-3.149
53	-3.179	-2.932	-3.072	-2.816
54	-3.048	-2.665	-2.812	-2.673
55	-2.814	-2.542	-2.580	-2.483
56	-2.533	-2.284	-2.274	-2.150
57	-1.835	-1.545	-1.554	-1.560
58	-1.493	-1.115	-1.121	-1.105
59	-1.231	0.150	-0.812	-0.894
60	-0.570	-0.299	-0.274	-0.413
61	-0.360	-0.195	-0.192	-0.236
62	-0.360	-0.181	-0.196	-0.253
63	-0.439	-0.263	-0.169	-0.228
64	-0.360	-0.172	-0.192	-0.253
65	-0.360	-0.195	-0.192	-0.253
66	0.849	0.952	0.961	1.087
67	0.591	0.748	0.651	0.366
68	-0.041	0.213	0.086	-0.156
69	-0.580	-0.376	-0.452	-0.536

TABULATED PRESSURE COEFFICIENTS

RUN 40, Q = 2.25 LB./FTSQ

ORIFICE NO.	CP VALUES AT ALPHA ANGLE SETTINGS 0	3	6	9
70	-0.893	-0.707	-0.675	-0.658
71	-1.226	-0.988	-0.812	-0.797
72	-0.992	-0.625	-0.657	-0.607
73	-0.701	-0.575	-0.474	-0.515
74	-0.566	-0.381	-0.351	-0.418
75	-0.439	-0.272	-0.256	-0.321
76	-0.360	-0.122	-0.196	-0.253
77	-0.397	-0.063	-0.041	-0.156
78	-0.252	0.009	-0.014	-0.131
79	-0.200	0.104	-0.028	-0.135

TABULATED PRESSURE COEFFICIENTS

RUN 41, Q = 3.00 LB./FTSQ

ORIFICE NO.	CP VALUES AT ALPHA ANGLE SETTINGS 0	3	6	9
1	-0.315	-1.582	-2.150	-2.969
2	-0.664	-1.800	-2.420	-3.128
3	-0.683	-1.702	-2.246	-2.790
4	-0.753	-1.663	-1.880	-2.372
5	-0.848	-1.488	-1.647	-1.859
6	-0.933	-1.390	-1.588	-1.663
7	-0.933	-1.463	-1.463	-1.582
8	-0.871	-1.463	-1.378	-1.462
9	-0.974	-1.582	-1.463	-1.445
10	-1.036	-1.582	-1.403	-1.462
11	-1.077	-1.488	-1.359	-1.329
12	-1.077	-1.488	-1.322	-1.406
13	-1.099	-1.484	-1.326	-1.336
14	-1.055	-1.445	-1.292	-1.206
15	-0.952	-1.245	-0.941	-0.830
16	-0.808	-0.835	-0.712	-0.591
17	-0.289	-0.501	-0.435	-0.394
18	-0.020	-0.211	-0.235	-0.328
19	0.872	0.971	0.921	0.672
20	0.793	0.990	0.981	0.918
21	0.655	0.932	1.000	1.000
22	0.556	0.739	0.981	1.000
23	0.437	0.546	0.723	0.857

TABULATED PRESSURE COEFFICIENTS

RUN 41, Q = 3.00 LB./FTSQ

ORIFICE NO.	CP VALUES AT ALPHA ANGLE SETTINGS 0	3	6	9
24	0.299	0.372	0.585	0.651
25	0.240	0.333	0.505	0.630
26	0.101	0.236	0.366	0.446
27	0.101	0.217	0.268	0.363
28	0.101	0.159	0.228	0.301
29	0.062	0.178	0.228	0.280
30	0.062	0.159	0.228	0.260
31	0.101	0.159	0.208	0.240
32	0.101	0.198	0.208	0.280
33	0.220	0.217	0.248	0.322
34	0.437	0.468	0.387	0.466
35	0.516	0.604	0.585	0.630
36	-1.077	-1.364	-0.838	-0.672
37	-0.602	-0.822	-0.627	-0.493
38	-0.436	-0.612	-0.439	-0.387
39	-0.370	-0.480	-0.398	-0.356
40	-0.226	-0.373	-0.306	-0.275
41	-0.226	0.383	-0.235	-0.198
42	-0.105	-0.330	-0.172	-0.198
43	0.635	0.662	0.782	0.733
44	0.596	0.623	0.664	0.672
45	0.556	0.526	0.565	0.569
46	0.437	0.410	0.486	0.445

TABULATED PRESSURE COEFFICIENTS

RUN 41, Q = 3.00 LB./FTSQ

ORIFICE NO.	CP VALUES AT ALPHA ANGLE SETTINGS 0	3	6	9
47	0.378	0.372	0.387	0.383
48	0.358	0.352	0.327	0.363
49	0.259	0.256	0.268	0.301
50	0.220	0.178	0.208	0.177
51	-4.253	-5.265	-4.420	-4.097
52	-3.734	-4.569	-3.814	-3.700
53	-3.318	-4.039	-3.418	-3.303
54	-3.134	-3.847	-3.211	-3.033
55	-2.946	-3.573	-2.997	-2.948
56	-2.582	-3.005	-2.328	-2.414
57	-1.916	-2.257	-1.795	-1.761
58	-1.452	-1.680	-1.244	-1.227
59	-1.161	-1.219	-0.816	-0.949
60	-0.499	-0.501	-0.346	-0.472
61	-0.392	-0.476	-0.335	-0.331
62	-0.392	-0.476	-0.398	-0.296
63	-0.311	-0.476	-0.335	-0.275
64	-0.418	-0.493	-0.398	-0.257
65	-0.392	-0.493	-0.317	-0.296
66	0.951	0.943	0.900	0.758
67	0.705	0.725	0.633	0.459
68	0.123	0.101	-0.002	-0.198
69	-0.517	-0.595	-0.546	-0.500

TABULATED PRESSURE COEFFICIENTS

RUN 41, Q = 3.00 LB./FTSQ

ORIFICE CP VALUES AT ALPHA ANGLE SETTINGS

NO.	0	3	6	9
70	-0.848	-1.125	-0.845	-0.682
71	-1.264	-1.582	-1.089	-0.851
72	-1.077	-1.343	0.027	-0.770
73	-0.848	-1.112	-0.712	-0.591
74	-0.517	-0.766	-0.524	-0.468
75	-0.436	-0.595	-0.398	-0.373
76	-0.311	-0.459	-0.272	-0.303
77	-0.226	-0.433	-0.213	-0.198
78	-0.123	-0.258	-0.128	0.417
79	-0.020	0.003	-0.095	-0.106

TABULATED PRESSURE COEFFICIENTS

RUN 42, Q = 5.00 LB./FTSQ

ORIFICE NO.	CP VALUES AT ALPHA ANGLE SETTINGS 0	3	6	9
1	-0.268	-0.978	-1.854	-2.842
2	-0.551	-1.275	-2.063	-2.933
3	-0.627	-1.226	-1.912	-2.657
4	-0.656	-1.130	-1.656	-2.257
5	-0.691	-1.059	-1.435	-1.696
6	-0.714	-1.012	-1.319	-1.526
7	-0.749	-0.998	-1.226	-1.444
8	-0.784	-0.998	-1.131	-1.318
9	-0.933	-1.057	-1.224	-1.375
10	-0.933	-1.057	-1.202	-1.296
11	-0.935	-1.016	-1.156	-1.237
12	-0.968	-1.045	-1.156	-1.217
13	-1.010	-1.010	-1.119	-1.176
14	-0.970	-0.998	-1.148	-1.111
15	-0.842	-0.839	-0.795	-0.817
16	-0.609	-0.558	-0.609	-0.597
17	-0.247	-0.265	-0.340	-0.370
18	-0.016	0.010	-0.202	-0.288
19	0.876	0.902	0.914	0.672
20	0.796	0.900	0.982	0.821
21	0.672	0.859	0.973	0.934
22	0.509	0.698	0.870	0.902
23	0.356	0.556	0.705	0.776

TABULATED PRESSURE COEFFICIENTS

RUN 42, Q = 5.00 LB./FTSQ

ORIFICE NO.	CP VALUES AT ALPHA ANGLE SETTINGS 0	3	6	9
24	0.286	0.436	0.577	0.662
25	0.193	0.354	0.306	0.587
26	0.135	0.258	0.346	0.465
27	0.077	0.183	0.286	0.356
28	0.077	0.112	0.240	0.295
29	0.029	0.165	0.193	0.248
30	0.089	0.114	0.193	0.246
31	0.069	0.136	0.193	0.238
32	0.089	0.122	0.224	0.248
33	0.147	0.218	0.240	0.295
34	0.403	0.411	0.449	0.421
35	0.507	0.562	0.577	0.569
36	-1.111	-1.143	-0.842	-0.721
37	-0.623	-0.666	-0.551	-0.530
38	-0.503	-0.460	-0.472	-0.483
39	-0.336	-0.391	-0.365	-0.380
40	-0.251	-0.300	-0.284	-0.323
41	-0.177	-0.149	-0.132	-0.278
42	-0.163	-0.082	-0.142	-0.209
43	0.647	0.643	0.660	0.650
44	0.531	0.539	0.577	0.571
45	0.438	0.423	0.494	0.455
46	0.356	0.403	0.457	0.299

TABULATED PRESSURE COEFFICIENTS

RUN 42, Q = 5.00 LB./FTSQ

ORIFICE NO.	CP VALUES AT ALPHA ANGLE SETTINGS 0	3	6	9
47	0.323	0.332	0.339	0.299
48	0.240	0.273	0.286	0.248
49	0.182	0.199	0.195	0.091
50	0.089	0.079	0.089	0.010
51	-3.763	-3.708	-4.065	-3.973
52	-3.344	-3.246	-3.296	-3.277
53	-2.982	-2.902	-2.895	-2.887
54	-2.767	-2.662	-2.668	-2.651
55	-2.623	-2.501	-2.517	-2.474
56	-1.954	-1.802	-1.714	-1.696
57	-1.425	-1.228	-1.140	-1.180
58	-0.925	-0.631	-0.522	-0.575
59	-0.516	-0.391	-0.365	-0.439
60	-0.388	-0.334	-0.365	-0.380
61	-0.388	-0.357	-0.353	-0.358
62	-0.388	-0.352	-0.353	-0.380
63	-0.413	-0.381	-0.400	-0.323
64	-0.388	-0.334	-0.351	-0.380
65	-0.353	-0.310	-0.332	-0.337
66	0.089	0.939	0.973	0.924
67	0.690	0.680	0.577	0.408
68	0.131	0.136	0.042	-0.183
69	-0.503	-0.414	-0.516	-0.620

TABULATED PRESSURE COEFFICIENTS

RUN 42, Q = 5.CC LB./FTSQ

ORIFICE NO.	CP VALUES AT ALPHA ANGLE SETTINGS 0	3	6	9
70	-0.896	-0.827	-0.762	-0.770
71	-1.319	-1.238	-1.051	-0.987
72	-1.148	-1.057	-0.877	-0.815
73	-0.902	-0.906	-0.714	-0.650
74	-0.563	-0.556	-0.551	-0.557
75	-0.408	-0.471	-0.379	-0.437
76	-0.305	-0.322	-0.295	-0.358
77	-0.212	-0.230	-0.239	-0.313
78	-0.144	-0.183	-0.181	-0.254
79	-0.086	-0.110	-0.119	-0.197

TABULATED PRESSURE COEFFICIENTS

RUN 43, Q = 10.00 LB./FTSQ

ORIFICE NO.	CP VALUES AT ALPHA ANGLE SETTINGS 0	3	6	9
1	-0.123	-0.881	-0.858	-2.965
2	-0.447	-1.176	-1.164	-3.108
3	-0.551	-1.168	-1.145	-2.840
4	-0.631	-1.137	-1.102	-2.440
5	-0.648	-1.028	-1.016	-1.821
6	-0.704	-1.010	-0.998	-1.665
7	-0.740	-0.987	-0.979	-1.571
8	-0.809	-0.985	-0.986	-1.446
9	-0.918	-1.096	-1.096	-1.477
10	-0.948	-1.095	-1.078	-1.422
11	-0.943	-1.090	-1.065	-1.353
12	-0.974	-1.096	-1.071	-1.327
13	-1.004	-1.101	-1.051	-1.315
14	-0.974	-1.058	-1.035	-1.202
15	-0.839	-0.851	-0.833	-0.909
16	-0.507	-0.553	-0.564	-0.678
17	-0.258	-0.283	-0.263	-0.430
18	-0.001	-0.061	-0.025	-0.315
19	0.888	0.948	0.996	0.741
20	0.764	0.946	0.941	0.879
21	0.634	0.850	0.862	1.010
22	0.452	0.672	0.686	0.966
23	0.323	0.518	0.518	0.816

TABULATED PRESSURE COEFFICIENTS

RUN 43, Q = 10.00 LB./FTSQ

ORIFICE NO.	CP VALUES AT ALPHA ANGLE SETTINGS 0	3	6	9
24	0.220	0.384	0.409	0.691
25	0.164	0.299	0.316	0.593
26	0.100	0.188	0.194	0.447
27	0.048	0.127	0.151	0.348
28	0.018	0.079	0.127	0.304
29	0.015	0.079	0.079	0.273
30	0.018	0.048	0.098	0.241
31	0.071	0.048	0.102	0.210
32	0.048	0.096	0.133	0.224
33	0.232	0.200	0.213	0.193
34	0.390	0.385	0.409	0.464
35	0.537	0.543	0.549	0.587
36	-1.347	-1.342	-1.316	-0.890
37	-0.787	-0.814	-0.802	-0.677
38	-0.485	-0.578	-0.570	-0.552
39	-0.414	-0.460	-0.460	-0.465
40	-0.313	-0.340	-0.313	-0.377
41	-0.252	-0.277	-0.258	-0.321
42	-0.135	-0.184	-0.142	-0.232
43	0.641	0.660	0.675	0.692
44	0.531	0.530	0.563	0.591
45	0.439	0.436	0.464	0.468
46	0.360	0.351	0.378	0.397

TABULATED PRESSURE COEFFICIENTS

RUN 43, Q = 10.00 LB./FTSQ

ORIFICE NO.	CP VALUES AT ALPHA ANGLE SETTINGS 0	3	6	9
47	0.299	0.281	0.311	0.335
48	0.246	0.217	0.244	0.266
49	0.164	0.149	0.176	0.160
50	0.079	0.048	0.078	0.053
51	-3.744	-3.739	-3.715	-3.778
52	-3.267	-3.243	-3.233	-3.298
53	-2.900	-2.894	-2.842	-2.927
54	-2.582	-2.589	-2.558	-2.602
55	-2.338	-2.264	-2.245	-2.259
56	-1.675	-1.591	-1.536	-1.453
57	-0.961	-0.790	-0.765	-0.603
58	-0.460	-0.469	-0.423	-0.441
59	-0.426	-0.465	-0.417	-0.440
60	-0.417	-0.441	-0.417	-0.441
61	-0.417	-0.435	-0.423	-0.440
62	-0.447	-0.442	-0.442	-0.450
63	-0.435	-0.473	-0.454	-0.471
64	-0.423	-0.460	-0.442	-0.438
65	-0.393	-0.417	-0.386	-0.409
66	0.965	0.947	0.971	0.991
67	0.719	0.684	0.684	0.510
68	0.171	0.126	0.126	-0.127
69	-0.505	-0.521	-0.534	-0.639

TABULATED PRESSURE COEFFICIENTS

RUN 43, Q = 10.CO LB./FTSQ

ORIFICE NO.	CP VALUES AT ALPHA ANGLE SETTINGS 0	3	6	9
70	-0.941	-0.943	-0.937	-0.883
71	-1.434	-1.432	-1.418	-1.065
72	-1.262	-1.285	-1.255	-0.928
73	-1.035	-1.071	-1.060	-0.778
74	-0.704	-0.753	-0.723	-0.678
75	-0.515	-0.576	-0.539	-0.522
76	-0.385	-0.442	-0.392	-0.422
77	-0.282	-0.331	-0.288	-0.357
78	-0.218	-0.283	-0.228	-0.295
79	-0.140	-0.184	-0.143	-0.209

TABULATED PRESSURE COEFFICIENTS

RUN 45, Q = 2.25 LB./FTSQ

ORIFICE NO.	CP VALUES AT ALPHA ANGLE SETTINGS 0	3	6	9
1	-1.146	-2.128	-3.182	-4.845
2	-1.376	-2.382	-3.316	-4.731
3	-1.376	-2.257	-2.777	-4.277
4	-1.347	-1.913	-2.606	-3.779
5	-1.239	-1.692	-1.996	-2.477
6	-1.185	-1.664	-1.734	-2.269
7	-1.347	-1.582	-1.706	-2.112
8	-1.269	-1.558	-1.601	-1.999
9	-1.514	-1.664	-1.730	-1.127
10	-1.538	-1.664	-1.730	-1.710
11	-1.568	-1.687	-1.730	-1.989
12	-1.729	-1.807	-1.782	-1.970
13	-1.837	-1.903	-1.863	-2.060
14	-2.004	-2.032	-1.944	-2.084
15	-2.112	-2.142	-2.049	-2.217
16	-2.357	-2.344	-2.258	-2.363
17	-3.229	-3.258	-3.158	-3.292
18	-8.522	-8.273	-8.178	-8.307
19	0.882	0.752	0.535	-0.023
20	0.808	0.905	0.746	0.440
21	0.882	0.829	0.793	0.766
22	0.585	0.803	0.886	0.875
23	0.510	0.676	0.722	0.821

TABULATED PRESSURE COEFFICIENTS

RUN 45, Q = 2.25 LB./FTSQ

ORIFICE NO.	CP VALUES AT ALPHA ANGLE SETTINGS 0	3	6	9
24	0.436	0.573	0.676	0.766
25	0.312	0.420	0.605	0.739
26	0.287	0.369	0.535	0.521
27	0.163	0.318	0.418	0.467
28	0.114	0.267	0.418	0.467
29	0.163	0.267	0.324	0.413
30	0.163	0.241	0.301	0.385
31	0.213	0.267	0.348	0.331
32	0.262	0.292	0.348	0.385
33	0.436	0.420	0.488	0.440
34	0.535	0.522	0.512	0.576
35	0.585	0.650	0.699	0.712
36	-33.214	-32.404	-31.954	-31.797
37	-25.304	-24.808	-24.514	-24.480
38	-18.653	-18.255	-17.942	-17.864
39	-13.737	-13.609	-13.346	-13.299
40	-10.179	-9.974	-9.688	-9.728
41	-7.518	-7.478	-7.354	-7.365
42	-3.092	-3.019	-2.844	-2.846
43	0.733	0.752	0.746	0.766
44	0.684	0.701	0.676	0.685
45	0.585	0.548	0.629	0.685
46	0.510	0.548	0.582	0.630

TABULATED PRESSURE COEFFICIENTS

RUN 45, Q = 2.25 LB./FTSQ

ORIFICE NO.	CP VALUES AT ALPHA ANGLE SETTINGS 0	3	6	9
47	0.510	0.548	0.605	0.549
48	0.461	0.522	0.512	0.576
49	0.485	0.369	0.488	0.576
50	0.461	0.446	0.465	0.521
51	-0.396	-0.581	-0.491	-0.564
52	-1.269	-1.410	-1.363	-1.511
53	-1.974	-2.032	-1.882	-2.112
54	-2.435	-2.411	-2.396	-2.558
55	-2.572	-2.641	-2.544	-2.648
56	-2.548	-2.645	-2.473	-2.610
57	-2.489	-2.511	-2.387	-2.482
58	-2.249	-2.272	-1.834	-2.217
59	-2.112	-2.214	-2.077	-2.141
60	-1.867	-1.917	-1.730	-1.757
61	-1.489	-1.529	-1.339	-1.407
62	-1.239	-1.213	-1.049	-1.113
63	-0.970	-0.974	-0.810	-0.881
64	-0.671	-0.777	-0.625	-0.545
65	-0.480	-0.519	-0.363	-0.384
66	-9.664	-9.782	-8.993	-8.771
67	-14.796	-14.462	-14.089	-14.004
68	-21.069	-20.564	-20.476	-20.251
69	-31.288	-30.632	-30.373	-30.135

TABULATED PRESSURE COEFFICIENTS

RUN 45, Q = 2.25 LB./FTSQ

ORIFICE NO.	CP VALUES AT ALPHA ANGLE SETTINGS 0	3	6	9
70	-37.969	-37.046	-36.731	-36.443
71	-40.493	-39.589	-39.160	-38.778
72	-36.454	-35.537	-35.164	-34.819
73	-29.779	-29.190	-28.687	-28.572
74	-25.471	-25.176	-24.853	-24.717
75	-19.275	-18.835	-18.656	-18.627
76	-14.472	-14.222	-13.713	-13.952
77	-11.267	-11.142	-10.845	-10.803
78	-8.547	-8.297	-8.040	-8.122
79	-2.999	-2.990	-2.763	-2.742

TABULATED PRESSURE COEFFICIENTS

RUN 46. Q = 3.00 LB./FTSQ

ORIFICE NO.	CP VALUES AT ALPHA ANGLE SETTINGS 0	3	6	9
1	-0.963	-1.862	-3.427	-5.169
2	-1.246	-2.094	-3.533	-5.045
3	-1.264	-1.958	-3.227	-4.579
4	-1.264	-1.753	-2.763	-3.977
5	-1.165	-1.483	-2.165	-2.841
6	-1.169	-1.394	-2.019	-2.547
7	-1.213	-1.371	-1.895	-2.416
8	-1.242	-1.316	-1.793	-2.167
9	-1.371	-1.432	-1.836	-2.246
10	-0.631	-1.432	-1.895	-2.205
11	-1.470	-1.487	-1.917	-2.149
12	-1.551	-1.562	-1.957	-2.228
13	-1.669	-1.644	-2.041	-2.276
14	-1.754	-1.295	-2.037	-2.276
15	-1.820	-1.678	-2.136	-2.325
16	-2.030	-1.866	-2.245	-2.423
17	-2.593	-2.449	-2.833	-2.999
18	-6.450	-5.997	-6.558	-6.723
19	0.951	0.893	0.546	0.043
20	0.877	0.951	0.816	0.430
21	0.804	0.951	0.893	0.777
22	0.600	0.855	0.932	0.951
23	0.526	0.681	0.758	0.932

TABULATED PRESSURE COEFFICIENTS

RUN 46, Q = 3.C0 LB./FTSQ

ORIFICE NO.	CP VALUES AT ALPHA ANGLE SETTINGS 0	3	6	9
24	0.360	0.604	0.719	0.797
25	0.341	0.507	0.623	0.719
26	0.194	0.391	0.468	0.604
27	0.175	0.333	0.449	0.526
28	0.157	0.294	0.352	0.410
29	0.138	0.256	0.333	0.372
30	0.101	0.217	0.275	0.352
31	0.194	0.256	0.352	0.352
32	0.212	0.333	0.314	0.352
33	0.360	0.449	0.488	0.507
34	0.489	0.565	0.565	0.584
35	0.600	0.700	0.700	0.700
36	-24.639	-22.817	-24.752	-25.484
37	-18.975	-17.552	-19.038	-19.596
38	-13.892	-12.785	-13.900	-14.281
39	-10.407	-9.589	-10.426	-10.722
40	-7.499	-6.936	-7.565	-7.769
41	-5.633	-5.198	-5.726	-5.869
42	-2.185	-2.019	-2.307	-2.386
43	0.693	0.758	0.797	0.797
44	0.637	0.739	0.777	0.739
45	0.526	0.642	0.662	0.642
46	0.508	0.604	0.604	0.604

TABULATED PRESSURE COEFFICIENTS

RUN 46, Q = 3.00 LB./FTSQ

ORIFICE NO.	CP VALUES AT ALPHA ANGLE SETTINGS 0	3	6	9
47	0.452	0.584	0.584	0.564
48	0.489	0.584	0.565	0.584
49	0.434	0.565	0.546	0.565
50	0.397	0.565	0.507	0.507
51	-0.940	-0.920	-1.245	-1.438
52	-1.677	-1.654	-2.037	-2.258
53	-2.269	-2.187	-2.581	-2.837
54	-2.597	-2.470	-2.909	-3.153
55	-2.737	-2.545	-2.986	-3.255
56	-2.593	-2.528	-2.862	-3.108
57	-2.472	-2.337	-2.741	-2.916
58	-2.185	-2.074	-2.424	-2.641
59	-2.104	-1.999	-2.329	-2.559
60	-1.695	-1.603	-1.946	-1.991
61	-1.353	-1.299	-1.552	-1.629
62	-1.044	-0.988	-1.231	-1.310
63	-0.782	-0.729	-0.972	-0.967
64	-0.554	-0.541	-0.720	-0.749
65	-0.330	-0.315	-0.446	-0.478
66	-5.917	-5.423	-5.952	-5.929
67	-10.263	-9.511	-10.324	-10.530
68	-15.364	-14.253	-15.454	-15.838
69	-23.318	-21.540	-23.270	-24.002

TABULATED PRESSURE COEFFICIENTS

RUN 46, Q = 3.00 LB./FTSQ

ORIFICE NO.	CP VALUES AT ALPHA ANGLE SETTINGS 0	3	6	9
70	-28.070	-26.136	-28.295	-29.073
71	-30.212	-27.959	-30.229	-31.112
72	-27.065	-25.046	-26.941	-27.907
73	-22.218	-20.563	-22.256	-22.911
74	-19.159	-17.780	-19.264	-19.732
75	-14.444	-13.427	-14.516	-14.856
76	-10.775	-9.978	-10.860	-11.091
77	-8.327	-7.694	-8.405	-8.597
78	-6.204	-5.744	-6.325	-6.426
79	-2.104	-1.883	-2.216	-2.250

TABULATED PRESSURE COEFFICIENTS

RUN 47, Q = 5.00 LB./FTSQ

ORIFICE NO.	CP VALUES AT ALPHA ANGLE SETTINGS 0	3	6	9
1	-0.852	-2.016	-3.207	-4.744
2	-1.221	-2.293	-3.331	-4.683
3	-1.223	-2.155	-3.041	-4.310
4	-1.174	-1.911	-2.583	-3.535
5	-1.098	-1.663	-1.992	-2.580
6	-1.115	-1.578	-1.821	-2.314
7	-1.115	-1.518	-1.772	-2.168
8	-1.174	-1.505	-1.703	-2.013
9	-1.329	-1.627	-1.776	-2.083
10	-1.359	-1.627	-1.776	-2.026
11	-1.392	-1.614	-1.729	-1.959
12	-1.461	-1.714	-1.763	-1.965
13	-1.558	-1.776	-1.821	-2.017
14	-1.605	-1.800	-1.843	-2.024
15	-1.603	-1.778	-1.789	-1.904
16	-1.653	-1.825	-1.821	-1.952
17	-1.901	-2.053	-2.078	-2.170
18	-3.937	-3.978	-4.008	-4.246
19	0.988	0.940	0.675	0.196
20	0.938	0.986	0.852	0.595
21	0.847	0.971	0.959	0.861
22	0.677	0.853	0.936	1.008
23	0.523	0.693	0.834	0.923

TABULATED PRESSURE COEFFICIENTS

RUN 47, Q = 5.CO LB./FTSQ

ORIFICE NO.	CP VALUES AT ALPHA ANGLE SETTINGS 0	3	6	9
24	0.424	0.585	0.698	0.824
25	0.331	0.482	0.625	0.742
26	0.247	0.363	0.495	0.595
27	0.197	0.287	0.411	0.510
28	0.152	0.260	0.361	0.449
29	0.150	0.232	0.338	0.425
30	0.150	0.249	0.314	0.388
31	0.150	0.236	0.290	0.379
32	0.210	0.254	0.314	0.377
33	0.374	0.411	0.446	0.508
34	0.487	0.545	0.567	0.584
35	0.616	0.656	0.675	0.691
36	-14.607	-14.974	-14.566	-13.430
37	-11.215	-11.557	-11.233	-11.332
38	-8.147	-8.421	-8.169	-8.251
39	-6.094	-6.261	-6.101	-6.050
40	-4.326	-4.587	-4.466	-4.502
41	-3.242	-3.408	-3.315	-3.365
42	-1.303	-1.367	-1.357	-1.398
43	0.703	0.729	0.735	0.752
44	0.642	0.669	0.675	0.691
45	0.556	0.593	0.601	0.608
46	0.523	0.542	0.541	0.558

TABULATED PRESSURE COEFFICIENTS

RUN 47, Q = 5.00 LB./FTSQ

ORIFICE NO.	CP VALUES AT ALPHA ANGLE SETTINGS 0	3	6	9
47	0.474	0.496	0.517	0.530
48	0.472	0.460	0.493	0.497
49	0.426	0.458	0.478	0.489
50	0.422	0.458	0.459	0.499
51	-1.964	-2.229	-2.206	-2.434
52	-2.476	-2.746	-2.767	-2.955
53	-2.773	-3.044	-3.052	-3.234
54	-2.955	-3.215	-3.246	-3.426
55	-2.970	-3.255	-3.225	-3.413
56	-2.763	-3.041	-3.030	-3.184
57	-2.594	-2.855	-2.815	-2.955
58	-2.292	-2.475	-2.443	-2.598
59	-2.057	-2.231	-2.182	-2.301
60	-1.709	-1.898	-1.849	-1.906
61	-1.327	-1.467	-1.208	-1.505
62	-1.005	-1.107	-1.130	-1.132
63	0.087	-0.808	-0.848	-0.853
64	-0.502	-0.559	-0.558	-0.589
65	-0.301	-0.361	-0.340	-0.371
66	-2.201	-2.291	-2.255	-2.183
67	-5.187	-5.379	-5.304	-5.383
68	-8.564	-8.899	-8.678	-8.822
69	-13.519	-13.972	-13.592	-13.801

TABULATED PRESSURE COEFFICIENTS

RUN 47, Q = 5.00 LB./FTSQ

ORIFICE NO.	CP VALUES AT ALPHA ANGLE SETTINGS 0	3	6	9
70	-16.660	-17.148	-16.684	-16.889
71	-17.841	-18.436	-17.876	-18.111
72	-16.049	-16.519	-16.069	-16.257
73	-13.152	-13.562	-13.126	-13.289
74	-11.323	-11.637	-11.304	-11.463
75	-8.508	-8.752	-8.534	-8.624
76	-6.271	-6.487	-6.349	-6.423
77	-4.794	-5.006	-4.850	-4.912
78	-3.609	-3.779	-3.723	-3.740
79	-1.254	-1.358	-1.310	-1.311

TABULATED PRESSURE COEFFICIENTS

RUN 48, Q = 10.00 LB./FTSQ

ORIFICE NO.	CP VALUES AT ALPHA ANGLE SETTINGS 0	3	6	9
1	-0.570	-1.381	-2.506	-3.945
2	-0.878	-1.647	-2.718	-3.993
3	-0.927	-1.611	-2.507	-3.655
4	-0.966	-1.464	-1.967	-3.026
5	-0.952	-1.275	-1.743	-2.236
6	-0.979	-1.235	-1.608	-2.084
7	-0.997	-1.222	-1.525	-1.964
8	-1.055	-1.200	-1.472	-1.825
9	-1.216	-1.318	-1.550	-1.852
10	-1.239	-1.331	-1.556	-1.819
11	-1.288	-1.336	-1.521	-1.777
12	-1.332	-1.401	-1.556	-1.777
13	-1.417	-1.429	-1.585	-1.770
14	-1.453	-1.424	-1.584	-1.740
15	-1.393	-1.336	-1.444	-1.590
16	-1.327	-1.263	-1.391	-1.536
17	-1.325	-1.259	-1.363	-1.505
18	-2.060	-2.042	-2.066	-2.181
19	0.947	0.975	0.808	0.433
20	0.887	1.000	0.918	0.729
21	0.769	0.970	0.976	0.933
22	0.573	0.804	0.915	0.968
23	0.414	0.650	0.771	0.875

TABULATED PRESSURE COEFFICIENTS

RUN 48, Q = 10.00 LB./FTSQ

ORIFICE NO.	CP VALUES AT ALPHA ANGLE SETTINGS 0	3	6	9
24	0.315	0.549	0.630	0.770
25	0.268	0.444	0.567	0.669
26	0.163	0.349	0.448	0.536
27	0.132	0.297	0.360	0.453
28	0.119	0.255	0.327	0.402
29	0.102	0.225	0.297	0.366
30	0.095	0.232	0.285	0.337
31	0.102	0.232	0.272	0.330
32	0.132	0.267	0.297	0.337
33	0.310	0.409	0.432	0.457
34	0.438	0.538	0.525	0.546
35	0.579	0.668	0.653	0.675
36	-7.661	-7.293	-7.352	-7.584
37	-5.920	-5.638	-5.678	-5.862
38	-4.321	-4.112	-4.161	-4.266
39	-3.167	-2.997	-3.052	-3.154
40	-2.244	-2.107	-2.167	-2.254
41	-1.655	-1.541	-1.608	-1.680
42	-0.712	-0.626	-0.710	-0.750
43	0.682	0.751	0.724	0.760
44	0.622	0.686	0.654	0.675
45	0.536	0.609	0.607	0.607
46	0.481	0.555	0.535	0.566

TABULATED PRESSURE COEFFICIENTS

RUN 48, Q = 10.00 LB./FTSQ

ORIFICE NO.	CP VALUES AT ALPHA ANGLE SETTINGS 0	3	6	9
47	0.450	0.532	0.512	0.530
48	0.426	0.509	0.489	0.511
49	0.414	0.476	0.460	0.487
50	0.416	0.478	0.466	0.482
51	-3.072	-3.038	-3.163	-3.384
52	-3.216	-3.198	-3.298	-3.535
53	-3.287	-3.226	-3.345	-3.559
54	-3.317	-3.221	-3.339	-3.546
55	-2.971	-3.162	-3.260	-3.441
56	-2.960	-2.880	-2.982	-3.149
57	-2.701	-2.625	-2.700	-2.852
58	-2.335	-2.172	-2.248	-2.368
59	-2.055	-0.027	-2.114	-2.146
60	-1.693	-1.602	-1.669	-1.743
61	-1.289	-1.193	-1.251	-1.269
62	-0.941	-0.840	-0.870	-0.858
63	-0.589	-0.487	-0.531	-0.526
64	-0.376	-0.281	-0.356	-0.393
65	-0.272	-0.240	-0.318	-0.375
66	-0.044	0.044	-0.031	-0.035
67	-1.938	-1.837	-1.926	-1.995
68	-4.033	-3.892	-3.950	-4.110
69	-6.845	-6.575	-6.684	-6.901

TABULATED PRESSURE COEFFICIENTS

RUN 48, Q = 10.CO LB./FTSQ

ORIFICE NO.	CP VALUES AT ALPHA ANGLE SETTINGS 0	3	6	9
70	-8.593	-8.244	-8.337	-8.568
71	-9.377	-8.964	-9.024	-9.294
72	-8.408	-8.028	-8.074	-8.321
73	-6.920	-6.599	-6.660	-6.847
74	-5.953	-5.238	-5.727	-5.873
75	-4.462	-4.247	-4.282	-4.429
76	-3.261	-3.096	-3.156	-3.263
77	-2.453	-2.308	-2.364	-2.453
78	-1.854	-1.736	-1.798	-1.874
79	-0.707	-0.630	-0.703	-0.750

TABLE V

TABULATED TOTAL HEAD RAKE

PRESSURE COEFFICIENTS

185

TABULATED PRESSURE COEFFICIENTS

RUN 14, Q = 2.25 LB./FTSQ

ORIFICE NO.	CP VALUES AT ALPHA ANGLE SETTINGS 0	3	6	9
1	22.969	22.927	22.885	22.056
2	48.534	48.861	48.765	46.977
3	37.315	37.717	37.407	36.111
4	25.324	25.594	25.378	24.575
5	14.175	14.176	13.995	13.747
6	5.995	6.014	6.030	5.947
7	1.735	1.657	1.593	1.892
8	0.089	0.060	0.063	0.273
9	0.178	0.129	0.119	0.365
10	0.787	0.634	0.765	0.937

TABULATED PRESSURE COEFFICIENTS

RUN 15, Q = 3.00 LB./FTSQ

ORIFICE CP VALUES AT ALPHA ANGLE SETTINGS

NO.	0	3	6	9
1	17.662	17.705	17.275	17.125
2	37.254	37.675	36.886	37.207
3	28.775	29.069	28.452	28.692
4	19.629	19.813	19.433	19.488
5	11.032	11.111	10.923	10.874
6	4.909	4.829	4.760	4.501
7	1.527	1.482	1.446	1.251
8	0.284	0.155	0.165	0.150
9	0.265	0.155	0.158	0.145
10	0.860	0.736	0.751	0.733

TABULATED PRESSURE COEFFICIENTS

RUN 16, Q = 5.00 LB./FTSQ

ORIFICE NO.	CP VALUES AT ALPHA ANGLE SETTINGS 0	3	6	9
1	12.138	10.544	9.804	9.901
2	26.381	24.237	24.717	25.481
3	20.403	18.812	19.218	19.675
4	13.970	12.950	13.216	13.498
5	8.053	7.508	7.679	7.831
6	3.646	3.446	3.595	3.519
7	1.139	1.121	1.145	1.056
8	0.103	0.145	0.097	0.055
9	0.071	0.009	-0.009	-0.136
10	0.412	0.371	0.299	0.223

TABULATED PRESSURE COEFFICIENTS

RUN 17, Q = 10.00 LB./FTSQ

ORIFICE NO.	CP VALUES AT ALPHA ANGLE SETTINGS 0	3	6	9
1	4.530	4.315	4.012	4.044
2	14.144	13.860	13.482	14.134
3	11.131	10.926	10.651	11.224
4	7.781	7.601	7.428	7.825
5	4.716	4.588	4.502	4.750
6	2.485	2.436	2.367	2.559
7	1.192	1.190	1.153	1.266
8	0.281	0.280	0.288	0.308
9	-0.185	-0.236	-0.286	-0.333
10	-0.338	-0.412	-0.494	-0.543

TABULATED PRESSURE COEFFICIENTS

RUN 18, Q = 2.25 LB./FTSQ

ORIFICE CP VALUES AT ALPHA ANGLE SETTINGS

NO.	0	3	6	9
1	0.667	0.738	0.831	0.722
2	0.266	-0.243	0.087	-0.016
3	0.291	-0.163	0.131	0.003
4	0.386	0.019	0.261	0.109
5	0.407	0.193	0.351	0.243
6	0.622	0.499	0.678	0.410
7	0.746	0.746	0.858	0.511
8	0.754	0.797	0.930	0.717
9	0.328	-0.134	0.432	0.166
10	-0.229	-1.216	-0.187	-0.418

TABULATED PRESSURE COEFFICIENTS

RUN 19, Q = 3.00 LB./FTSQ

ORIFICE CP VALUES AT ALPHA ANGLE SETTINGS

NO.	0	3	6	9
1	0.744	0.725	0.886	0.848
2	0.186	0.063	0.040	-0.015
3	0.271	0.091	0.040	-0.074
4	0.387	0.252	0.147	0.190
5	0.449	0.458	0.419	0.207
6	0.653	0.722	0.672	0.437
7	0.760	0.876	0.886	0.680
8	0.810	0.845	0.909	0.866
9	0.292	0.265	0.250	0.310
10	-0.297	-0.382	-0.466	-0.338

TABULATED PRESSURE COEFFICIENTS

RUN 20, Q = 5.00 LB./FTSQ

ORIFICE NO.	CP VALUES AT ALPHA ANGLE SETTINGS 0	3	6	9
1	0.848	0.832	0.814	0.774
2	0.188	0.137	0.010	-0.062
3	0.240	0.200	0.041	-0.026
4	0.361	0.351	0.227	0.043
5	0.567	0.507	0.395	0.218
6	0.745	0.806	0.667	0.402
7	0.898	0.938	0.900	0.669
8	0.944	0.938	0.973	0.892
9	0.355	0.362	0.382	0.274
10	-0.402	-0.378	-0.449	-0.467

TABULATED PRESSURE COEFFICIENTS

RUN 21, Q = 10.00 LB./FTSQ

ORIFICE NO.	CP VALUES AT ALPHA ANGLE SETTINGS 0	3	6	9
1	0.809	0.865	0.839	0.839
2	0.139	0.110	0.027	-0.298
3	0.225	0.191	0.079	-0.253
4	0.359	0.336	0.221	-0.117
5	0.575	0.557	0.428	0.115
6	0.788	0.803	0.686	0.464
7	0.919	0.941	0.900	0.793
8	0.941	0.954	0.936	0.961
9	0.378	0.361	0.370	0.221
10	-0.415	-0.469	-0.428	-0.783

TABULATED PRESSURE COEFFICIENTS

RUN 23, Q = 2.25 LB./FTSQ

ORIFICE NO.	CP VALUES AT ALPHA ANGLE SETTINGS 0	3	6	9
1	35.000	35.010	35.721	35.733
2	54.746	54.927	56.224	56.614
3	42.438	42.370	43.430	43.755
4	29.444	29.386	30.203	30.390
5	17.827	17.716	18.108	18.024
6	9.167	8.927	9.418	9.231
7	3.888	3.762	3.342	3.875
8	1.004	0.843	1.066	0.956
9	-.197	-0.226	-.312	-0.178
10	-.483	-0.591	-.601	-0.496

TABULATED PRESSURE COEFFICIENTS

RUN 24, Q = 3.00 LB./FTSQ

ORIFICE CP VALUES AT ALPHA ANGLE SETTINGS

NO.	0	3	6	9
1	27.785	26.212	22.550	21.999
2	44.272	41.766	36.324	35.780
3	34.213	32.276	28.158	27.720
4	23.698	22.386	19.586	19.299
5	14.261	13.402	11.730	11.471
6	7.345	6.940	6.142	5.941
7	3.228	3.157	2.856	2.608
8	1.016	1.013	0.959	0.784
9	0.017	0.153	0.134	0.118
10	-0.302	-0.230	-0.210	-0.195

TABULATED PRESSURE COEFFICIENTS

RUN 25, Q = 5.00 LB./FTSQ

ORIFICE NO.	CP VALUES AT ALPHA ANGLE SETTINGS			
	0	3	6	9
1	14.024	14.175	14.203	13.501
2	23.553	24.019	24.658	24.866
3	18.323	18.699	19.257	19.331
4	12.777	13.000	13.416	13.501
5	7.721	7.852	8.063	8.192
6	4.067	4.198	4.296	4.302
7	2.043	2.085	2.091	2.123
8	1.173	1.192	1.142	1.202
9	0.696	0.740	0.772	0.827
10	0.102	0.160	0.148	0.259

TABULATED PRESSURE COEFFICIENTS

RUN 26, Q = 10.00 LB./FTSQ

ORIFICE NO.	CP VALUES AT ALPHA ANGLE SETTINGS 0	3	6	9
1	6.326	6.036	5.597	5.593
2	13.454	13.305	12.808	13.117
3	10.572	10.466	10.155	10.369
4	7.446	7.345	7.157	7.300
5	4.598	4.492	4.437	4.532
6	2.485	2.478	2.456	2.476
7	1.383	1.392	1.384	1.369
8	1.035	1.054	1.024	0.988
9	0.984	0.996	0.989	0.987
10	0.832	0.846	0.831	0.852

TABULATED PRESSURE COEFFICIENTS

RUN 27, Q = 2.25 LB./FTSQ

ORIFICE NO.	CP VALUES AT ALPHA ANGLE SETTINGS			
	0	3	6	9
1	0.924	0.886	0.825	0.862
2	0.427	0.352	0.142	0.113
3	0.530	0.535	0.142	0.135
4	0.591	0.535	0.320	0.187
5	0.615	0.666	0.455	0.281
6	0.797	0.825	0.591	0.427
7	0.956	0.933	0.825	0.720
8	0.980	0.956	0.933	0.840
9	1.060	1.036	0.933	0.935
10	1.031	1.064	0.933	0.961

TABULATED PRESSURE COEFFICIENTS

RUN 28, Q = 3.00 LB./FTSQ

ORIFICE NO.	CP VALUES AT ALPHA ANGLE SETTINGS 0	3	6	9
1	0.907	0.818	0.929	0.853
2	0.370	0.101	0.120	-0.008
3	0.495	0.331	0.203	0.024
4	0.535	0.485	0.343	0.161
5	0.661	0.564	0.502	0.259
6	0.745	0.718	0.736	0.498
7	0.929	0.835	0.868	0.695
8	1.014	0.934	1.016	0.874
9	1.014	0.951	1.076	0.951
10	1.014	0.938	1.034	1.011

TABULATED PRESSURE COEFFICIENTS

RUN 29, Q = 5.00 LB./FTSQ

ORIFICE NO.	CP VALUES AT ALPHA ANGLE SETTINGS 0	3	6	9
1	0.775	0.806	0.853	0.846
2	0.298	0.286	0.137	-0.052
3	0.368	0.301	0.194	-0.002
4	0.484	0.488	0.311	0.126
5	0.589	0.582	0.443	0.256
6	0.728	0.687	0.664	0.422
7	0.868	0.852	0.800	0.755
8	0.916	0.936	0.878	0.883
9	0.932	0.936	0.913	1.038
10	0.969	0.934	0.936	1.038

TABULATED PRESSURE COEFFICIENTS

RUN 30, Q = 10.00 LB./FTSQ

ORIFICE NO.	CP VALUES AT ALPHA ANGLE SETTINGS 0	3	6	9
1	2.395	0.864	0.866	0.863
2	0.783	0.311	0.135	0.059
3	1.073	0.397	0.178	0.084
4	1.308	0.497	0.310	0.176
5	1.745	0.604	0.496	0.357
6	2.161	0.729	0.692	0.576
7	2.450	0.840	0.829	0.747
8	2.740	0.910	0.927	0.893
9	2.807	0.967	0.985	0.948
10	2.814	0.982	0.985	0.967

TABULATED PRESSURE COEFFICIENTS

RUN 50, Q = 2.25 LB./FTSQ

ORIFICE NO.	CP VALUES AT ALPHA ANGLE SETTINGS			
	0	3	6	9
1	3.471	3.321	3.013	2.999
2	68.352	63.894	55.805	55.306
3	55.180	51.667	45.073	44.703
4	36.700	34.663	30.306	30.087
5	21.071	19.879	17.290	17.241
6	10.559	10.202	8.908	8.650
7	0.597	0.566	0.526	0.488
8	0.649	0.737	0.592	0.630
9	1.008	1.107	0.807	0.832
10	1.110	1.025	0.909	0.903

TABULATED PRESSURE COEFFICIENTS

RUN 51, Q = 3.00 LB./FTSQ

ORIFICE NO.	CP VALUES AT ALPHA ANGLE SETTINGS 0	3	6	9
1	2.423	17.697	2.578	2.381
2	43.956	344.469	45.952	44.402
3	35.767	280.001	37.495	36.284
4	23.995	188.698	25.293	24.434
5	13.658	106.709	14.456	13.980
6	6.814	52.000	7.119	6.827
7	0.409	1.949	0.401	0.353
8	0.568	3.317	0.524	0.481
9	0.951	0.840	0.961	0.932
10	0.979	6.570	0.971	0.833

N.G.

TABULATED PRESSURE COEFFICIENTS

RUN 52, Q = 5.00 LB./FTSQ

ORIFICE NO.	CP VALUES AT ALPHA ANGLE SETTINGS 0	3	6	9
1	1.587	1.552	1.665	1.601
2	26.247	26.864	28.167	28.341
3	21.459	21.919	23.011	23.122
4	14.496	14.712	15.527	15.656
5	8.271	8.463	8.885	8.962
6	4.090	4.133	4.413	4.344
7	0.288	0.217	0.256	0.171
8	0.357	0.303	0.283	0.222
9	0.813	0.758	0.764	0.729
10	0.965	0.960	0.999	0.994

TABULATED PRESSURE COEFFICIENTS

RUN 53, Q = 10.00 LB./FTSQ

ORIFICE NO.	CP VALUES AT ALPHA ANGLE SETTINGS 0	3	6	9
1	1.009	0.967	0.998	1.002
2	14.180	13.630	14.294	14.281
3	11.837	11.374	12.057	12.118
4	8.100	7.804	8.285	8.371
5	4.619	4.418	4.696	4.757
6	2.184	2.014	2.121	2.135
7	-0.038	-0.126	-0.229	-0.245
8	-0.268	-0.406	-0.526	-0.551
9	-0.211	-0.389	-0.402	-0.543
10	-0.025	-0.389	-0.527	-0.576

TABULATED PRESSURE COEFFICIENTS

RUN 54, Q = 2.25 LB./FTSQ

ORIFICE NO.	CP VALUES AT ALPHA ANGLE SETTINGS 0	3	6	9
1	0.113	0.753	0.984	0.897
2	0.113	0.014	-0.014	-0.037
3	0.113	0.113	0.052	0.022
4	0.113	0.263	0.297	0.140
5	0.113	0.317	0.485	0.355
6	0.113	0.345	0.613	0.532
7	0.113	-0.140	-0.136	-0.171
8	0.113	-0.652	-0.735	-0.794
9	0.113	-0.652	-0.824	-0.794
10	0.113	-0.729	-0.824	-0.885

N-G.

206

TABULATED PRESSURE COEFFICIENTS

RUN 55, Q = 3.00 LB./FTSQ

ORIFICE NO.	CP VALUES AT ALPHA ANGLE SETTINGS 0	3	6	9
1	0.759	0.794	0.831	0.805
2	0.165	0.217	0.154	0.115
3	0.252	0.255	0.076	0.040
4	0.338	0.313	0.256	0.080
5	0.443	0.449	0.397	0.190
6	0.462	0.562	0.415	0.301
7	0.082	0.118	0.016	-0.042
8	-0.362	-0.302	-0.372	-0.338
9	-0.377	-0.298	-0.379	-0.381
10	-0.362	-0.322	-0.410	-0.403

TABULATED PRESSURE COEFFICIENTS

RUN 56, Q = 5.00 LB./FTSQ

ORIFICE NO.	CP VALUES AT ALPHA ANGLE SETTINGS 0	3	6	9
1	0.866	0.847	0.896	0.875
2	0.280	0.224	0.170	0.158
3	0.340	0.237	0.092	0.063
4	0.429	0.361	0.221	0.148
5	0.541	0.493	0.403	0.305
6	0.603	0.591	0.559	0.402
7	0.106	0.048	0.009	-0.021
8	-0.282	-0.375	-0.401	-0.319
9	-0.295	-0.386	-0.413	-0.375
10	-0.303	-0.362	-0.413	-0.375

TABULATED PRESSURE COEFFICIENTS

RUN 57, Q = 10.00 LB./FTSQ

ORIFICE NO.	CP VALUES AT ALPHA ANGLE SETTINGS 0	3	6	9
1	0.870	0.860	0.866	0.917
2	0.201	0.196	0.125	0.108
3	0.285	0.249	0.125	0.054
4	0.393	0.384	0.251	0.176
5	0.555	0.536	0.443	0.364
6	0.691	0.601	0.606	0.522
7	0.083	0.056	0.039	0.019
8	-0.347	-0.363	-0.377	-0.390
9	-0.347	-0.384	-0.397	-0.390
10	-0.364	-0.382	-0.397	-0.432

TABLE VI

TABULATED SURFACE AND RAKE PRESSURE DISTRIBUTIONS FOR $C_j = \infty (q = 0)$

210

TABULATED PRESSURE DATA

RUN 1, Q = 0.0 LB./FTSQ

ORIFICE NO.	PRESSURE ~ LB/FTSQ AT ALPHA = 0
	0
1	-0.126
2	-0.305
3	-0.126
4	0.011
5	-0.126
6	-0.305
7	-0.179
8	-0.179
9	-0.368
10	-0.368
11	-0.599
12	-0.714
13	-0.714
14	-0.903
15	-1.134
16	-1.660
17	-3.382
18	-10.661
19	0.221
20	0.347
21	0.347
22	0.336
23	0.347

211

TABULATED PRESSURE DATA

RUN 1, Q = 0.0 LB./FTSQ

ORIFICE PRESSURE ~ LB/FTSQ AT ALPHA = 0

NO.	0
24	0.221
25	0.168
26	0.168
27	-0.074
28	0.105
29	0.105
30	0.168
31	0.168
32	0.158
33	0.168
34	0.168
35	0.231
36	-18.602
37	-14.138
38	-10.073
39	-7.416
40	-5.105
41	-4.853
42	-4.328
43	-0.063
44	0.168
45	0.105
46	0.105

TABULATED PRESSURE DATA

RUN 1, Q = 0.0 LB./FTSQ

ORIFICE NO.	PRESSURE ~ LB/FTSQ AT ALPHA = 0
	0
47	-0.074
48	-0.074
49	-0.126
50	-0.126
51	-0.903
52	-0.011
53	0.168
54	0.168
55	-0.011
56	-0.084
57	-0.126
58	-0.105
59	-0.105
60	-0.305
61	-0.305
62	-0.074
63	-0.420
64	-0.368
65	-0.368
66	-26.701
67	-26.522
68	-27.825
69	-30.262

TABULATED PRESSURE DATA

RUN 1, Q = 0.0 LB./FTSQ

ORIFICE NO.	PRESSURE ~ LB/FTSQ AT ALPHA = 0
70	-31.144
71	-30.767
72	-27.226
73	-21.375
74	-18.245
75	-13.624
76	-10.136
77	-8.246
78	-7.405
79	-5.273

TABULATED PRESSURE DATA

RUN 13, Q = 0.0 LB./FTSQ

ORIFICE NO.	PRESSURE ~ LB/FTSQ AT ALPHA = 0
	0
1	58.844
2	119.744
3	92.104
4	61.801
5	35.586
6	14.573
7	3.979
8	0.309
9	0.0
10	0.013

TABULATED PRESSURE DATA

RUN 22, Q = 0.0 LB./FTSQ

ORIFICE NO.	PRESSURE ~ LB/FTSQ AT ALPHA = 0
	0
1	73.262
2	113.091
3	87.633
4	60.648
5	34.867
6	16.832
7	5.759
8	0.230
9	-1.541
10	-1.717

TABULATED PRESSURE DATA

RUN 31, Q = 0.0 LB./FTSQ

ORIFICE NO.	PRESSURE ~ LB/FTSQ AT ALPHA = 0
1	-0.286
2	-0.286
3	-0.286
4	-0.488
5	-0.477
6	-0.753
7	-0.530
8	-0.530
9	-0.647
10	-0.647
11	-0.647
12	-0.827
13	-0.827
14	-1.007
15	-1.092
16	-1.781
17	-3.042
18	-6.625
19	0.0
20	0.0
21	0.0
22	-0.011
23	-0.011

TABULATED PRESSURE DATA

RUN 31, Q = 0.0 LB./FTSQ

ORIFICE NO.	PRESSURE ~ LB/FTSQ AT ALPHA = 0
	0
24	-0.011
25	-0.011
26	-0.085
27	-0.085
28	-0.085
29	-0.286
30	-0.286
31	-0.286
32	-0.286
33	-0.286
34	-0.233
35	-0.095
36	-2.989
37	-2.321
38	-1.548
39	-0.530
40	-0.519
41	-1.198
42	-2.502
43	-0.233
44	-0.233
45	-0.064
46	-0.159

TABULATED PRESSURE DATA

RUN 31, Q = 0.0 LB./FTSQ

ORIFICE NO.	PRESSURE ~ LB/FTSQ AT ALPHA = 0
	0
47	-0.233
48	-0.233
49	-0.286
50	-0.350
51	-0.530
52	0.064
53	0.064
54	-0.053
55	-0.053
56	-0.286
57	-0.350
58	-0.350
59	-0.530
60	-0.530
61	-0.530
62	-0.466
63	-0.466
64	-0.286
65	-0.530
66	-16.239
67	-14.988
68	-14.628
69	-14.268

TABULATED PRESSURE DATA

RUN 31, Q = 0.0 LB./FTSQ

ORIFICE NO.	PRESSURE ~ LB/FTSQ AT ALPHA = 0
	0
70	-13.791
71	-12.709
72	-10.791
73	-8.416
74	-7.038
75	-5.311
76	-4.081
77	-3.519
78	-3.466
79	-3.466

TABULATED PRESSURE DATA

RUN 44, Q = 0.0 LB./FTSQ

ORIFICE NO.	PRESSURE ~ LB/FTSQ AT ALPHA = 0 0
1	-0.424
2	-0.658
3	-0.658
4	-0.902
5	-0.902
6	-0.668
7	-0.658
8	-0.658
9	-0.955
10	-0.955
11	-0.902
12	-1.018
13	-1.018
14	-1.241
15	-1.496
16	-2.036
17	-4.179
18	-16.971
19	-0.244
20	-0.244
21	-0.244
22	-0.424
23	-0.414

TABULATED PRESSURE DATA

RUN 44, Q = 0.0 LB./FTSQ

ORIFICE NO.	PRESSURE ~ LB/FTSQ AT ALPHA = 0
	0
24	-0.414
25	-0.414
26	-0.414
27	-0.414
28	-0.414
29	-0.424
30	-0.424
31	-0.424
32	-0.424
33	-0.308
34	-0.318
35	-0.286
36	-72.496
37	-55.123
38	-40.157
39	-30.600
40	-22.656
41	-17.151
42	-6.905
43	-0.244
44	-0.233
45	-0.233
46	-0.212

222

TABULATED PRESSURE DATA

RUN 44, Q = 0.0 LB./FTSQ

ORIFICE NO.	PRESSURE ~ LB/FTSQ AT ALPHA = 0
	0
47	-0.244
48	-0.244
49	-0.477
50	-0.477
51	-1.252
52	-0.297
53	-0.180
54	-0.424
55	-0.424
56	-0.477
57	-0.477
58	-0.424
59	-0.424
60	-0.477
61	-0.477
62	-0.658
63	-0.658
64	-0.297
65	-0.668
66	-36.752
67	-40.751
68	-50.381
69	-69.749

TABULATED PRESSURE DATA

RUN 44, Q = 0.0 LB./FTSQ

ORIFICE NO.	PRESSURE ~ LB/FTSQ AT ALPHA = 0
	0
70	-82.827
71	-87.791
72	-78.987
73	-64.637
74	-55.748
75	-42.257
76	-32.212
77	-25.159
78	-18.890
79	-6.576

TABULATED PRESSURE DATA

RUN 49, Q = 0.0 LB./FTSQ

ORIFICE NO.	PRESSURE ~ LB/FTSQ AT ALPHA = 0
	0
1	6.716.
2	135.473
3	109.779
4	73.935
5	43.446
6	22.315
7	1.076
8	0.0
9	0.0
10	0.177

DISCUSSION OF LOW-SPEED WIND TUNNEL TESTS OF A QUASI-TWO DIMENSIONAL EJECTOR-AUGMENTED JET FLAP AIRFOIL

This report presents the results of low-speed wind tunnel tests of a quasi-two dimensional ejector-augmented jet flap airfoil. The primary purpose of these tests was to obtain data for use in evalutaing the theoretical approach proposed in Ref. 1* for predicting the behavior of ejector-augmented jet flap systems. In this reference a numerical solution has been devised for the two-dimensional potential flow around a powered augmentor wing section as represented by an embedded vortex distribution technique.

The present wind tunnel tests were conducted in the closed, three-dimensional test section of the GALCIT** ten-foot wind tunnel during the period May 8-10, 1973. The work was performed under NASA Ames Research Center Grant No. UT-290-SC-2001.

Model, test set-up and Procedures

The model used for these tests was constructed primarily from wood with an internal metal air supply system for the ejector and static pressure orifices at center-span for measuring the static pressure distribution. The model consisted of a main wing, a flap set at 30 degrees relative to the wing chord plane, a shroud with adjustable height placed above the flap and set at 32 degrees relative to the wing chord plane, an ejector located in the main wing and elliptically shaped end plates. One end plate incorporated a flush lucite window to permit the observation of surface attached tuft behavior between the flap and shroud during portions of the testing. The model had a design wing chord of 24 inches, and a span between end plates of 36 inches.

The gap between the main wing lower surface and the flap was sealed closed with tape in an attempt to more nearly represent the math-

*Ref. 1. L. B. Sidor, An Investigation of the Ejector-Powered Jet Flap. A.E. Thesis, California Institute of Technology, 1974.

**Guggenheim Aeronautical Laboratory, California Institute of Technology.

ematical model specified in Ref. 1 which does not provide for airflow thru this gap. The 2 degree convergence angle between the shroud and the flap chord planes resulted in a 3.4 degree total divergence angle between the flap upper surface and the shroud lower surface. This was considered conservative for the existence of fully attached flow in this region.

The ejector incorporated a simple two-dimensional exit slot which measured 0.09 ± 0.005 inch high at the exit plane. The ejector or auxiliary air trajectory was adjusted such that the vertical centerline of this air would be tangent with the flap leading edge radius. The auxiliary air was then to provide a sink effect, with only relatively small amounts of mass addition, for the entrainment of much larger amounts of freestream air entering between the wing upper surface and the shroud. No attempt was made to promote the mixing of the freestream and auxiliary air in the region between the flap and shroud. Additional information related to the model is presented in Tables I-B, II-A and III and on Figs. 2 and 3.

In order to measure the total pressure distribution across the exit plane of the flap-shroud system (a primary parameter in Ref. 1) a total head rake was constructed as shown on Fig. 4. The rake was installed for those test runs where rake pressures were recorded as indicated on the Index of Runs. The rake was located at center-span and supported by a section of streamlined tubing attached between the end plates. The plane of symmetry of the streamlined tubing was oriented at 24 degrees relative to the wing chord plane which was calculated to be the nominal downwash angle in the region occupied by the tubing. Additional detail concerning the installation of the rake is presented in Table II-B with a photograph on Photo Page 5.

The model was supported in the wind tunnel on the standard three-strut system for the ten-foot wind tunnel external balance. A sketch of the wind tunnel air path and external balance is presented on Fig. 1.

The two main support bayonets were attached to plates on the model located outboard of the end plates. The tail support strut was attached to a U-shaped extension boom from the end plates. Vertical movement of the tail support strut resulted in a change in angle of attack

of the model, which was pitched about a line coincident with the intersection of the wing 0.25 chord and the wing chord plane. Photographs of the model supported in the wind tunnel are presented on Photo Pages 4 and 5.

Auxiliary air, for the model ejector, was supplied by the supersonic wind tunnel compressor system. Air flow control was maintained by a valve in the main air supply line and monitered by the pressure difference from a 3.5 inch venturi flow meter (see Fig. 3). The auxiliary air volume flow was held constant at $Q_e = 21.45$ ft^3/sec (measured at the venturi) during test runs where $C_j \neq 0$. This resulted in a constant auxiliary air weight flow of 0.83 lb/sec. The auxiliary air momentum coefficient C_j, was varied during the tests by changing the freestream dynamic pressure q, as shown on the Index of Runs. The auxiliary air velocity at the mid span of the ejector exit was calculated to be 741.6 ft/sec using the measured exit temperature of the auxiliary airstream and the static pressures on the flap and shroud in the region of the exit. The orifices on the flap and shroud nearest to the ejector were approximately 0.5 inch from the exit plane and a smooth fairing between measured static pressures was used to approximate the static pressure at the exit.

Prior to the tests and with the complete model assembled a total pressure survey was performed along the complete span at the ejector exit. The total pressure was found to vary less than 0.6 percent along the span except for 2.5 inches inboard of each end plate. In these two regions the total pressure was deficient by approximately 50 percent due to internal losses in the plennum just inboard of the air supply hoses. The result was an ejector exit velocity which was of the order of 30 percent low in these regions. This should not however affect the pressure data recorded at center span.

During the auxiliary air flow calibration, checks were also made to determine if choking had occured within the air supply system or at the ejector exit. There was no evidence that the airflow was choked anyhwere in the system and a uniform increase in exit total pressure could be obtained over the center 85 percent of the span by opening the supply pipe valve further. However, for a significent increase in ejector airflow it was found to be difficult to hold this airflow steady over the ten minute period required for a test run and therefore the lower ejector air

setting was selected for the experiments.

The tunnel airstream dynamic pressure settings used for these tests were corrected for the effects of solid and wake blockage using the following formula:

$$q = q_{\mu} (1 + 2\epsilon)$$

where ϵ is the blockage factor dependent upon model shape and volume (or frontal area for bluff shapes) and tunnel test section shape and cross-sectional area; q_{μ} is the dynamic pressure of the airstream without the model present. The correction includes the effects of the model with endplates and the portion of auxiliary air supply hoses and pressure tubing exposed to the airstream, and accounts for the increase in air velocity over the model due to Bernoulli's principle.

Data recorded during these tests include static pressure data from flush surface orifices located around the mid-spans of the main wing, flap and shroud as shown on Fig. 2; total pressure data from the rake previously discribed and shown on Fig. 4; and photographs of the behavior of tufts (strands of standard darning cotton) attached to the upper surfaces of the wing and shroud. No attempt was made to record force and moment data from the external balance system due to interference effects of the auxiliary air supply hoses.

Flexible tubing was used to connect the model static pressure orifices and the rake total pressure orifices to a 100-tube multimanometer board. The pressure data were acquired simultaneously for each point of a test run by photographing the manometer board. After processing, the film was projected onto a ground glass screen where precise measurements of the manometer fluid (alcohol) heights were made utilizing an adjustable hairline connected to a slide wire with the output automatically digitized onto IBM cards through a digital voltmeter. As an initial step in the data reduction program these data were reduced to pressure coefficients (C_{p_m} defined in Table I) by computer.

Test Results

The complete set of pressure coefficients calculated from data recorded during these tests are presented in tabular form in Tables IV, V and VI. Table IV contains the C_p values from the model surface pressure orifices which are listed versus orifice number (ref. Fig. 2 and

Table III), run number and angle of attack. The total pressure rake data are presented in Table V versus rake orifice number (see Fig. 4), run number and angle. The data presented in Table VI were calculated from data recorded from both the surface pressure orifices and the rake with $q = 0$ and therefore these data are not dimensionless coefficients as presented in Tables IV and V. The values presented in Table VI were calculated in the same manner as used for the C_p values in the previous tables by assuming $q \equiv 1$ lb/ft^2, and therefore the values in this table are actually pressure differences (the difference between the pressure acting at orifice m and atmospheric pressure) denoted in lb/ft^2. Complete test conditions for data of any test run are given by the Index of Runs.

Lift and drag coefficients, C_L and C_D, were calculated by integration of the surface static pressure coefficients as indicated under Definition of Coefficients in Table I. These integrations were performed by computer separately for the main wing with flap and for the shroud. The resulting data were plotted and faired with smooth continuous lines and from these fairings the wing-flap and shroud data were summed to form C_L and C_D. These lift and drag coefficients are presented in plotted form versus geometric angle of attack for the various shroud positions tested on Figs. 5-7 for the model without the ejector operating and on Figs. 8-10 with the ejector operating.

To demonstrate the overall effects of the ejector operating at various C_j values, total force coefficients C_{L_T} and C_{D_T} were calculated as indicated on Table I. These coefficients include the reaction of the momentum in the ejector airflow and are, except for skin friction, the force coefficients which would be expected from force balance measurements. These data are presented in plotted form on Figs. 11-13 for the various angles of attack and shroud height positions of the tests and are useful when comparing these test results with other work.

Immediately prior to the first test run strands of standard darning cotton (tufts) were attached to the upper surface of the wing, flap and shroud and to the lower surface of the shroud with streamwise strips of Scotch brand cellophane tape. The behavior of the tufts was observed for the full range of test conditions and shroud positions anticipated for the tests. For runs 6-8 a portion of the tuft strips were replaced on the upper wing and shroud surfaces and photographs were taken to record

the tuft behavior with the shroud set in the center position of $h/c_s = 0.225$. Examples of these photographs are presented on Photo Pages 1-3. Unfortunately adequate lighting for photographs could not be obtained in the region between the flap and shroud.

From the tuft observations the airflow between the flap upper surface and shroud lower surface was steady and fully attached to both surfaces for all test conditions. At the highest shroud position of $h/c_s = 0.270$ however some unsteadiness in the tufts attached to the aft 30% of shroud existed when $q = 0$ indicating possible incipient separation for this region and test condition. With some freestream flow, $q = 2.25$ lb/ft^2 for example, this condition was completely eliminated and the tufts were again steady and tight against the shroud surface. Also, with $Q_e = 21.45$ lb/ft^2 and $q = 0$ ($C_j = \infty$), entrainment of the free air into the region between the flap and shroud appeared to be excellent for all test h/c_s values as observed with a 6 inch long strand of knitting wool attached to the end of a pole and used as a visual probe. The photograph on Photo Page 1 gives an indication of the region of entrained flow from over the main wing which extends up to approximately the 30% chord line and also shows flow entering from above the shroud leading edge as evidenced by the pulling in of the tufts attached to the shroud above this leading edge.

For finite C_j values ($q \neq 0$) airflow over the wing was fully attached for all h/c_s and α_g settings. Examples of the tuft behavior on the upper wing surface are shown for the maximum finite C_j value and minimum C_j value ($C_j \neq 0$) on Photo Pages 2 and 3 respectively. Flow separation did occur however over the aft 50% of the shroud upper surface for the two lower test C_j values of 0.33 and 0.65. Angle of attack and shroud height had only minor effects on this region of flow separation (see Photo Pages 2 and 3).

From a review of the basic force data, C_L and C_D, presented on Figs. 5-7 for $C_j = 0$ and on Figs. 8-10 for $C_j \neq 0$, the following comments can be made. The force coefficients, primarily C_L, behaved in a reasonably linear manner with angle of attack for all test shroud positions and C_j values. There is some increase in the level of C_L and C_D with increasing shroud height for $C_j = 0$ and $C_j \neq 0$ and in the level of C_L with q for $C_j = 0$. The lift curve slopes however appear to be essentially constant with h/c_s and q for $C_j = 0$ and with h/c_s and C_j for $C_j \neq 0$. From

Figs. 5-7 $(dC_L/d\alpha_g)_{C_j=0} \pm 0.045$/deg. and from Figs. 8-10 $(dC_L/d\alpha_g)_{C_j=0} \pm 0.058$/deg. It is worth mentioning that the lift and drag coefficients of the shroud tend to be constant with α_g for both the blowing and non-blowing cases and the lift curve slope is therefore that of the basic flapped airfoil.

The fact that the lift coefficient tends to decrease with increasing test airstream velocity suggests that the behavior of C_L and C_D with q is not simply due to Reynolds number (see Figs. 5-7). While the test Reynolds numbers (see Table II-B) were somewhat low for a 65 series airfoil, the behavior of C_L and C_D with α_g does not suggest erratic characteristics such as found for these airfoils at the lower Reynolds numbers ($R \leq 0.15 \times 10^6$).

In addition the levels of C_L and $dC_L/d\alpha_g$, at least for tests where $C_j = 0$, are low when compared to values calculated using thin airfoil theory for a flat plate with $\delta_f \approx 30^o$. These calculations yield C_L values of the order of two times those obtained from the experiments and a lift curve slope of at least 0.08/deg. Of course these values should be reduced somewhat to account for the fact that model end plates do not result in true two-dimensional flow and the experimental values of C_L and dC_L/α_g should be increased by 8 percent to account for the 26 inch wing-flap chord used for data reduction in place of the more usual design chord of 24 inches.

In an attempt to explain the aforementioned anomalies in the experimental data the surface static pressure coefficients were examined. These data in general look well behaved and normal everywhere except for the data recorded from the pressure side of the wing in the region of the wing-flap intersection. In this region (primarily orifice nos. 35, 43 and 44 as shown on Fig. 2) the C_p values increase from approximately 0.5 to approximately 0.7 or 0.8 with some dependence on α_g. This behavior can be followed by scanning the data in Table IV, and suggests that a separated region exists in the knee on the lower surface of the wing. It is unfortunate that tuft behavior could not be observed in this region due to the model end plates but it is suspected that a recirculating flow existed for all tests in this separated region at the intersection of the wing and flap and was probably caused by sealing the gap between the

Vertical Section through 10-Ft. Wind Tunnel
2 Parameter 6 Component Suspension System
Guggenheim Aeronautics Laboratory
California Institute of Technology

GALCIT Rep. 926

Fig. 1

wing and flap lower surfaces. This recirculating flow may well have been deformed depending on freestream q and α_g resulting in changes in the effective wing camber, wing thickness and thickness distribution. This type of behavior would explain the variations in C_L and C_D with q and at least part of the deficiencies in C_L and $dC_L/d\alpha_g$.

To complete the experimental data review the total pressure rake data presented in Table V were examined. It should be pointed out here that rake orifice no. 1 was always lined up with the flap T.E. and for runs where $h/c_s = 0.180$ orifice nos. 1-6 covered the area between the flap and shroud; for $h/c_s = 0.225$ orifice nos. 1-9 covered the area with orifice no. 9 at the shroud T.E.; and for $h/c_s = 0.270$ all ten orifices where data were recorded are necessary to cover the area between the flap and shroud.

The C_p values representing the total pressure distribution at the exit plane between the flap and shroud are seen to vary enormously across this space with the variation dependent primarily upon C_j but with little, if any affect due to angle of attack. To graphically show this behavior, data from test runs selected randomly for each test h/c_s are presented on Figs. 14-16. The non-uniformity in the C_p distributions when $C_j \neq 0$ indicates poor mixing between the auxiliary airstream from the ejector and the entrained air entering the region between the flap and shroud. However, the existance of C_p values much greater than 1 in the region of the shroud for $h/c_s = 0.180$ while the C_p values for the larger h/c_s settings were progressively lower indicates that mixing was better for the lower shroud setting. Had mixing in this region been a clear test objective, additional shroud angle settings could have been evaluated along with screens or low pressure loss lifting surfaces placed between the flap and shroud to promote mixing and provide a more uniform exit velocity profile.

Guggenheim Aeronautical Laboratory
California Institute of Technology

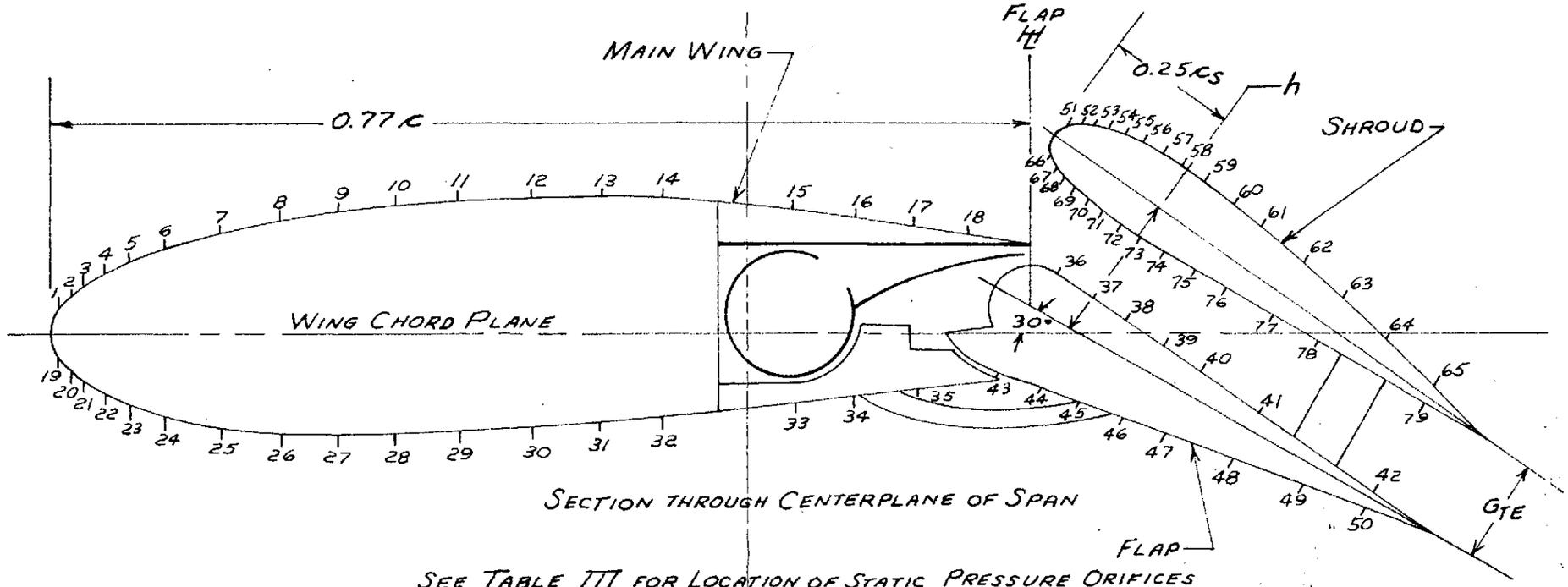

SECTION THROUGH CENTERPLANE OF SPAN

SEE TABLE III FOR LOCATION OF STATIC PRESSURE ORIFICES

235

SKETCH OF MODEL SHOWING STATIC PRESSURE ORIFICE LOCATIONS

A

B

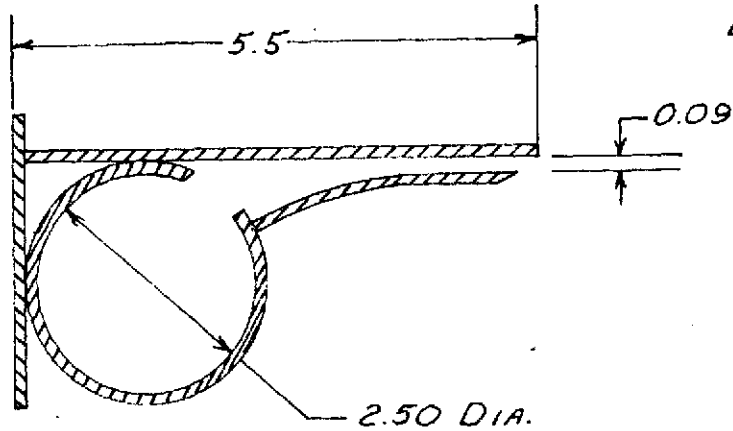

DIMENSIONS IN INCHES

SECTION A-A

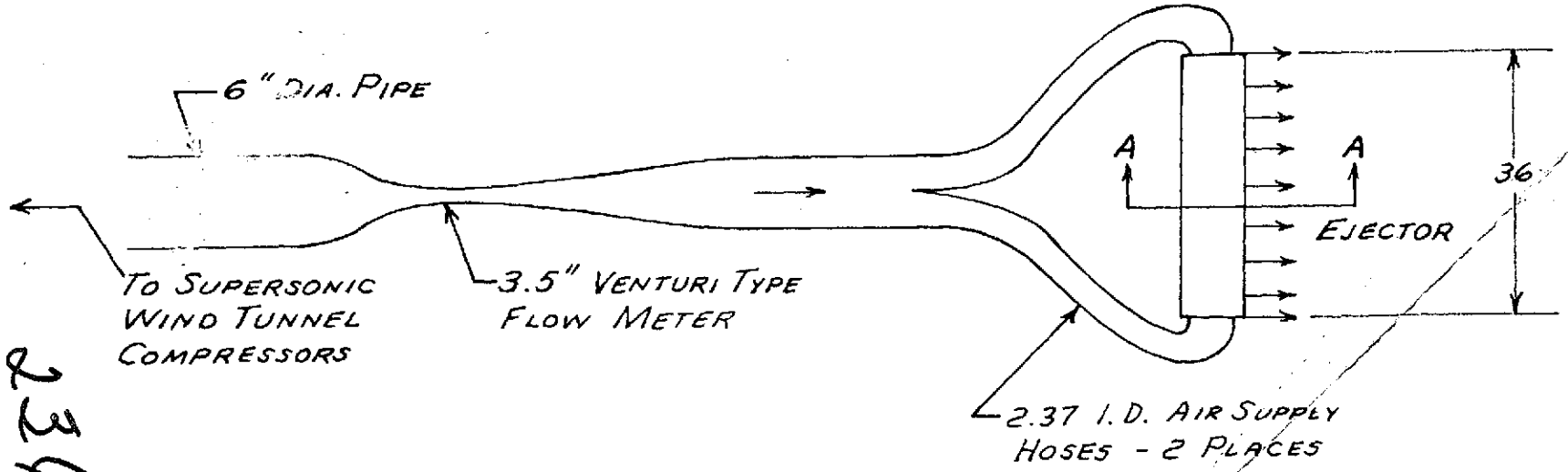

SKETCH SHOWING AUXILLARY AIR SUPPLY SYSTEM

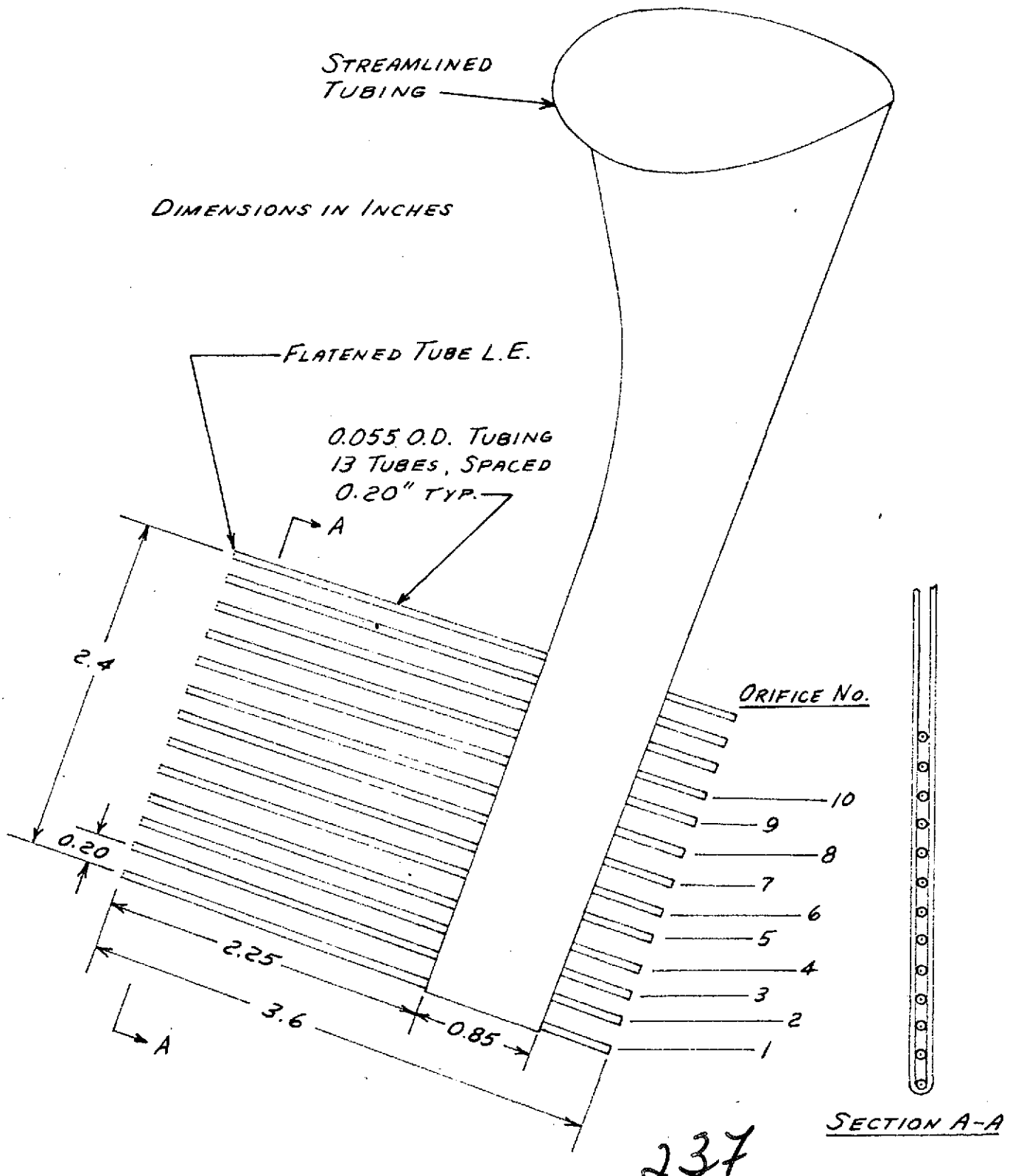

237

SKETCH SHOWING TOTAL HEAD RAKE

BASIC CONFIGURATION, $h/c_3 = 0.225$
$C_j = 0$

o	q = 10.0	LB/FT^2,	RUN 12
Δ	" = 5.0	"	" 11
□	" = 3.0	"	" 10
▽	" = 2.25	"	" 9

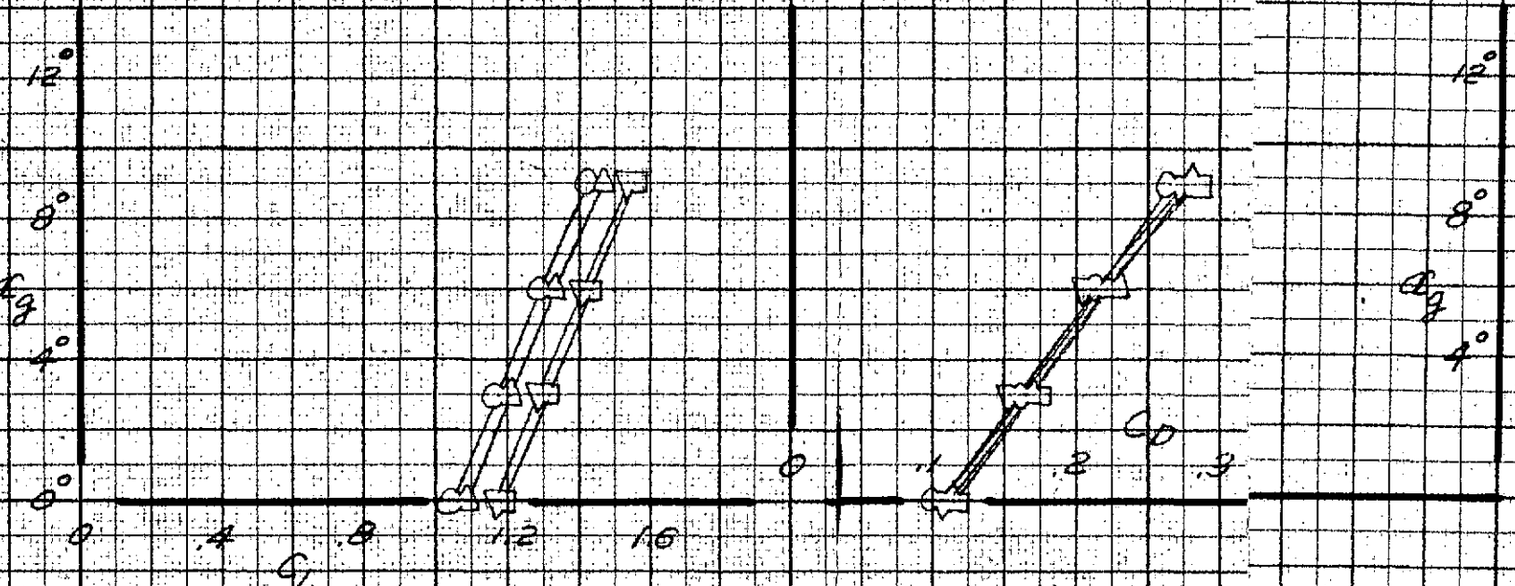

239

FORCE COEFFICIENTS DETERMINED FROM SURFACE PRESSURE INTEGRATION FOR THE MODEL WITHOUT BLOWING AND $h/c_3 = 0.225$

C_L, C_D VS. α_g

A

B

BASIC CONFIGURATION, $h/c_s = 0.180$
$C_J = 0$

○	q = 10.0	LB/FT^2,	RUN 43
△	" = 5.0	" ,	" 42
□	" = 3.0	" ,	" 41
▽	" = 2.25	" ,	" 40

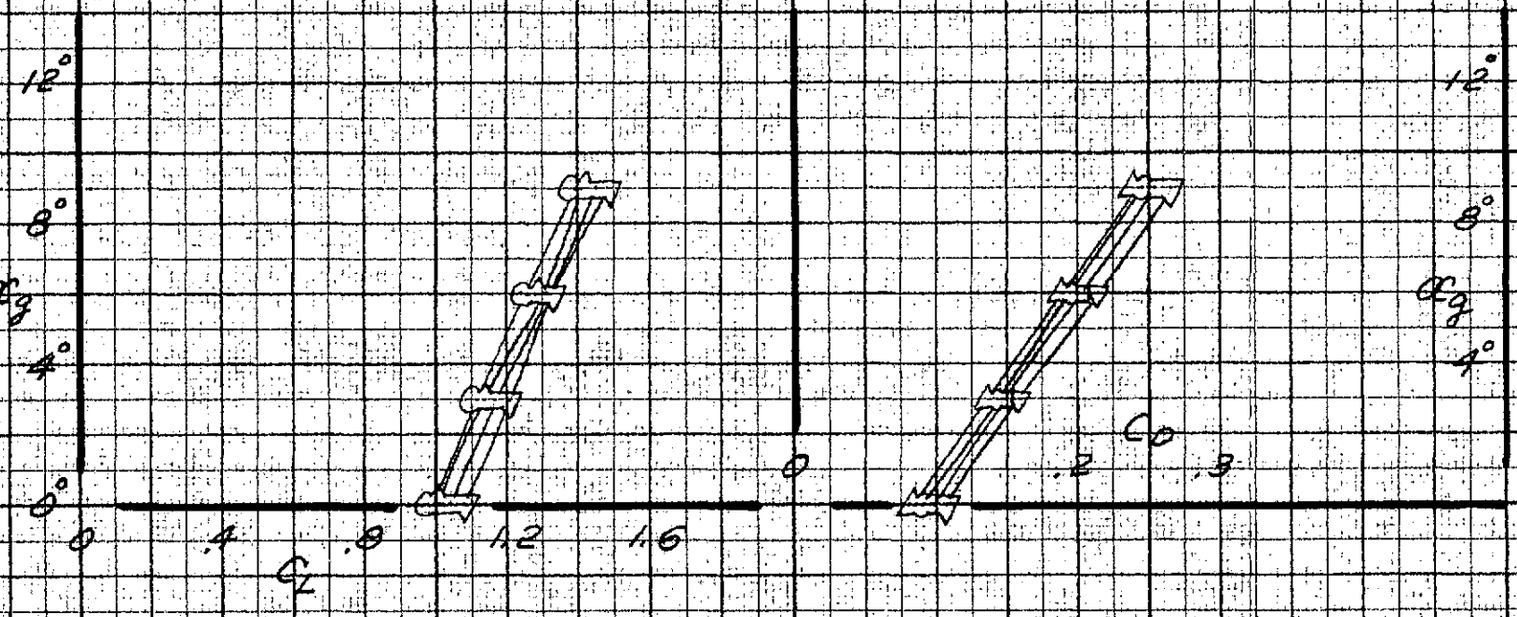

FORCE COEFFICIENTS DETERMINED FROM SURFACE PRESSURE INTEGRATION FOR THE MODEL WITHOUT BLOWING AND $h/c_s = 0.180$

C_L, C_D VS. α_g

BASIC CONFIGURATION, $h/c_0 = 0.270$
$C_j = 0$

○	q = 10.0	LB/FT^2,	RUN 39
△	" = 5.0	"	" 38
□	" = 3.0	"	" 37
▽	" = 2.25	"	" 36

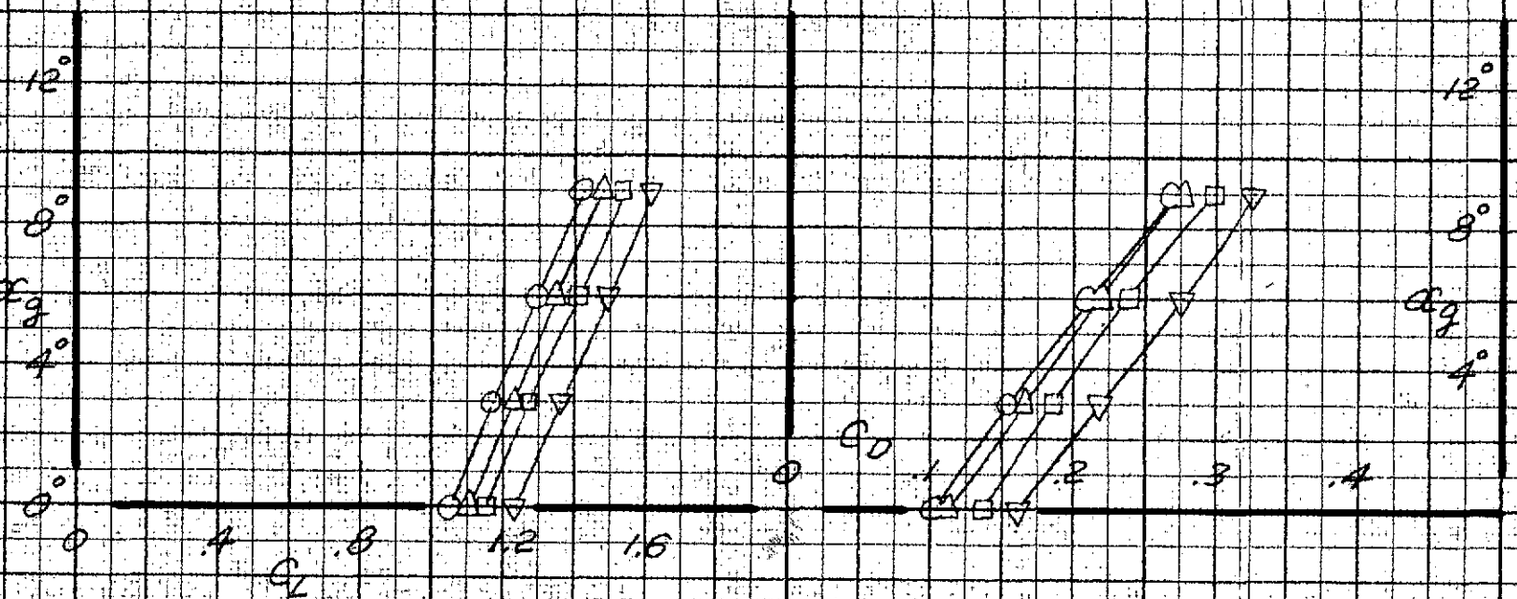

140

FORCE COEFFICIENTS DETERMINED FROM SURFACE PRESSURE INTEGRATION FOR THE MODEL WITHOUT BLOWING AND $h/c_0 = 0.270$

C_L, C_D VS. α_g

BASIC CONFIGURATION, $h/c_r = 0.180$

○	q = 10.0 LB/FT²,	C_J = 0.33,	RUN	48
△	" = 5.0 "	" = 0.66,	"	47
□	" = 3.0 "	" = 1.09,	"	46
▽	" = 2.25 "	" = 1.45,	"	45

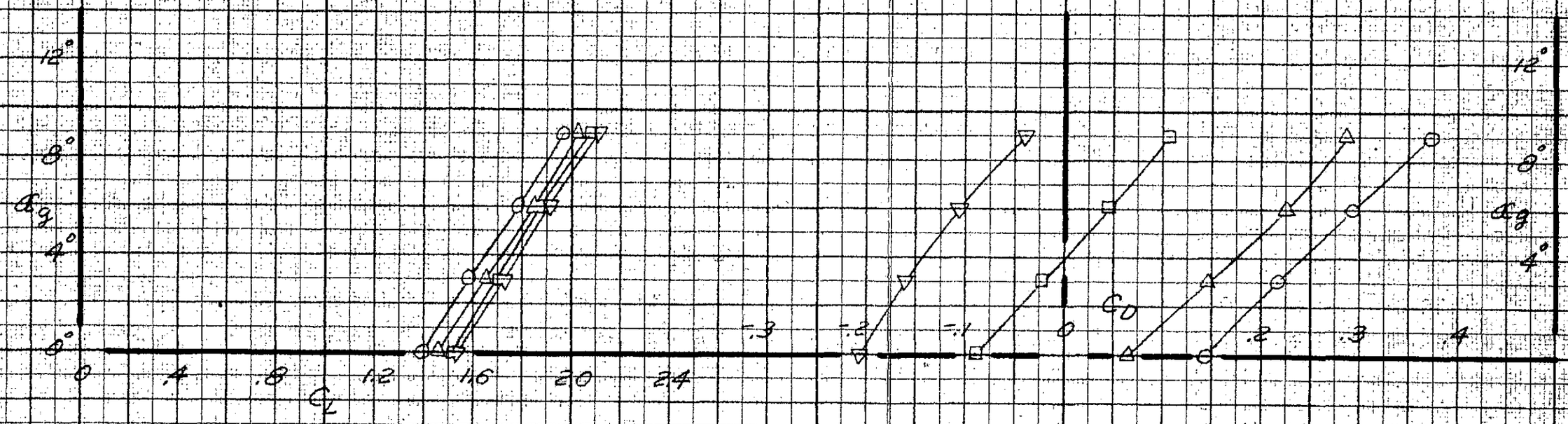

241

A

FORCE COEFFICIENTS DETERMINED FROM SURFACE PRESSURE INTEGRATION FOR THE MODEL WITH BLOWING AND $h/c_r = 0.180$

C_L, C_D VS. α_g

B

BASIC CONFIGURATION, $h/c_s = 0.225$

o	q = 10.0	LB/FT^2,	C_j = 0.33,	RUN	5
Δ	" = 5.0	"	" = 0.66,	"	4
□	" = 3.0	"	" = 1.09,	"	3
▽	" = 2.25	"	" = 1.45,	"	2

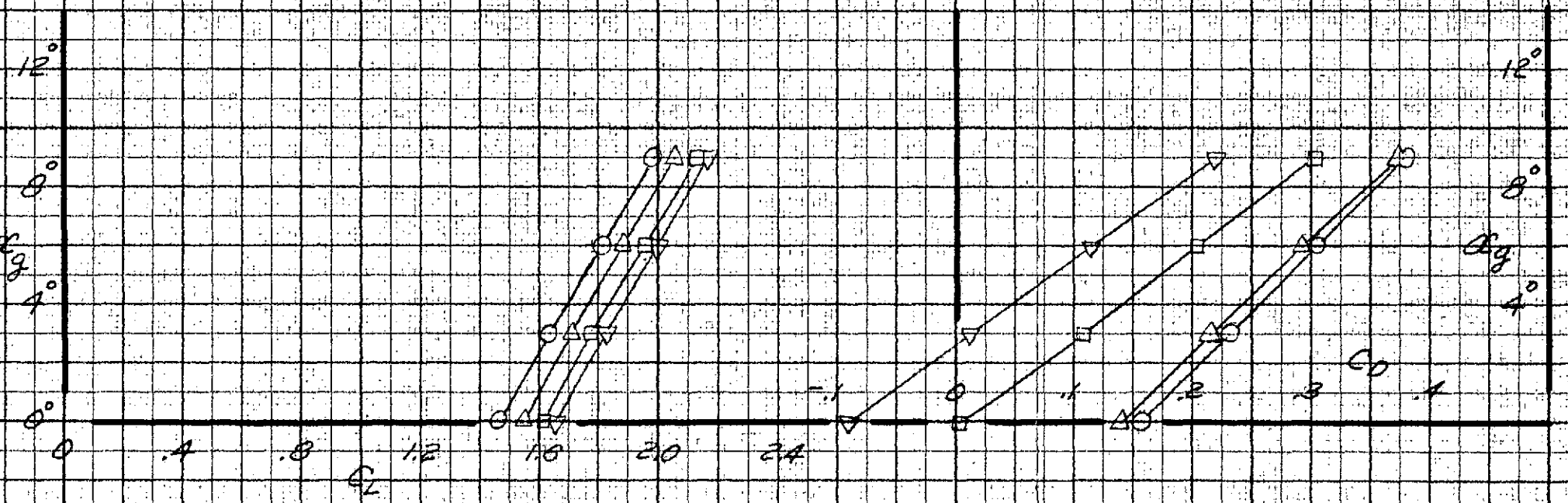

242

A

FORCE COEFFICIENTS DETERMINED FROM SURFACE PRESSURE INTEGRATION FOR THE MODEL WITH BLOWING AND $h/c_s = 0.225$

C_L, C_D VS. α_g

B

BASIC CONFIGURATION, $h/c_s = 0.270$

○	q = 10.0 LB/FT²,	C_f = 0.33,	RUN	35
△	" = 5.0 "	" = 0.66,	"	34
□	" = 3.0 "	" = 1.00,	"	33
▽	" = 2.25 "	" = 1.45,	"	32

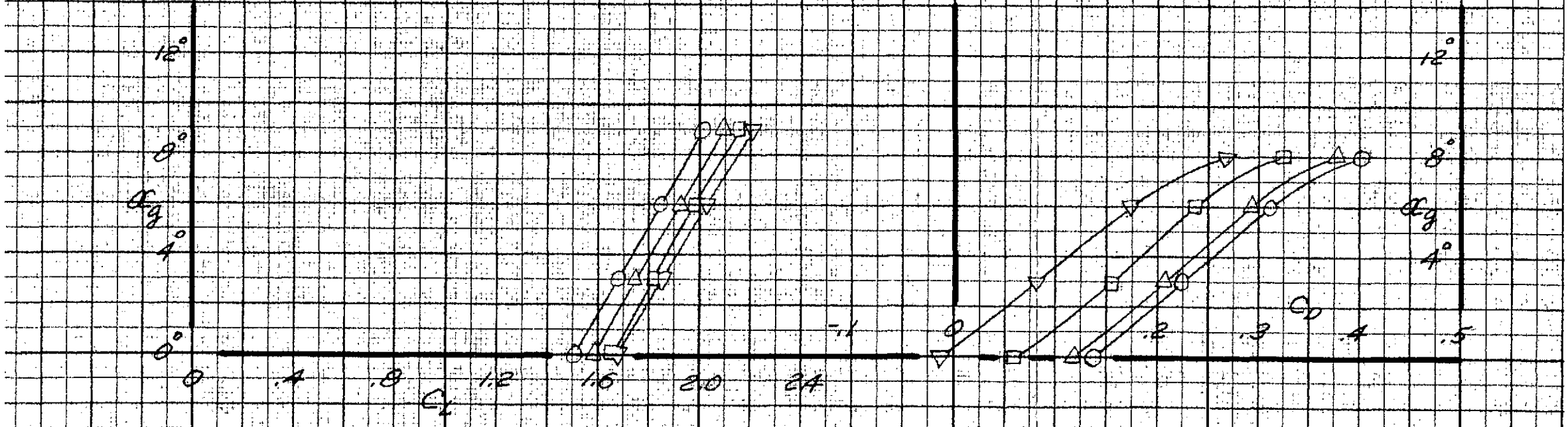

FORCE COEFFICIENTS DETERMINED FROM SURFACE PRESSURE INTEGRATION FOR THE MODEL WITH BLOWING AND $h/c_s = 0.270$

C_L, C_D VS. α_g

BASIC CONFIGURATION, $h/c_s = 0.180$

○ $\alpha_g = 0°$
△ " $= 3°$
□ " $= 6°$
▽ " $= 9°$

} RUNS* 40, 43, 45-48

*AT $C_j = 0$ NON-TAGGED DATA FOR $q = 10$ LB/FT^2
TAGGED " " " $= 2.25$ "

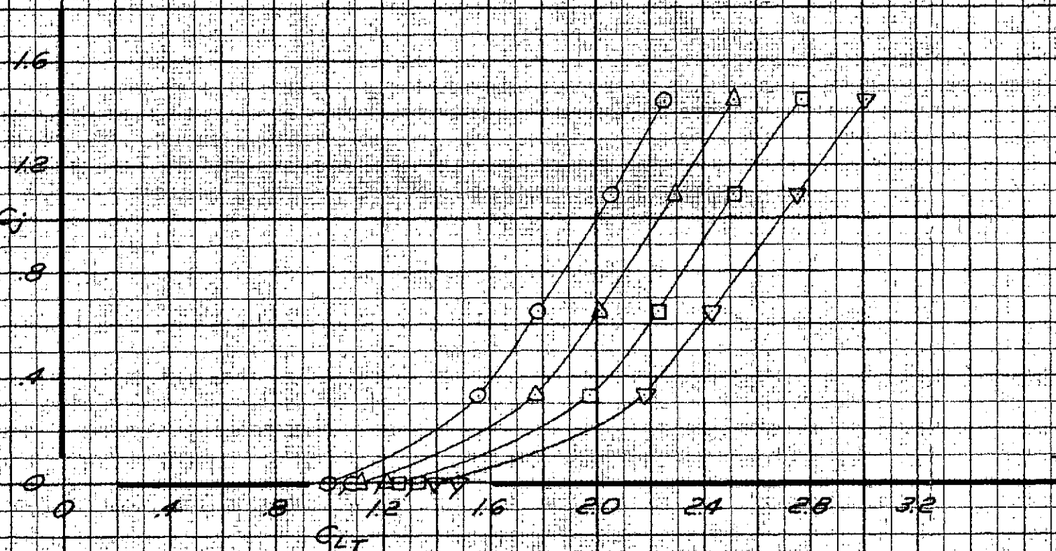

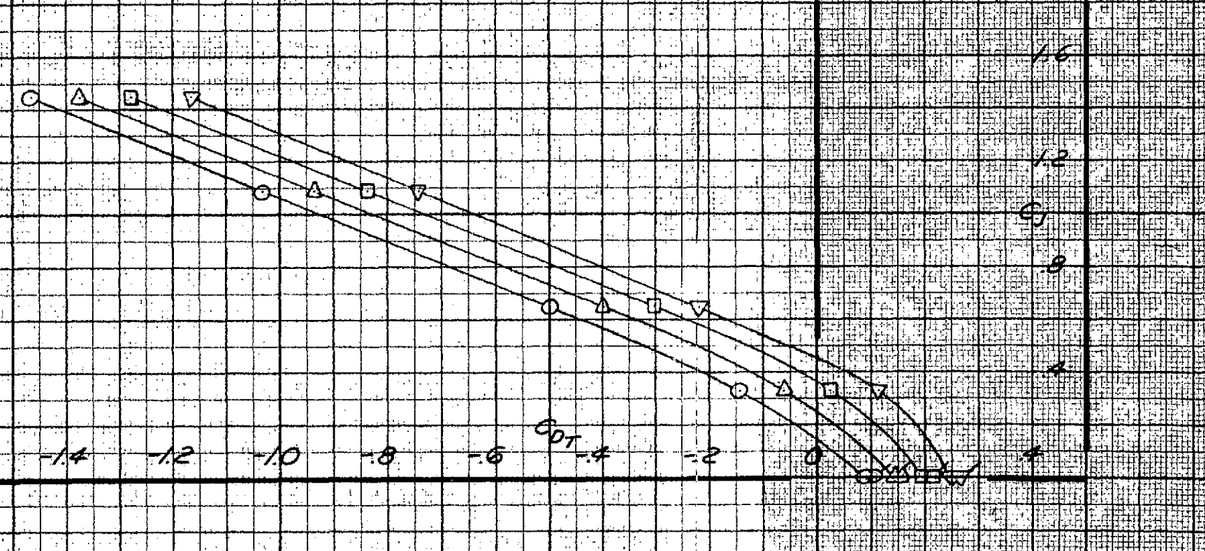

EFFECTS OF BLOWING ON THE TOTAL FORCE COEFFICIENTS WITH THE MODEL AT VARIOUS ANGLES OF ATTACK AND $h/c_s = 0.180$

C_{LT}, C_{DT} VS. C_j

BASIC CONFIGURATION, $h/c_s = 0.225$

- ○ $\alpha_g = 0°$
- △ " $= 3°$
- □ " $= 6°$
- ▽ " $= 9°$

} RUNS* 2-5, 9, 12

*AT $C_j = 0$ NON-TAGGED DATA FOR $q = 10$ LB/FT^2
TAGGED " " " $= 2.25$ "

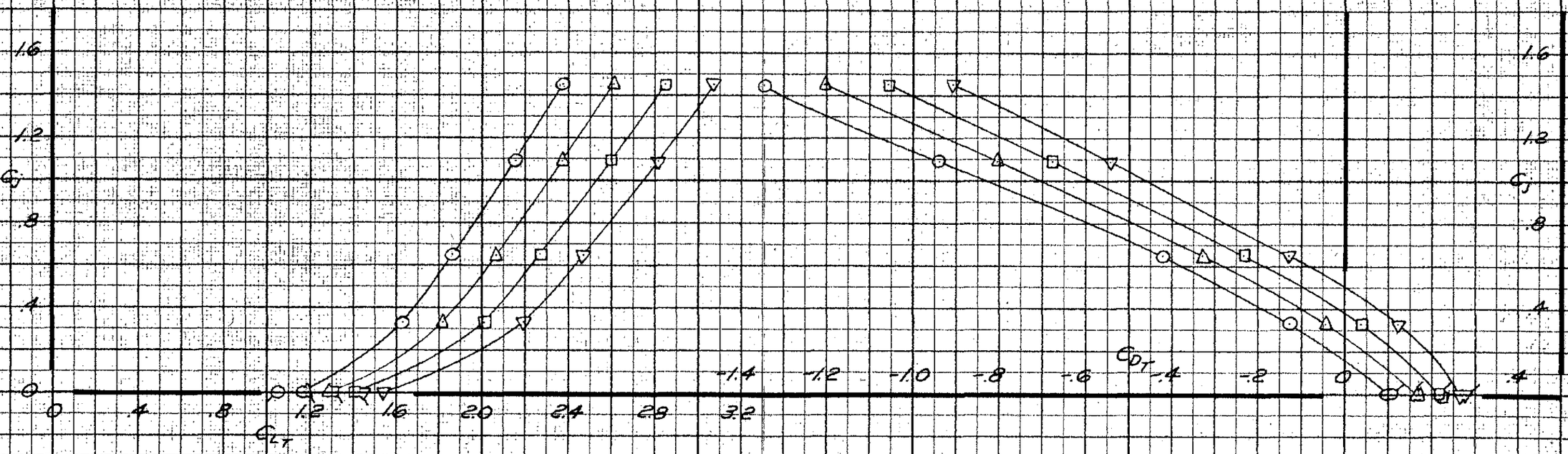

EFFECTS OF BLOWING ON THE TOTAL FORCE COEFFICIENTS WITH THE MODEL AT VARIOUS ANGLES OF ATTACK AND $h/c_s = 0.225$

C_{L_T}, C_{D_T} VS. C_j

BASIC CONFIGURATION, $h/c_s = 0.270$

○ $\alpha_g = 0°$
△ " $= 3°$
□ " $= 6°$
▽ " $= 9°$
} RUNS* 32-36, 39

*AT $C_J = 0$ NON-TAGGED DATA FOR $q = 10$ LB/FT^2
TAGGED " " " $= 2.25$ "

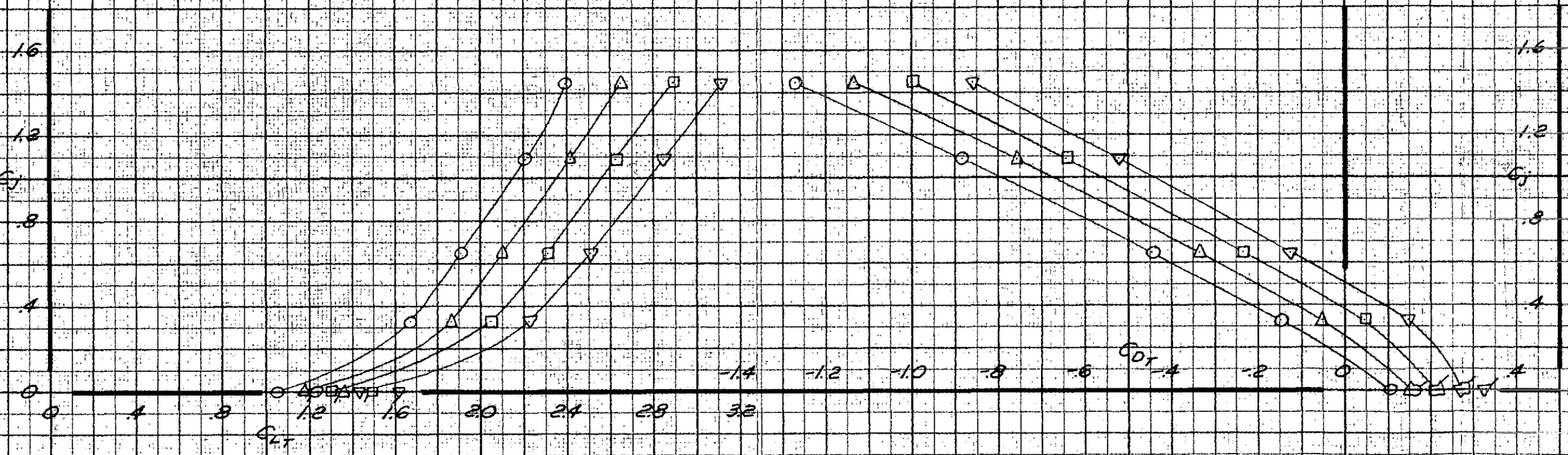

EFFECTS OF BLOWING ON THE TOTAL FORCE COEFFICIENTS WITH THE MODEL AT VARIOUS ANGLES OF ATTACK AND $h/c_s = 0.270$

C_{L_T}, C_{D_T} VS. C_J

BASIC CONFIGURATION, $h/c_s = 0.180$
$q = 50$ LB/FT.^{2}

○	$\alpha_g = 0°$	$C_j = 0.65$	RUN	52
△	" $= 3°$	" = "	"	"
□	" $= 6°$	" = "	"	"
▽	" $= 9°$	" = "	"	"
○	" $= 0°$	" = 0	"	56
△	" $= 3°$	" = "	"	"
□	" $= 6°$	" = "	"	"
▽	" $= 9°$	" = "	"	"

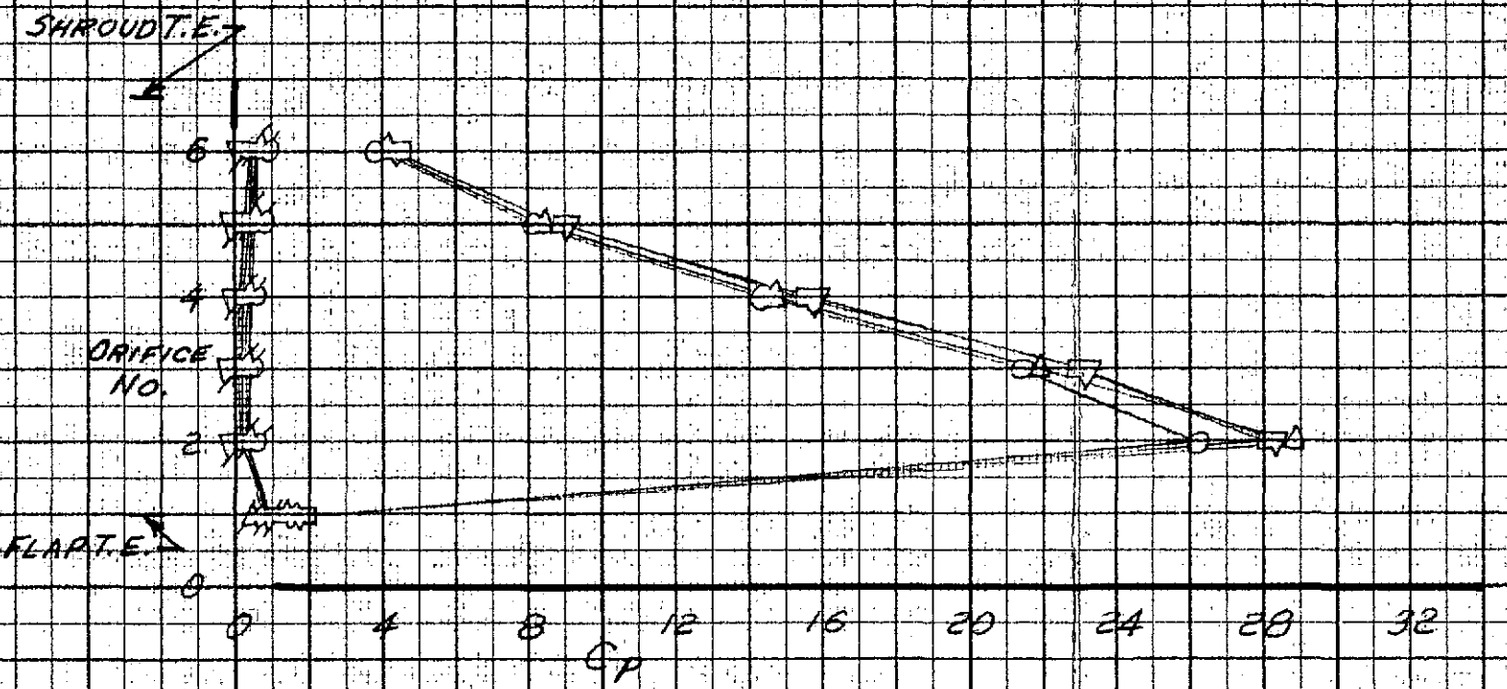

247

EXAMPLE TOTAL HEAD PRESSURE DISTRIBUTIONS BETWEEN THE FLAP AND SHROUD TRAILING EDGES WITH $h/c_s = 0.180$

C_p VS. ORIFICE NO.

A

B

BASIC CONFIGURATION, $h/c_s = 0.285$
$\theta = 10.0 < \theta/\alpha_T^2$

o	$\alpha_g = 0°$	$C_j = 0.33$	RUN	17	
Δ	" = 3°	" = "	"	"	
□	" = 6°	" = "	"	"	
▽	" = 9°	" = "	"	"	
○	" = 0°	" = 0	"	21	
△	" = 3°	" = "	"	"	
□	" = 6°	" = "	"	"	
▽	" = 9°	" = "	"	"	

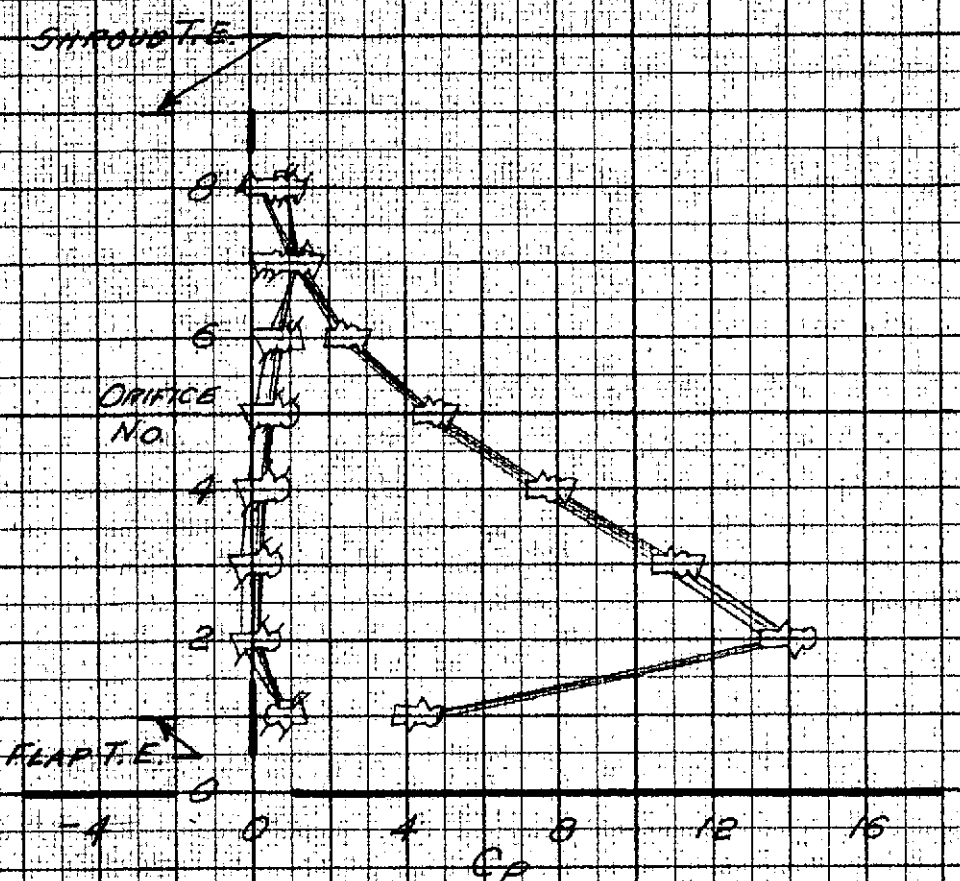

EXAMPLE TOTAL HEAD PRESSURE DISTRIBUTIONS BETWEEN THE FLAP AND SHROUD TRAILING EDGES WITH $h/c_s = 0.285$

C_p VS. ORIFICE NO.

A

B

BASIC CONFIGURATION, $h/c_s = 0.270$
$q = 2.25$ LB/FT^2

○	$\alpha_s = 0°$,	$C_j = 1.45$,	RUN	23	
△	" $= 3°$,	" =	" ,	"	"
□	" $= 6°$,	" =	" ,	"	"
▽	" $= 9°$,	" =	" ,	"	"
○	" $= 0°$,	" =	0 ,	"	27
△	" $= 3°$,	" =	" ,	"	"
□	" $= 6°$,	" =	" ,	"	"
▽	" $= 9°$,	" =	" ,	"	"

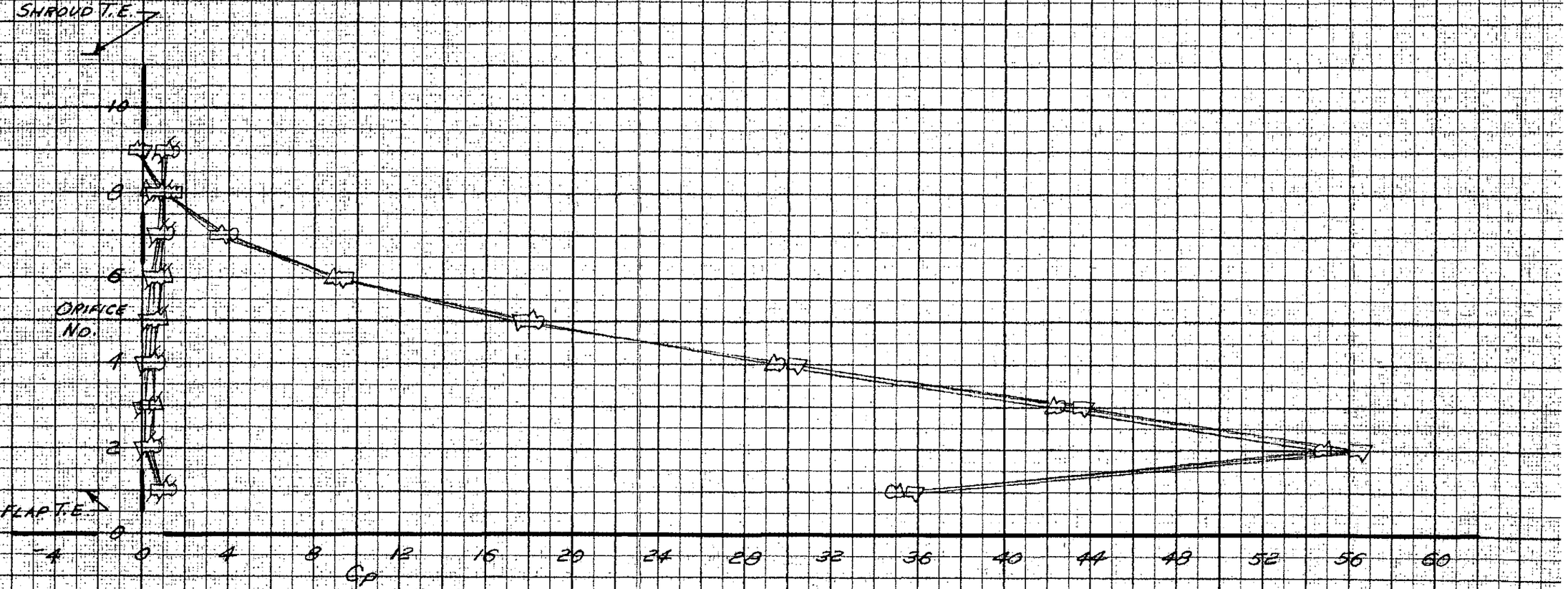

EXAMPLE TOTAL HEAD PRESSURE DISTRIBUTIONS BETWEEN THE FLAP AND SHROUD TRAILING EDGES WITH $h/c_s = 0.270$

C_p VS. ORIFICE No.

A B C

FLOW VISUALIZATION PHOTOGRAPHS

Showing flow over top (low pressure) surface

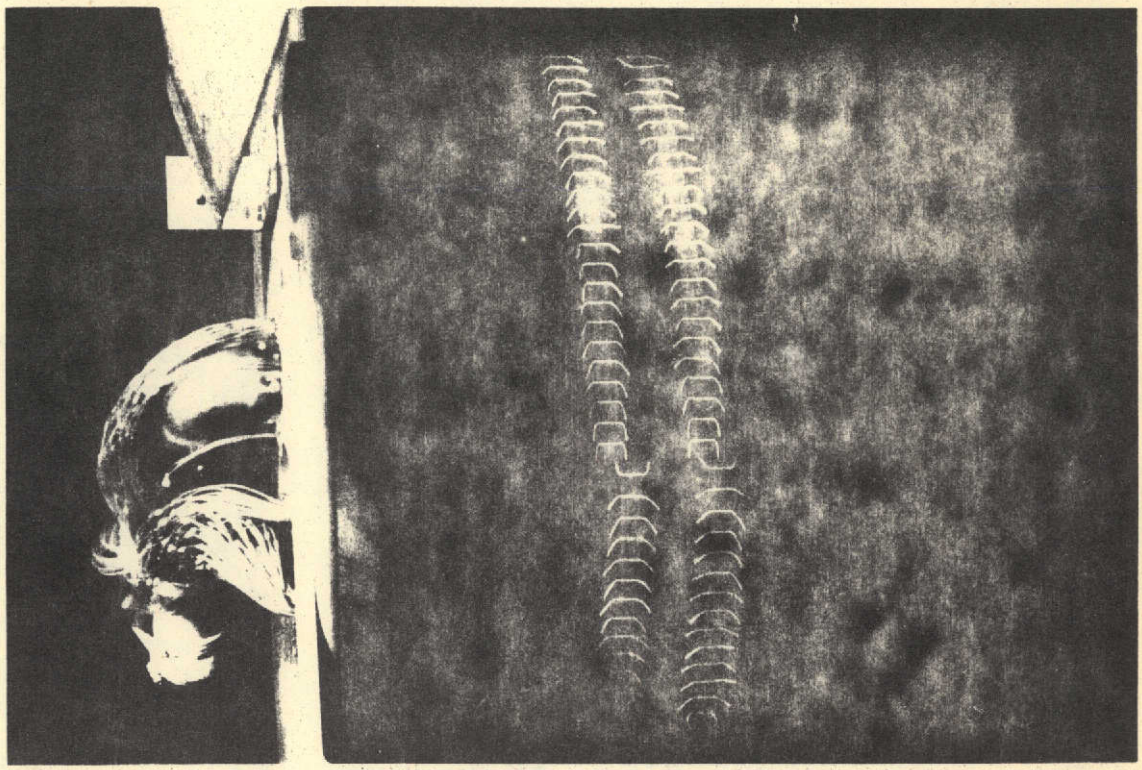

$C_j = \infty$, $q = 0$, $\alpha_g = 0°$, Run 6

250

$C_j = 1.45$, $q = 2.25$, Run 7

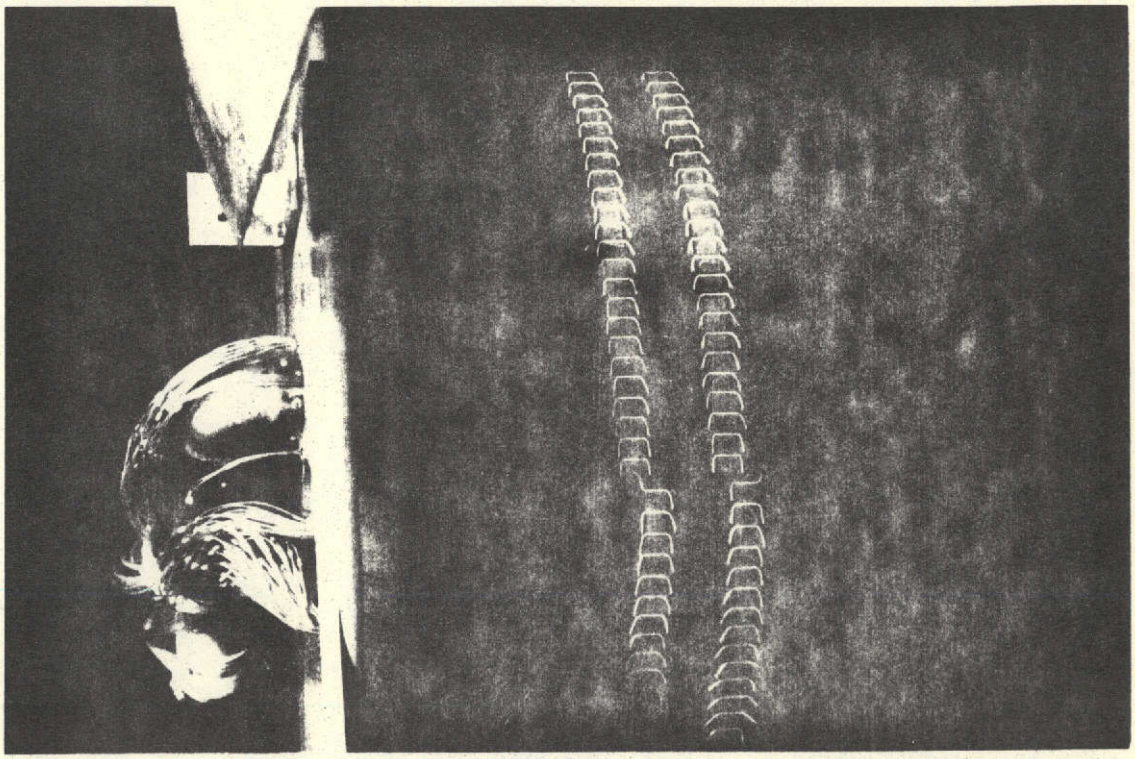

$\alpha_g = 0°$

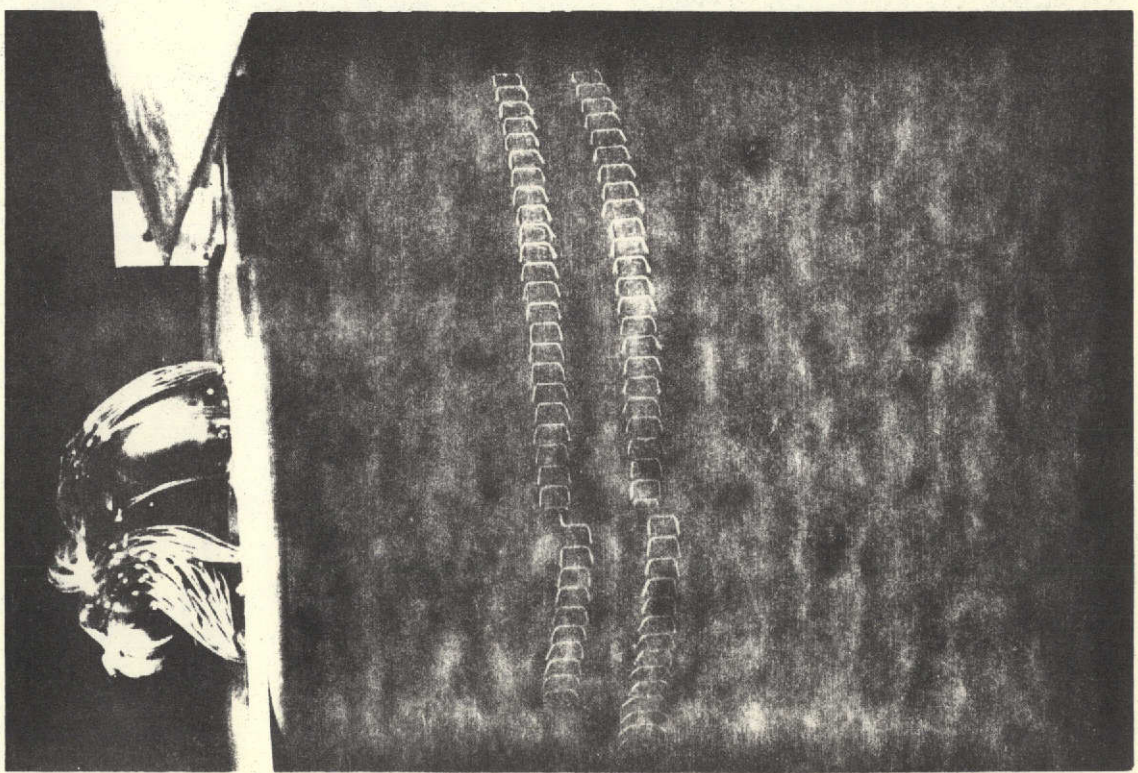

$\alpha_g = 9°$

251

$C_j = 0.33$, $q = 10$ lb/ft^2, Run 8

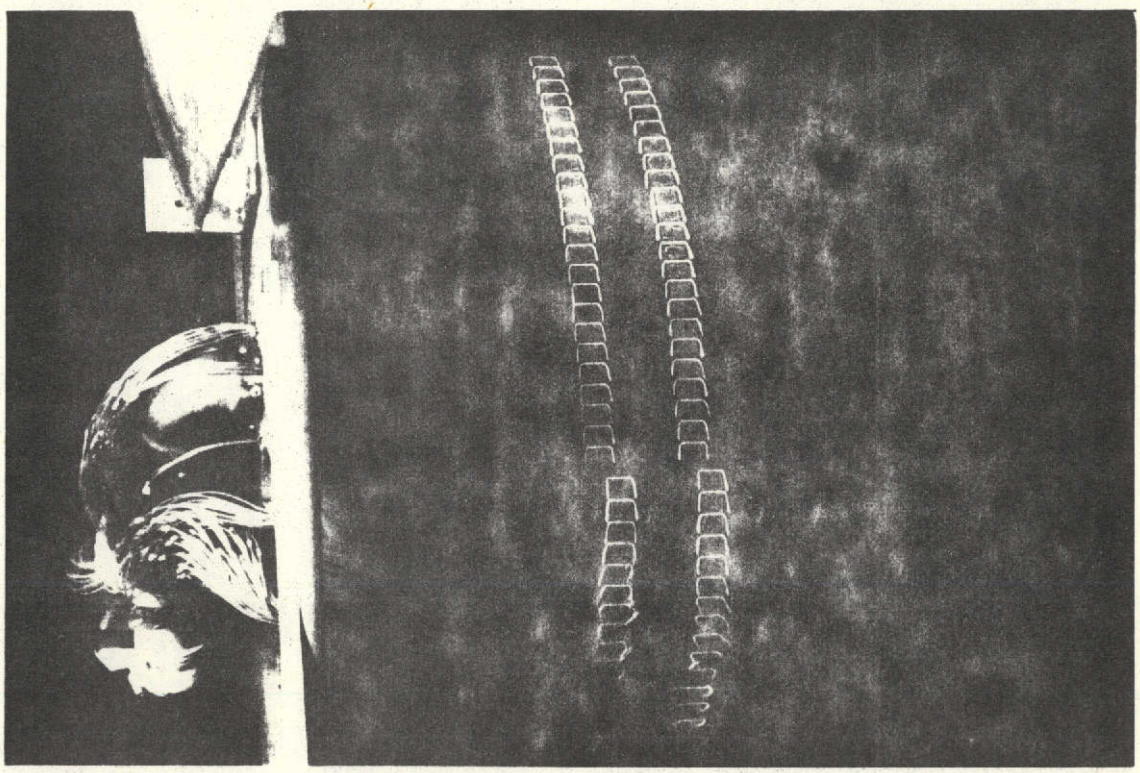

$\alpha_g = 0°$

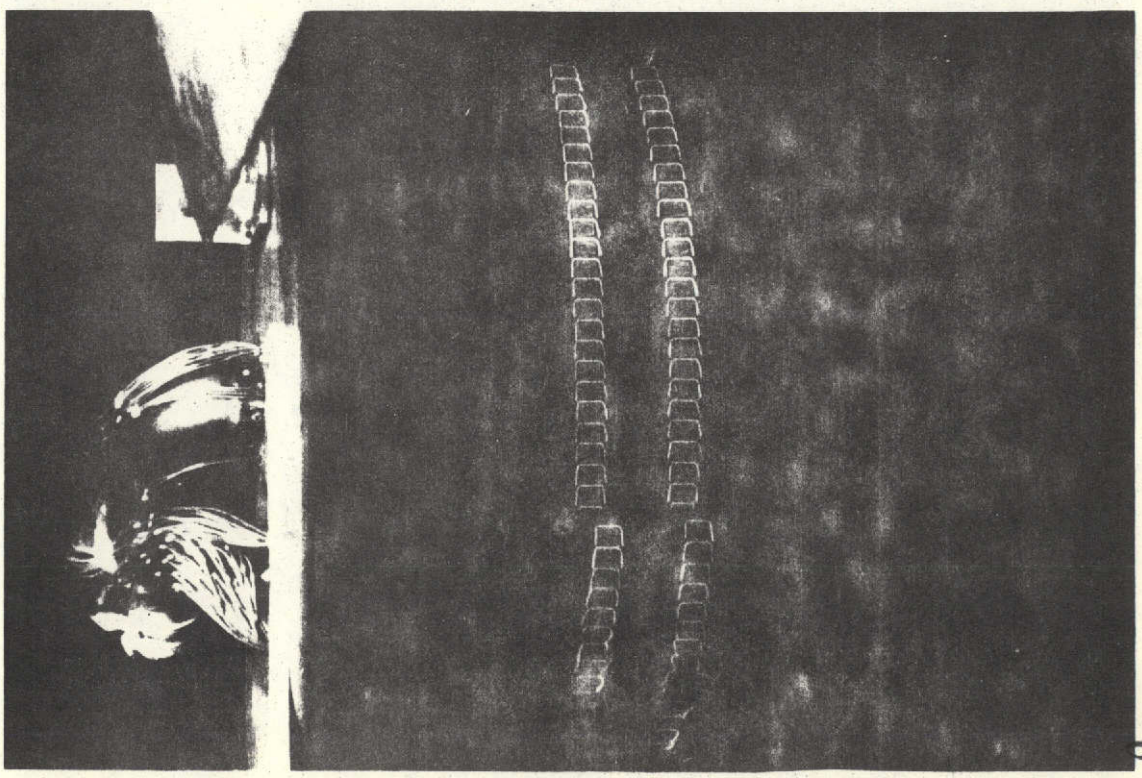

$\alpha_g = 9°$

952

MODEL PHOTOGRAPHS

Basic model with auxiliary air supply lines

and surface static pressure orifices connected

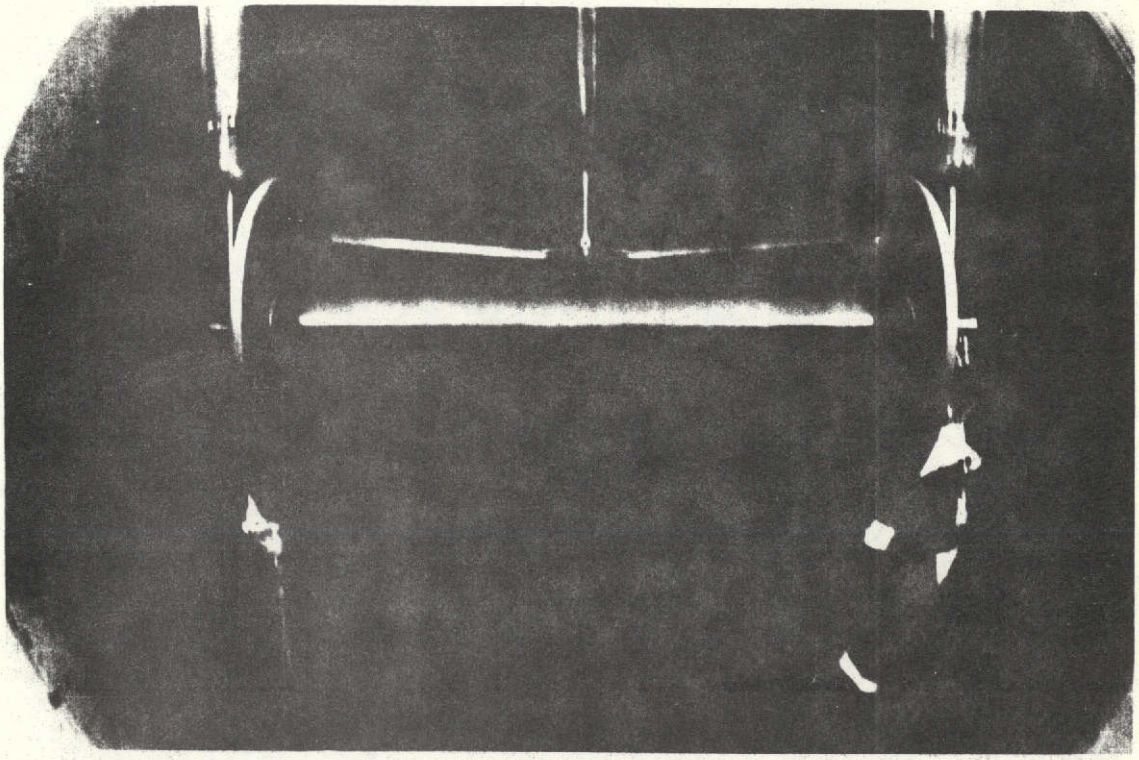

Front view

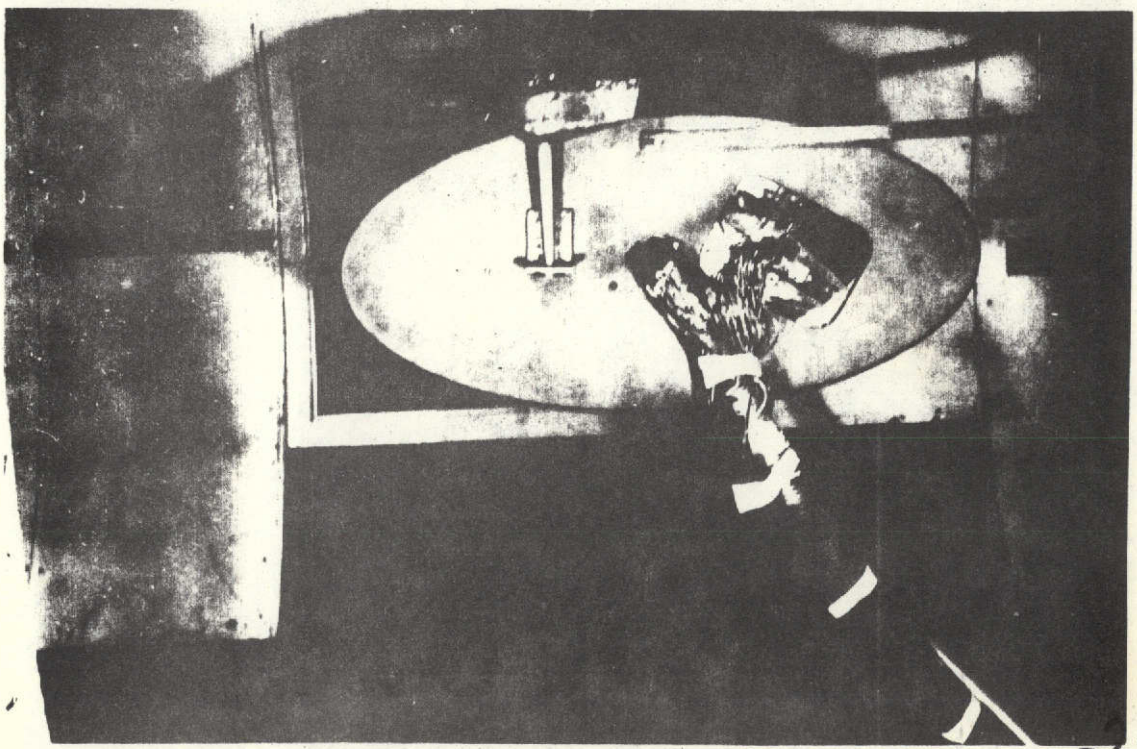

Side view

253

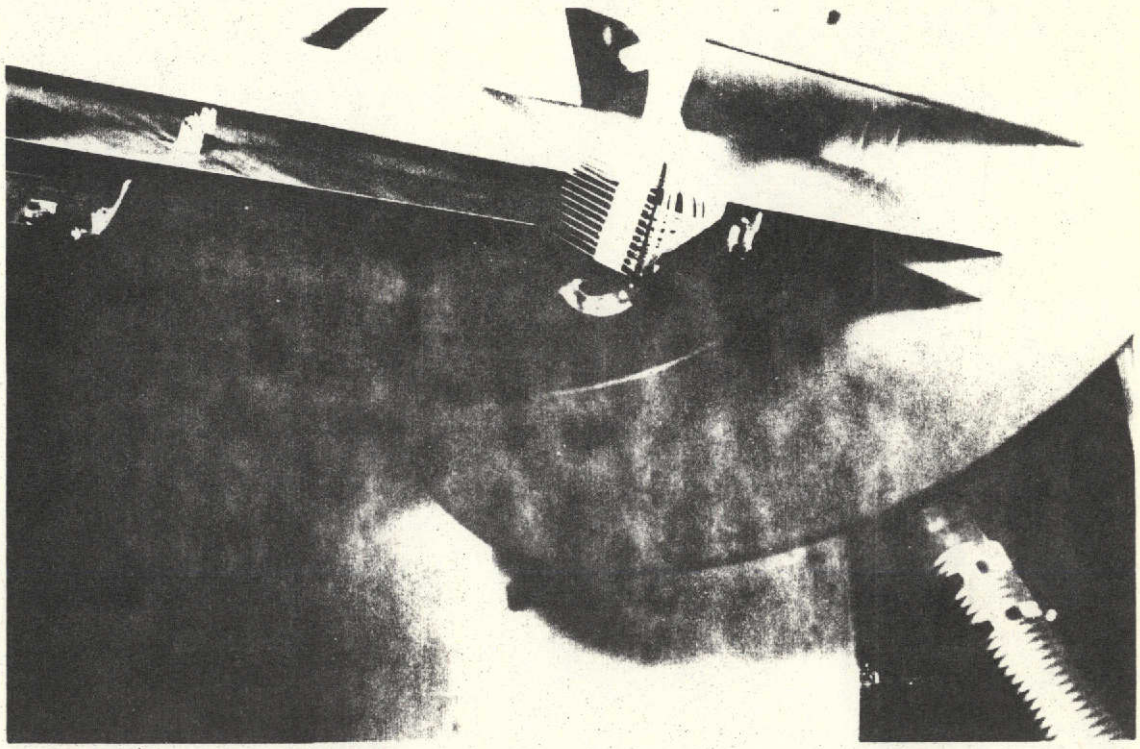

View showing total head rake located at flap-shroud exit plane

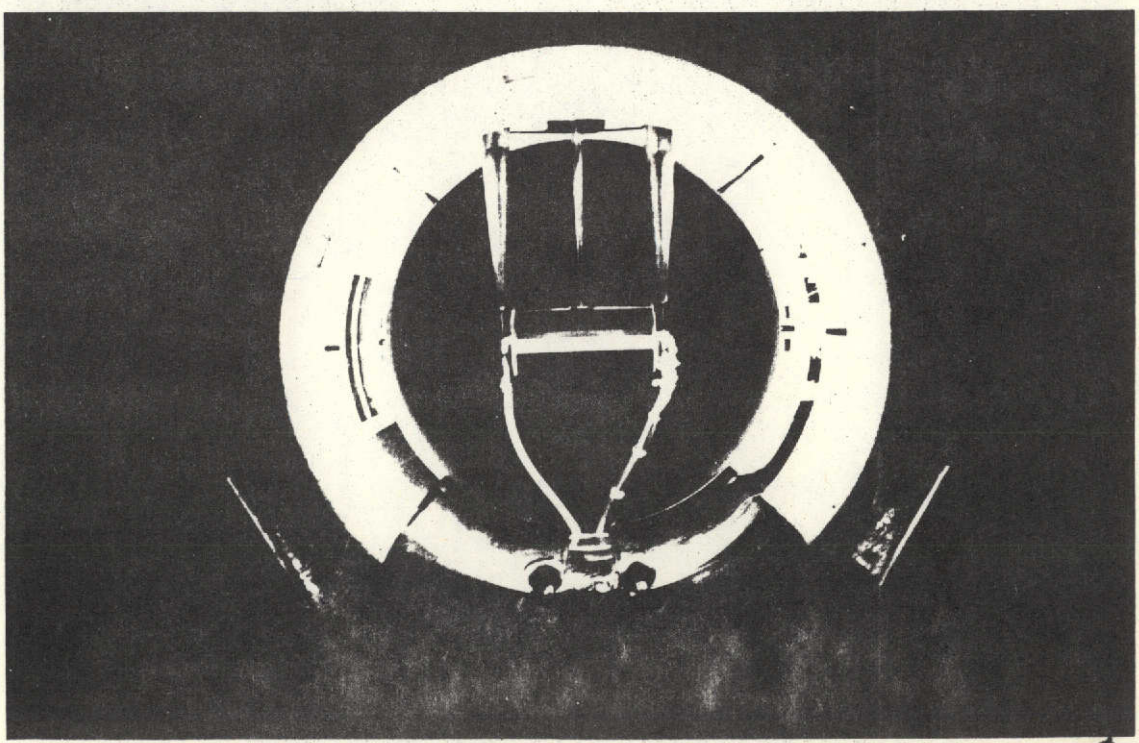

254

Front view showing model installation

Now with respect to the environments that we are going to try, Figure 6-34 shows a spectral distribution of incident radiation, obtained from C. H. Kiu using the Aerotherm code. The bottom curve is without any mass addition, the top curve is with mass addition. It is for the Saturn nominal atmosphere near peak heating, and is for the proper mass addition at that flight velocity. The point I want to make is that you can reflect, essentially from about 0.5 to 6 ev radiation, that is, you can reflect most of this incident radiation and that's the attractive thing.

Figure 6-35 shows one of the environments, i.e. for the Uranus cool dense atmosphere; twenty-five degree entry angle. This raw heating data was obtained from Aerotherm. The radiative pulse is significantly bigger than the convective pulse. The net heating that the wall sees for this code is shown on the right. You don't know this in advance, it is worked out as the solution proceeds, so I'm jumping ahead here. But, you can see the radiation is hardly influenced at all by the material response; that is, there's very little coupling, but the convective is almost wiped out. So, this is very strongly a radiative environment.

Figure 6-36 shows the environment for the Saturn nominal atmosphere. The raw heating data is predominantly convective, with just one kw/cm^2 radiative spike, but when you translate that into what the wall actually sees, it turns out it's mostly radiative. It's enhanced, also, by ablation as other speakers have presented. The radiation increases to about 1.6 kilowatts; convective is knocked down to 1.2 or thereabout.

Figure 6-37 shows the result of exercising this new code, and this is a code that we are just beginning to really exercise in a production mode; so, all of these results are fairly new. This is a 25° entry into the Uranus cool dense atmosphere, for which we saw the environment in Figure 6-35. This is a time history of the exposed surface that's ablating, and the rear surface. You can see that the front surface heats up very rapidly, starts ablating almost at once and then as the radiation pulse comes on,